

# Frequency Diverse Arrays: Fundamentals, Key Insights, and Future Directions

Bang Huang, Member, IEEE, Sajid Ahmed, Senior Member, IEEE, Wenkai Jia, Mohamed-Slim Alouini, Fellow, IEEE, and Wen-Qin Wang Senior Member, IEEE

Abstract—Frequency diverse arrays (FDA) have attracted sustained interest as a promising architecture for introducing range-dependent responses into array systems. Unlike conventional phased arrays (PA), whose transmit behavior is primarily angle-dependent, FDA employs inter-element frequency offsets to generate time- and range-dependent phase structures, thereby producing a joint time–range–angle array response. Despite extensive research, the physical meaning of FDA-induced degrees of freedom remains debated, particularly in relation to range–angle coupling, the feasibility of time-invariant focusing, and the distinction between frequency-driven and waveform-driven range selectivity. This paper reexamines FDA from a structural and manifold-based perspective. A central contribution is the introduction of an irreducibility criterion, which distinguishes genuine range-domain physical degrees of freedom from effects that can be reproduced by equivalent signal-processing transformations. Based on this perspective, PA, multiple-input multiple-output (MIMO), FDA, and FDA–MIMO are comparatively interpreted according to the physical origin of their effective degrees of freedom, including spatial phase, waveform orthogonality, frequency gradients, and their interaction. The paper further clarifies the role of frequency across different array paradigms, contrasts FDA with time-coding-based architectures, and explains how key FDA properties such as manifold expansion, range–angle coupling, time variation, and multi-frequency diversity translate into system capabilities. Building on these structural insights, the paper connects FDA to a broad range of radar and communication functionalities, including parameter estimation, target detection, imaging, physical-layer security, and integrated sensing and communication. It also discusses major limitations and open issues, including hardware realizability, wideband constraints, experimental reproducibility, near-field modeling, and the physical boundary of time-invariant focusing. Overall, this survey aims to clarify what is fundamentally distinctive about FDA, identify the conditions under which its gains are physically meaningful, and outline promising directions for future research in next-generation sensing and communication systems.

Index Terms—Frequency diverse array (FDA), multiple-input multiple-output (MIMO), phased arrays (PA), radar applications, communication applications, range-angle dependence.

Bang Huang is a postdoctoral fellow with King Abdullah University of Science and Technology (KAUST), CEMSE division, Thuwal 23955-6900, Saudi Arabia. Besides, he was a PhD student from School of Information and Communication Engineering, University of Electronic Science and Technology of China, Chengdu, 611731, P. R. China. (e-mail: bang.huang@kaust.edu.sa) (Corresponding author: Bang Huang).

Sajid Ahmed and Mohamed-Slim Alouini are with King Abdullah University of Science and Technology (KAUST), CEMSE division, Thuwal 23955-6900, Saudi Arabia (e-mails: sajid.ahmed@kaust.edu.sa; slim.alouini@kaust.edu.sa).

Wenkai Jia and Wen-Qin Wang are with the School of Information and Communication Engineering, University of Electronic Science and Technology of China, Chengdu, 611731, P. R. China. (e-mails: mrwenkaij@126.com; wqwang@uestc.edu.cn).

## I. Introduction

### A. Background and Motivation

Modern sensing and communication systems have evolved through a progressive expansion of exploitable signal dimensions [1], [2]. In radar systems, early designs primarily relied on echo detection and propagation delay estimation, with signal processing largely confined to the time domain [3]. The introduction of pulse compression enabled energy focusing via matched filtering, improving range resolution and partially suppressing uncorrelated interference [4]. Subsequently, pulse-Doppler radar incorporated Doppler frequency shifts, introducing a frequency-domain discrimination dimension and enabling joint time–frequency processing [5]. Further advances were achieved through phased-array (PA) radar, which introduced spatial-domain processing via beamforming and directional selectivity [6]. Combined with space–time adaptive processing (STAP), modern radar systems now operate in a joint space–time domain, significantly enhancing detection performance in complex environments [7], [8].

A similar evolution can be observed in communication systems, whose development has also been marked by the progressive exploitation of new transmission dimensions. Early communication systems relied primarily on time-domain signaling, where information delivery and user access were largely organized over time. Subsequent advances extended communication design into the code domain, exemplified by code-division multiple access (CDMA) [9], [10], which enabled multiuser separation through spreading codes and provided enhanced robustness against interference. The frequency domain was progressively incorporated into communication system design, initially through frequency-division multiplexing and multiple-access schemes such as frequency-division multiple access (FDMA) [11], [12], and later in a more structured manner through multicarrier techniques such as orthogonal frequency division multiplexing (OFDM) [13], [14], which improved spectral efficiency and facilitated reliable transmission over frequency-selective channels. More recently, multiple-input multiple-output (MIMO) [15]–[18] technology has elevated the spatial domain into a fundamental communication resource, enabling spatial multiplexing, beamforming, and diversity gains. Taken together, these advances reflect a broader evolution from one-dimensional signaling toward the joint exploitation of time, code, frequency, and space.

Despite these advances, a common limitation persists across both radar and communication systems: while time, frequency, code, and spatial dimensions have been extensively exploited, the range dimension remains largely passive [19], [20]. In conventional array systems, the array response is primarily a function of angle, whereas range information is only implicitly embedded in propagation delay or path loss, rather than being explicitly controllable as a design variable. Existing approaches attempt to utilize range information through waveform design or receiver processing, such as matched filtering or delay estimation. However, these mechanisms operate mainly in the signal processing stage, without fundamentally altering the propagation structure of the transmitted field. As a result, range cannot be directly incorporated into the array response in the same manner as angle in phased arrays or space in MIMO systems. This limitation becomes particularly critical in emerging scenarios, including range-dependent interference suppression, ambiguity resolution, near-field communications, holographic MIMO, physical-layer security, and integrated sensing and communication (ISAC), where fine-grained control over the range dimension is highly desirable. These challenges motivate the need for array architectures that can explicitly incorporate range into the design space.

## B. The Concept of Frequency Diverse Array

Motivated by the aforementioned limitations, particularly the lack of controllable range-domain response in conventional array systems, the frequency diverse array (FDA) emerges as a natural extension that enables the explicit incorporation of the range dimension into array design. The concept of FDA was first introduced by Antonik in 2006 at the IEEE Radar Conference [21]. Unlike conventional phased arrays (PAs), where all elements operate at a common carrier frequency, FDA assigns slightly different carrier frequencies to different array elements, i.e.,  $f_m = f_c + \Delta f_m$ . Although seemingly minor, this modification fundamentally alters the propagation-induced phase structure [22]–[24]. Since the radiated field from each element accumulates phase according to its own carrier frequency over the propagation delay, the inter-element phase difference becomes a function not only of angle, but also of range and time.

For a conventional far-field phased array, the transmit array response at an instantaneous snapshot is determined primarily by angular steering, while range enters only through common propagation delay and attenuation rather than as an independently controllable array-response dimension [25], [26]. In contrast, the element-dependent frequency offsets in FDA introduce additional time- and range-dependent phase terms, resulting in a transmit response that depends jointly on time, range, and angle. Consequently, the array manifold is extended from  $\mathbf{a}(\theta)$  to a higher-dimensional representation  $\mathbf{a}(t, r, \theta)$ . This structural extension gives rise to several distinctive phenomena, including range–angle coupling, time-varying

beam scanning, and dynamic focusing behavior. Unlike conventional arrays that form essentially static beams, FDA produces a spatiotemporal energy distribution that evolves continuously over time, often visualized as a trajectory in the range–angle plane. These properties create new opportunities for range-aware beam synthesis, ambiguity shaping, interference suppression, and ISAC design. At the same time, the resulting range dependence is intrinsically coupled with temporal evolution, which fundamentally distinguishes FDA from conventional static-beam array architectures.

Importantly, FDA should not be understood as merely introducing frequency diversity into an array. Its real significance lies in altering the dimensionality of the array manifold itself, by embedding range and time into the propagation-induced response. In this sense, FDA extends the conventional angle-dependent array model toward a joint time–range–angle representation. The canonical FDA usually employs linear frequency increments across the aperture. However, this simplest form also reveals intrinsic range–angle coupling and time-varying focusing behavior, which soon motivated a broad family of generalized FDA architectures, including nonlinear-offset, random-offset, time-modulated, subarray, and geometry-modified designs. These developments mark an important transition from the original FDA concept toward a richer research landscape centered on controllable propagation-structure design [27]–[42]. This evolutionary trajectory, together with the subsequent emergence of FDA–MIMO and other related range–angle responsive architectures, is reviewed next.

## C. Research History for FDA

Since its introduction by Antonik in 2006 [21], FDA research has evolved from a concept centered on unusual transmit beampattern phenomena into a broader framework for propagation-structure engineering. Early patents, doctoral-level investigations, and later prototype studies further indicate that FDA quickly attracted attention beyond purely conceptual analysis [22], [43]–[45]. As also reflected in later overview and survey articles [24], the development of FDA has not proceeded merely as a chronological accumulation of applications, but rather through a sequence of conceptual reinterpretations, structural extensions, and task-driven generalizations. From this perspective, the evolution of FDA research can be broadly understood through four interconnected stages, as shown in Fig. 1.

(i) Concept emergence and phenomenon discovery (2006–2013): The earliest studies were primarily devoted to understanding the unconventional transmit behavior induced by element-dependent frequency offsets [21], [22]. Relative to conventional phased arrays, FDA exhibited range–angle coupling, time-varying beam scanning, and dynamic focusing effects, thereby extending the array response from an angle-only description to a joint time–range–angle structure [46]–[48]. During this stage, the

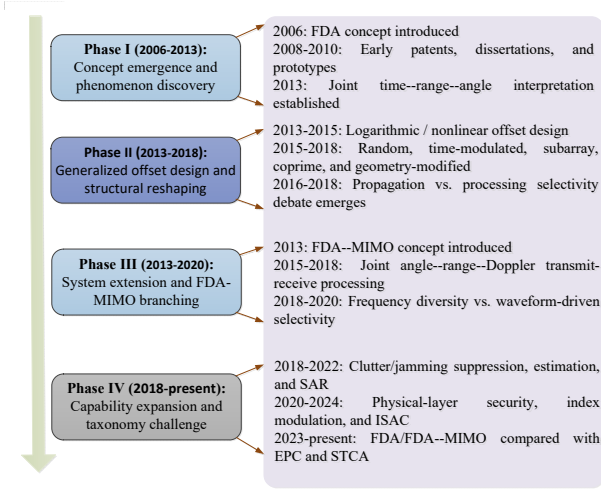


Fig. 1: Representative development trajectory of FDA research, from concept emergence to generalized structural redesign, FDA-MIMO branching, capability expansion, and taxonomy-oriented comparison.

main research effort focused on revealing these phenomena, clarifying their physical origin, and assessing whether the resulting range dependence could be interpreted as a genuine new structural degree of freedom [22]–[24]. At the same time, the canonical FDA with linear frequency increments quickly exposed its intrinsic limitations: the transmit response was strongly range–angle coupled, and the focusing behavior was generally nonstationary rather than permanently fixed at a prescribed location [49]–[51]. These observations triggered extensive discussions on the physical interpretability of FDA focusing and the feasibility of time-invariant beamforming.

(ii) Generalized offset design and structural reshaping (2013–2018): Once the basic FDA mechanism became better understood, research rapidly moved beyond the original linear-offset configuration. A wide range of generalized FDA architectures were proposed, including logarithmic-offset FDA [27], nonlinear polynomial-offset FDA [30], random-offset and logarithmic-random-offset FDA [38], [39], time-modulated and sparse FDA [52], [53], subarray-based FDA [54]–[57], coprime FDA [58], [59], and geometry-modified FDA such as semicircular or nonuniform-spacing structures [60]–[62]. Related efforts also explored beampattern synthesis using windowing, weighting, Costas-type offsets, and intelligent optimization methods in order to improve focusing, reduce sidelobes, or achieve range–angle decoupling [32]–[35], [40]–[42]. Although these variants differ in implementation, they were largely motivated by a common objective: to reshape the propagation-induced phase structure so as to mitigate range–angle coupling, improve focusing behavior, suppress sidelobes, or enhance controllability in the range–angle plane. In this sense, the evolution from linear FDA to generalized FDA should not be understood as a simple accumulation of design variants, but as a deeper transition

from phenomenon observation to manifold engineering.

A particularly important thread in this stage concerned attempts to realize quasi-static or time-invariant focusing. Pulse-based FDA, optimized offset design, and receive-assisted equivalent focusing schemes were all proposed to approximate or synthesize more stable range–angle responses. However, these efforts also made clear that one must carefully distinguish between genuinely propagation-induced range dependence and range selectivity that is produced only after matched filtering, coding, or transmit–receive synthesis [49]–[51], [63]. This distinction later became central to the interpretation of FDA-like architectures more broadly.

(iii) System extension and architectural branching (2013–2020): As FDA matured, the research frontier expanded from single-aperture coherent FDA toward multi-channel and hybrid architectures, most notably FDA-MIMO [64]–[67]. By combining frequency offsets with waveform orthogonality, FDA-MIMO enlarged the design space and enabled joint transmit–receive processing in angle, range, and Doppler. This significantly accelerated research in range-ambiguous clutter suppression, deceptive jamming mitigation, target localization, and adaptive detection [68]–[77]. At the same time, FDA-MIMO also introduced an important structural ambiguity: once waveform orthogonality and receiver-side matched filtering are incorporated, the effective system degrees of freedom may arise jointly from propagation-level frequency diversity and signal-processing-level waveform diversity. As a result, the relationship between coherent FDA and FDA-MIMO is not merely a matter of implementation, but a question of mechanism origin. This is also why the evolution of FDA research cannot be fully understood without explicitly distinguishing propagation-driven array effects from processing-driven virtual responses.

(iv) Capability expansion, cross-domain applications, and taxonomy challenge (since 2018): With the proliferation of FDA variants and FDA-MIMO architectures, the field increasingly moved toward application-oriented development. FDA-related techniques have been applied to a broad range of tasks, including range-ambiguous clutter suppression [78]–[81], deceptive jamming suppression [82], [83], target detection and parameter estimation [84]–[88], synthetic aperture radar (SAR) imaging [89]–[94], low-probability-of-intercept (LPI) radar [95], [96], physical-layer security [97]–[104], and ISAC [105]–[107]. During this stage, FDA was no longer viewed merely as a source of unusual beampatterns, but increasingly as a flexible mechanism for shaping propagation structures to satisfy task-specific objectives. Accordingly, design criteria also evolved from qualitative beampattern visualization toward performance-oriented metrics such as ambiguity suppression, estimation accuracy, interference rejection, identifiability, secrecy enhancement, and sensing–communication integration.

In parallel, the literature also began to discuss FDA and FDA-MIMO together with other array paradigms capable of generating range–angle dependent responses,

such as element–pulse coding (EPC) arrays and space–time coding arrays (STCA) [108]–[120]. This broader comparison is highly significant, because it reveals that not all range–angle dependent responses arise from the same mechanism. For some architectures, the additional selectivity is rooted in transmit-side propagation physics; for others, it is produced through coding, pulse diversity, or receiver-side synthesis. Consequently, a key issue in the modern FDA literature is no longer only how to generate range-dependent beampatterns, but how to interpret their physical origin, distinguish genuine and synthesized degrees of freedom, and classify related architectures within a unified structural taxonomy.

It is also worth noting that the historical development of FDA research has included not only theoretical analysis and numerical design, but also patents, prototype exploration, and experimental validation [22], [43], [44], [121]. The literature has reported early proof-of-concept platforms and later prototype demonstrations, indicating that FDA has evolved beyond a purely conceptual topic [22], [121]. Nevertheless, compared with the diversity of theoretical models, experimental validation remains relatively limited, and many important issues—including hardware complexity, coherent implementation, waveform calibration, and practical robustness—are still far from fully resolved.

Overall, the historical evolution of FDA suggests that the field has progressed through a clear internal logic: from discovering unconventional range–angle–time behavior, to redesigning the array structure for better controllability, to branching into FDA–MIMO and related architectures, and finally to expanding toward diverse sensing and communication tasks. Yet despite this rich development, several foundational questions remain open: whether truly time-invariant focusing is physically achievable, whether range–angle coupling should be viewed as a useful degree of freedom or a design burden, and how FDA, FDA–MIMO, EPC, STCA, and related architectures should be positioned within a unified modeling framework. These unresolved issues strongly motivate the need for a structural re-examination of FDA research.

Motivated by these observations, this paper revisits FDA and its related architectures from a unified signal modeling and taxonomy perspective. Rather than organizing the literature solely by application domain, we aim to establish a principled mapping from design mechanism to manifold structure, from manifold structure to exploitable degrees of freedom, and from these degrees of freedom to sensing and communication capabilities.

#### D. Core Innovations and Key Debates of FDA

Although FDA has been extensively studied, its essential innovation and the boundary of its claimed capabilities remain subjects of ongoing debate. Much of the existing literature interprets FDA from application-oriented, beampattern-oriented, or architecture-oriented viewpoints. In contrast, we revisit FDA from a structural

perspective and argue that its significance lies not merely in generating range-dependent responses, but in altering how propagation variables enter the array manifold itself. From this viewpoint, FDA exhibits several core innovations, while also raising a number of unresolved debates concerning the physical meaning, structural origin, and practical validity of its claimed degrees of freedom.

1) From Angle-Only Response to a Joint Time–Range–Angle Manifold: The most fundamental distinction of FDA lies in introducing inter-element frequency gradients across the array aperture. Unlike conventional phased arrays, whose manifold is essentially angle-dependent at an instantaneous snapshot, FDA embeds range dependence directly into the propagation process through element-dependent carrier frequencies. As a result, the array response is extended from an angle-only representation  $\mathbf{a}(\theta)$  to a higher-dimensional manifold  $\mathbf{a}(t, R_0, \theta)$ . This transformation constitutes a genuine structural extension of the array model, enabling joint dependence on time, range, and angle. At the same time, it also introduces intrinsic time variation and range–angle coupling, which fundamentally distinguish FDA from conventional static-beam array architectures.

2) Frequency as a Propagation-Domain Design Variable: A second conceptual innovation of FDA is that frequency is no longer used merely as a signal-domain resource for multiplexing, waveform construction, or spectral allocation. Instead, FDA employs frequency offsets to generate phase gradients across the array aperture, thereby making frequency a propagation-domain design variable. This shift is conceptually important: the role of frequency is moved from shaping the transmitted signal alone to shaping how the signal propagates and interferes across space. In other words, FDA does not simply use different frequencies; it uses frequency differences to alter the spatial-temporal structure of the transmitted field. This naturally raises a fundamental question: do such frequency gradients create genuinely new physical degrees of freedom, or do they merely re-parameterize effects that can already be synthesized through other means?

3) From Beamforming to Propagation-Structure Shaping: The above viewpoint leads to a broader reinterpretation of what FDA contributes to array design. In conventional arrays, beamforming is typically performed over a fixed manifold, where the main task is to optimize weights, phases, or waveforms under a given propagation structure. FDA goes one step further: rather than operating solely on top of a fixed angular manifold, it modifies the mechanism by which the manifold itself is generated. Hence, FDA should not be understood merely as another beam synthesis technique, but as a framework for propagation-structure shaping. Its novelty lies in altering how time, range, and angle jointly enter the array response, thereby transforming the design problem from beam control over a given manifold to structural control over the manifold-forming process itself.

4) Irreducibility as a Criterion for Genuine Physical Degrees of Freedom: From this structural perspective,

the mere existence of frequency offsets is not sufficient to claim new physical degrees of freedom. We argue that a more meaningful criterion is irreducibility. Specifically, a range-dependent phase term should be regarded as a genuine physical degree of freedom only if it cannot be removed, absorbed, or equivalently transformed away without collapsing the underlying propagation structure into an angle-only or waveform-synthesized form. If the apparent range dependence can be eliminated through equivalent linear compensation, matched filtering, coding synthesis, or other receiver-side transformations, then the resulting selectivity does not necessarily correspond to an independent propagation-domain degree of freedom. Under this viewpoint, the key issue is not whether range-dependent responses can be observed, but whether they are intrinsically embedded in the propagation manifold itself. Only when the range-dependent phase structure is irreducible in this sense does FDA introduce a genuinely new physical design dimension. This criterion also has an important implication for FDA-MIMO. If range is not merely a delay-domain quantity but an irreducible parameter embedded in the transmit-receive manifold, then distance estimation may no longer need to be interpreted exclusively within the classical pulse-compression framework. Under such a viewpoint, range could in principle be treated as a manifold parameter, much like angle in phased arrays, thereby opening the possibility of a manifold-based ranging paradigm. This, in turn, raises the further question of whether range resolution should still be defined solely by waveform bandwidth, or instead by the distinguishability and identifiability of range-dependent manifold responses.

5) Key Debates in FDA Research: The above structural insights, especially the criterion of irreducibility for genuine physical degrees of freedom, lead to several fundamental debates that continue to shape the interpretation of FDA and FDA-related architectures:

- Time-invariant focusing: whether strictly time-invariant spatial focusing can be achieved under nonzero frequency gradients, or whether such focusing is inherently dynamic in FDA-like architectures;
- Range-angle coupling: whether the coupling observed in FDA should be interpreted as a useful structural degree of freedom or as an additional source of design complexity and signal-processing burden;
- Origin of selectivity: whether the observed range-dependent response is induced directly by propagation physics or synthesized through coding, matched filtering, or receiver-side processing;
- Ranging paradigm: whether range should still be interpreted exclusively under the classical delay-resolution framework, or whether the embedding of range into the transmit-receive manifold opens the possibility of manifold-based ranging and a corresponding redefinition of range resolution;
- Paradigm interpretation: whether FDA-MIMO should be understood primarily as a frequency-driven extension of FDA or as a waveform-driven

hybrid architecture whose additional selectivity is not purely propagation-originated;

- Practical realizability: how hardware nonidealities, bandwidth limitations, calibration errors, coherence requirements, and implementation complexity affect the existence and usability of the theoretically claimed degrees of freedom.

Among the above issues, this paper places particular emphasis on three major structural debates, namely the physical feasibility of time-invariant focusing, the interpretation of range-angle coupling as either redundancy or exploitable DoF, and the taxonomy of FDA-MIMO with respect to propagation-driven versus processing-driven selectivity. The remaining debates, especially those related to manifold-based ranging and practical realizability, are also discussed throughout the paper, but are treated primarily as forward-looking perspective questions and implementation-level challenges rather than as fully resolved theoretical conclusions.

Among these open perspective questions, one particularly intriguing issue arises in the context of FDA. If range is explicitly embedded into the transmit-receive manifold, then distance information may no longer need to be interpreted exclusively through the conventional delay-domain framework. This raises the possibility that range could be estimated, at least in principle, as a structural parameter of the array manifold, in a manner conceptually analogous to angle estimation in phased arrays, rather than solely through pulse compression and matched filtering. Under such a viewpoint, the classical definition of range resolution based only on waveform bandwidth may no longer be sufficient. Instead, range resolution may need to be reconsidered from a manifold-discrimination perspective, for example through distinguishability, identifiability, or Fisher-information-based metrics of range-dependent steering responses.

Taken together, these debates suggest that FDA should be interpreted not simply as a special waveform configuration or a modified array structure, but as a structural extension of the propagation manifold. For this reason, FDA is more appropriately understood through a framework that links design mechanism, manifold transformation, and exploitable capability, rather than through application categories alone. This perspective also motivates the structural taxonomy adopted in the remainder of this paper.

## E. Contributions and Organization

To address the above challenges and establish a unified understanding of FDA, this paper develops a structure-oriented framework that connects array design variables, propagation-induced manifold structure, physical degrees of freedom, and ultimately system capabilities. Rather than treating FDA as a collection of application-specific techniques, we reinterpret it as a propagation-structure-driven array paradigm and revisit its related architectures from a unified taxonomic perspective.

The main contributions of this paper are summarized as follows:

- Unified structural taxonomy of array paradigms: We establish a unified signal and array-level framework covering PA, FDA, MIMO, and FDA-MIMO, and show that these paradigms can be distinguished according to the physical source of their degrees of freedom. In particular, PA is interpreted as a spatial-phase-driven paradigm, MIMO as a waveform-orthogonality-driven paradigm, FDA as a frequency-gradient-driven paradigm, and FDA-MIMO as a frequency-waveform jointly driven paradigm. This taxonomy provides a clearer physical interpretation of how different array architectures generate their effective capabilities.
- Clarification of the role of frequency across different systems: We systematically analyze the fundamentally different roles of frequency in FDMA/OFDM-type systems and FDA-type systems. In contrast to FDMA and OFDM, where frequency mainly serves as a multiplexing, modulation, or indexing resource, FDA employs inter-element frequency offsets to reshape the propagation kernel itself. This distinction clarifies why FDA should not be reduced to a conventional frequency-domain communication or signal-processing mechanism.
- Irreducibility criterion for genuine range-domain DoFs: We introduce an irreducibility criterion to distinguish genuinely new physical range-domain DoFs from equivalent processing-level reformulations. Under this viewpoint, frequency offsets alone do not automatically imply a new physical DoF; a genuine range DoF arises only when the resulting range-phase-gradient structure is irreducible and cannot be removed without collapsing the system into an angle-only or waveform-synthesized form. This provides a physics-grounded answer to the long-standing question of whether FDA truly introduces a new distance-related design dimension.
- The answers to three central structural debates: Based on the proposed framework, we provide unified answers to three long-standing structural debates in FDA research, namely the physical feasibility of time-invariant focusing, the interpretation of range-angle coupling as redundancy or exploitable DoF, and the taxonomy of FDA-MIMO in terms of propagation-driven versus processing-driven selectivity. We further discuss manifold-based ranging and practical realizability as two forward-looking debates that remain open, thereby distinguishing between questions that can be structurally clarified within the present framework and those that still require future theoretical and experimental investigation.
- Systematic classification of FDA-MIMO realizations: We classify FDA-MIMO architectures according to their orthogonality mechanisms, namely waveform-orthogonal and frequency-orthogonal realizations, and clarify how these mechanisms affect the preservation, suppression, or reconstruction of propagation-induced range dependence. This classification explains why FDA-MIMO may exhibit different range-angle behaviors at the propagation level and the equivalent processing level, and provides a more precise answer to the question of what should and should not be regarded as FDA-originated.
- Manifold-based explanation of core FDA phenomena: From the perspective of manifold expansion, we systematically analyze the intrinsic time variability, frequency-gradient effect, beam scanning behavior, range-angle coupling, integrated transmit beam pattern, ambiguity-function structure, and scattering-response characteristics of FDA. This provides a coherent physical interpretation of how element-dependent carrier frequencies reshape the propagation manifold from  $\mathbf{a}(\theta)$  to  $\mathbf{a}(t, r, \theta)$ .
- Unified comparison with time-coding array paradigms: We establish a structural comparison between frequency-gradient-driven FDA/FDA-MIMO and time-coding-driven architectures such as EPC arrays and STCA. Although these systems may produce similar range-angle dependent responses at the output level, we show that their underlying mechanisms are fundamentally different: FDA creates physical range dependence through propagation-phase gradients, whereas EPC/STCA mainly generate processing-induced range selectivity through temporal coding and receiver-side synthesis.
- Capability mapping from mechanism to function: We build a capability-oriented mapping framework that connects FDA-induced structural properties to system-level functionalities. In particular, we identify three representative FDA capabilities, including range-angle selectivity, time-evolving beam control, and frequency-domain diversity, and show how they arise from the underlying propagation structure. This framework bridges the gap between abstract DoF analysis and practical sensing/communication functions.
- Task-oriented review of radar and communication applications: Using the above framework, we systematically review how FDA capabilities translate into practical advantages across radar and communication applications. On the radar side, we analyze parameter estimation and target localization, target detection under range-ambiguous clutter, deceptive jamming and high-speed-target scenarios, anti-jamming and anti-deception processing, LPI radar, high-resolution wide-swath imaging, and target tracking. On the communication side, we further review FDA-enabled physical-layer security, index modulation, and FDA-based ISAC, thereby showing how the same propagation-structure mechanism manifests across sensing and communication tasks.
- Critical discussion of limitations and future directions: Finally, we discuss the current limitations of

FDA research and identify future directions, including near-field modeling, wideband applicability, hardware coherence constraints, experimental validation, the feasibility of manifold-based ranging, and the integration of FDA with emerging near-field/holographic MIMO and next-generation ISAC systems.

<b>I. Introduction</b>	
A. Background and Motivation	B. The Concept of Frequency Diverse Array
C. Research History for FDA	D. Core Innovations and Key Debates of FDA
E. Contributions and Organization	
<b>II. The Evolution of the FDA</b>	
A. Phased Array Beam Steering	B. Frequency Diverse Array
C. From Phased Array to FDA-MIMO: Taxonomy and Expansion of the Design Space	
D. Design Variables and DoF: A Physical-Layer Criterion vs. Equivalent-Layer Phenomena	
E. The Answers to Three Major Structural Debates	
<b>III. Fundamental Design Dimensions of FDA: From Mechanism to Structural Abstraction</b>	
A. Time Variability as Manifold Expansion	
B. Frequency Gradient and Scanning Mechanism	
C. Range–Angle Coupling in the FDA Manifold	
D. Integrated Transmit Beampattern from a Manifold Perspective	
E. Ambiguity-Function Interpretation of the FDA Manifold	
F. Scattering Response from a Manifold Perspective	
<b>IV. Frequency-Gradient and Time-Coding Array Paradigms</b>	
A. Propagation Phase and Design Dimensions	
B. Frequency-Driven Paradigm: FDA and FDA–MIMO	
C. Time-Coding-Driven Paradigm I: EPC	
D. Time-Coding-Driven Paradigm II: STCA	
E. Structural Comparison of Array Paradigms	
<b>V. FDA System Capability Mapping Framework</b>	
A. Range–Angle Selectivity	
B. Time-Evolving Beam Control	
C. Frequency-Domain Diversity	
D. Capability Mapping Summary	
<b>VI. FDA Applications Across Radar Task Families</b>	
A. Parameter Estimation and Target Localization	
B. Target Detection in Complex Environments	
C. Anti-Deception and Anti-Jamming	
D. Low-Probability-of-Intercept Radar	
E. Imaging and Wide-Area Surveillance	
F. Target Tracking and Adaptive Sensing	
G. Summary and Key Insight	
<b>VII. Extensions Toward Communications and Integrated Sensing and Communications (ISAC)</b>	
A. Physical-Layer Secure Communications	
B. Index Modulation and Hybrid Transmission Schemes	
C. FDA-Enabled ISAC Systems	
<b>VIII. Limitations, Misconceptions, and Future Research Directions</b>	
A. On the Feasibility of Time-Invariant Focusing	
B. Near-Field and Far-Field Applicability Boundary	
C. Frequency-Offset Constraints under Wideband Conditions	
D. Experimental Validation and Dataset Challenges	
E. Future Research Directions	
F. Concluding Perspective	
<b>IX. Conclusion</b>	

Fig. 2: Organization of this paper.

The organization of this paper is illustrated in Fig. 2. Specifically, Section I introduces the background and motivation of FDA, together with its basic concept, research history, core innovations, and key debates. Section II presents the evolution from phased arrays to FDA and FDA–MIMO, and develops a unified array taxonomy, a physical-layer DoF criterion, and unified answers to three major structural debates. Section III analyzes the fundamental design dimensions of FDA from a manifold perspective, including time variability, frequency-gradient-induced beam scanning, range–angle coupling, integrated transmit beampatterns, ambiguity-function char-

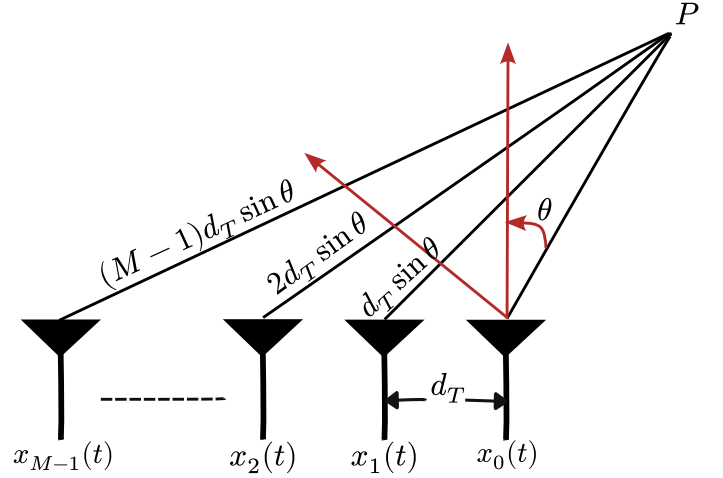


Fig. 3: Geometry of a uniform linear transmit array with  $M$  antennae and inter-element-spacing of  $d_T$  showing the angle-dependent path differences toward a far-field point  $P$ .

acteristics, and scattering responses. Section IV compares frequency-gradient-driven FDA paradigms with time-coding-based array architectures, including EPC and STCA, from a unified structural viewpoint. Section V establishes an FDA capability mapping framework that links structural mechanisms to representative system capabilities. Section VI reviews FDA applications across major radar task families, including parameter estimation, target detection, anti-jamming, LPI radar, imaging, and target tracking. Section VII extends the discussion to communication and integrated sensing and communication (ISAC) systems, with particular emphasis on physical-layer security, index modulation, and FDA-enabled ISAC architectures. Section VIII discusses current limitations, common misconceptions, and future research directions. Finally, Section IX concludes the paper.

## II. The Evolution of the FDA

This section aims to clarify how the FDA evolves from conventional array architectures and why it should be regarded as an independent array paradigm rather than a minor variation of phased arrays or MIMO radar. To this end, we first establish a unified modeling starting point based on a uniform linear array (ULA), and then compare the array-factor structures and effective degrees of freedom of PA, MIMO, FDA, and FDA–MIMO. Building on this framework, we further clarify the distinct role of frequency in FDA as compared with conventional frequency-domain mechanisms such as FDMA and OFDM, and discuss two representative implementation routes for FDA–MIMO. Finally, this unified perspective naturally leads to an open structural question: once range has entered the array manifold through frequency-induced phase gradients, is the conventional pulse-compression-based treatment of the range dimension still indispensable, or should FDA motivate a different view of range processing?

We begin with the standard transmit model of a ULA, which serves as the common reference for all subsequent developments. Consider a ULA with  $M$  transmit antenna elements and  $d_T = \lambda/2$  inter-element spacing, as shown in Fig. 3. The signal transmitted by the  $m$ -th antenna is written as

$$x_m(t) = A_m e^{j(2\pi f_c t + \phi_o)}, \quad (1)$$

where  $A_m$  and  $\phi_m$  are the amplitude and phase applied to the signal transmitted by the  $m$ -th element, respectively, while  $f_c$  is the carrier frequency. The position of the  $m$ -th antenna relative to the reference antenna located at the origin can be found as

$$d_m = m d_T, \quad m = 0, 1, \dots, M-1. \quad (2)$$

Under the far-field approximation, the wavefront observed at a distant point can be approximated as planar. Accordingly, for a target located at range  $R_o$  and direction  $\theta$  with respect to the reference antenna (the rightmost element), the propagation distance associated with the  $m$ -th element is given by

$$R_m = R_o + m d_T \sin \theta. \quad (3)$$

The propagation delay associated with the  $m$ -th element is given by

$$\tau_m(\theta) = \frac{R_o + m d_T \sin \theta}{c}, \quad (4)$$

where  $c$  denotes the speed of light. The contribution of the  $m$ -th antenna element at the target is given by

$$r_m(t, \theta) = A_m e^{j(2\pi f_c (t - \tau_m(\theta)) + \phi_o)},$$

Aggregating the contributions from all transmit antenna elements, the received signal can be expressed as

$$\begin{aligned} r(t, \theta) &= \sum_{m=0}^{M-1} A_m e^{j(2\pi f_c (t - \tau_m(\theta)) + \phi_o)}, \\ &= \sum_{m=0}^{M-1} A_m e^{j(2\pi f_c t - 2\pi \frac{R_o}{\lambda} + \phi_o)} e^{-j2\pi \frac{m d_T \sin \theta}{c}}. \end{aligned} \quad (5)$$

For the given value of  $R_o$ , the amplitude of the overall received signal depends on the angular location  $\theta$ . This angular dependence forms the basis for directional transmission using controlled phase excitation across the array elements.

### A. Phased Array Beam Steering

A uniform linear array can operate as a phased array when a controlled phase shift is applied across its antenna elements as shown in Fig. 4. By properly selecting the excitation phases, the radiated signals from different elements combine constructively in a desired direction and destructively in other directions. This enables electronic steering of the main beam without physically rotating the array. With these pre-compensated phases, the transmitted signal from the  $m$ -th antenna element can be expressed

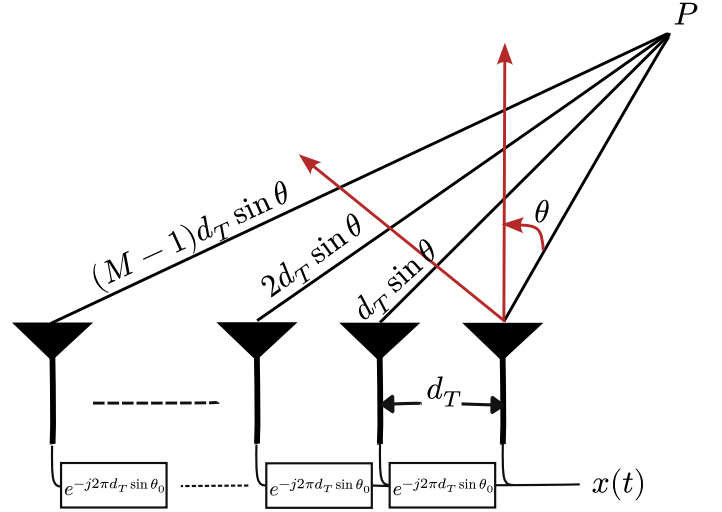


Fig. 4: In phased-array, the progressive phase shifts across antenna elements steer the beam in the direction  $\theta_0$ .

as

$$x_m(t) = A_m e^{j(2\pi f_c t + 2\pi f_c \frac{d_m \sin \theta_o}{c} + \phi_o)}.$$

The relative phase of the transmit signal from the  $m$ -th antenna element is then

$$\phi_m(t, \theta) = 2\pi f_c \frac{d_m \sin \theta_o}{c}.$$

Accordingly, the combined received signal from all transmit antenna elements at point  $P$  is given by

$$r(t, \theta) = e^{j2\pi(f_c t - \frac{R_o}{\lambda})} \sum_{m=0}^{M-1} \tilde{A}_m e^{j2\pi f_c (\frac{d_m \sin \theta_o}{c} - \frac{d_m \sin \theta}{c})}, \quad (6)$$

where  $\tilde{A}_m = A_m e^{j\phi_o}$ . The term inside the summation defines the array factor, which governs the directional radiation pattern of the phased array:

$$\text{AF}(\theta) = \sum_{m=0}^{M-1} \tilde{A}_m e^{j2\pi f_c (\frac{d_m \sin \theta_o}{c} - \frac{d_m \sin \theta}{c})}. \quad (7)$$

Therefore, by controlling the excitation phases  $\theta_o$ , the array radiation can be focused toward the intended direction  $\theta_0$ . However, despite this beam-steering capability, a conventional phased array exhibits a radiation pattern that is solely angle-dependent in the far field and does not provide range-dependent focusing. This angle-only dependence limits the capability of phased arrays in applications requiring joint range and angle localization.

### B. Frequency Diverse Array

To overcome the angle-only limitation of the phased array, the FDA extends the phased-array concept by introducing small frequency increments across the transmitting elements, resulting in a beampattern that depends on both range and angle. In an FDA system, the carrier frequency

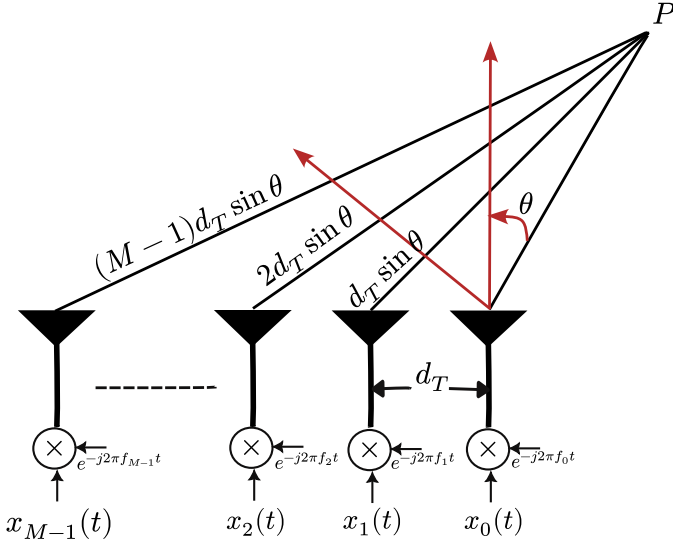


Fig. 5: In an FDA, each antenna element slightly offset the carrier frequency.

of the  $m$ -th antenna element is defined as [122]

$$f_m = f_c + \Delta f_m, \quad m = 0, 1, \dots, M-1, \quad (8)$$

where  $\Delta f_m$  represent the frequency offset of the  $m$ -th antenna. The offset frequency can vary linearly, for example  $\Delta f_m = m f_a$ , or it can be assigned independently for each antenna element. Assuming  $\Delta f_m \ll f_c$ , the phase term of the received signal associated with the signal transmitted from the  $m$ th antenna can be written as [84], [123], [124]

$$\phi_m^{\text{FDA}}(t, R_o, \theta) = 2\pi \left( \Delta f_m t - \Delta f_m \frac{R_o}{c} - f_c \frac{d_m \sin \theta}{c} \right).$$

This leads to the array factor (AF)

$$\text{AF}(t, R_o, \theta) = \sum_{m=0}^{M-1} e^{j\phi_m(t, R_o, \theta)}. \quad (9)$$

In the PA case, we only have the spatial phase term, whereas FDA additionally introduces two phase components that are linear in both time and range. In particular, the terms  $\Delta f_m t$  and  $-\Delta f_m \frac{R_o}{c}$  introduce phase variations with respect to  $t$  and  $R_o$ , respectively. These terms induce controllable phase gradients whose slopes are directly governed by the frequency offset  $\Delta f_m$ . Consequently, unlike phased arrays, FDA systems inherently couple time and range through a common parameter, enabling joint control of the spatio-temporal-range response within the array manifold.

Under the unified model given in (9), different array paradigms can be distinguished by how the design-variable space is expanded or constrained. In simple terms, the more adjustable parameters, or degrees of freedom (DoFs), an array has, the greater its flexibility in controlling the beam pattern across different domains. In the following, we discuss the beam patterns of several representative antenna array configurations:

a) Phased-Array: Spatial-Phase Driven. When  $\Delta f_m = 0$ , the propagation-induced phase across the transmit aperture reduces to a purely spatial term, namely

$$\phi_m^{\text{PA}}(\theta) = -2\pi f_c \frac{d_m \sin \theta}{c}, \quad (10)$$

which depends only on the angular variable [125], [126]. Therefore, the effective DoFs arise exclusively from spatial phase steering,

b) FDA: Frequency-gradient driven. When  $\Delta f_m \neq 0$ , the element-dependent carrier  $f_m$  yields an additional time-range phase gradient [19], [20], [22], [127], i.e.,

$$\phi_m^{\text{FDA}}(t, R, \theta) = \phi_m^{\text{PA}}(\theta) + 2\pi \Delta f_m t - 2\pi \Delta f_m \frac{R}{c}. \quad (11)$$

The second and third terms constitute explicit time and range phase gradients across the aperture, fundamentally altering the interference structure formed during propagation.

As a result, the system DoFs expand to

$$\text{DoF}_{\text{FDA}} = \text{Space} \oplus \text{Frequency}. \quad (12)$$

c) MIMO: Waveform-Orthogonality Driven. Consider a MIMO system with  $M$  transmit antennas and  $N$  receive antennas. The  $m$ th transmit element radiates an orthogonal baseband waveform  $x_m(t)$  at a common carrier frequency  $f_c$  (i.e., no frequency gradient is applied). Let  $d_n^{\text{R}}$  and  $d_m^{\text{T}}$  denote the locations of the  $n$ th receive and  $m$ th transmit antenna elements from the reference transmit and receive antennas, respectively. For a colocated Tx/Rx array with element locations  $\{d_n^{\text{R}}\}$  and  $\{d_m^{\text{T}}\}$ , define the virtual position  $d_{n,m}^{\text{V}} \triangleq d_m^{\text{T}} + d_n^{\text{R}}$ , and the corresponding virtual phase as the propagation-kernel phase associated with  $(m, n)$ .

Under the narrow-band far-field approximation, the received signal at the  $n$ -th receive channel can be written as [128]

$$y_n(t) = \sum_{m=0}^{M-1} \alpha x_m(t - \tau) e^{-j2\pi f_c \frac{d_{n,m}^{\text{V}} \sin \theta}{c}} + w_n(t), \quad (13)$$

where  $\tau = 2R/c$  and  $\alpha$  collects the scattering and propagation coefficients and  $w_n(t)$  represents noise term. By matched filtering with  $x_m(t)$  (waveform separability), one obtains the  $m$ -th virtual channel [129], [130]

$$z_{n,m} \triangleq \int y_n(t) x_m^*(t - \tau) dt \approx \alpha e^{-j2\pi f_c \frac{d_{n,m}^{\text{V}} \sin \theta}{c}}, \quad (14)$$

which exhibits the standard Tx-Rx separable spatial phase (virtual array) at a single carrier. Hence, the phase term of MIMO can be expressed as

$$\phi_{n,m}^{\text{MIMO}}(\theta) = -2\pi f_c \frac{d_{n,m}^{\text{V}} \sin \theta}{c}, \quad (15)$$

with  $\text{DoF}_{\text{MIMO}} = \text{Space} \oplus \text{Waveform}$ . Further, we have the compact virtual array factor [131], [132]

$$\text{AF}_{\text{MIMO}}(\theta) \triangleq \sum_{n=0}^{N-1} \sum_{m=0}^{M-1} e^{-j2\pi f_c \frac{d_{n,m}^V \sin \theta}{c}}. \quad (16)$$

This explicitly shows that MIMO expands DoF via the virtual aperture  $\{d_{n,m}^V\}$ , i.e.,  $\text{Space}_{\text{Tx}} \oplus \text{Space}_{\text{Rx}}$ .

d) FDA-MIMO: Composite Expansion. If an frequency coding is further imposed across transmit elements, while maintaining waveform orthogonality  $\{x_m(t)\}$ , then the received signal becomes [133]

$$y_n(t) = \sum_{m=0}^{M-1} \alpha x_m(t - \tau) e^{-j2\pi \frac{\Delta f_m}{c} R} \times e^{j2\pi \Delta f_m t} e^{-j2\pi f_c \frac{d_{n,m}^V \sin \theta}{c}} + w_n(t). \quad (17)$$

After matched filtering with  $x_m(t)$ , the  $m$ -th virtual channel is (up to a constant scaling) [134]

$$z_{n,m} \approx \alpha e^{j2\pi \Delta f_m t} e^{-j2\pi \frac{\Delta f_m}{c} R} e^{-j2\pi f_c \frac{d_{n,m}^V \sin \theta}{c}}. \quad (18)$$

Therefore, the composite phase structure can thus be written as

$$\phi_{n,m}^{\text{FDA-MIMO}}(t, R, \theta) = 2\pi f_c \frac{d_{n,m}^V \sin \theta}{c} + 2\pi \Delta f_m t - 2\pi \frac{\Delta f_m}{c} R,$$

where the DoF are determined by the combined contributions of spatial, frequency, and waveform domains:

$$\text{DoF}_{\text{FDA-MIMO}} = \text{Space} \oplus \text{Frequency} \oplus \text{Waveform}. \quad (19)$$

Accordingly, the compact virtual FDA array factor is

$$\text{AF}_{\text{FDA-MIMO}}(t, R, \theta) \triangleq \sum_{n=0}^{N-1} \sum_{m=0}^{M-1} e^{j\phi_{n,m}^{\text{FDA-MIMO}}(t, R, \theta)}. \quad (20)$$

#### Remark 1: Alignment with the Unified AF in (9)

- The AF expressions of MIMO and FDA-MIMO follow a mathematical form similar to that of FDA.
- In contrast to PA and FDA, MIMO introduces a virtual array that effectively enlarges the aperture, thereby improving spatial (angular) resolution.
- FDA-MIMO further exploits  $\Delta f_m$  to induce time- and range-dependent phase gradients, in addition to the virtual aperture.

This taxonomy underscores that the FDA is neither a special case of MIMO radar nor a simple variant of PA radar. Instead, it represents an independent paradigm that extends the array manifold through frequency gradients.

To illustrate the distinctions among these paradigms, we present a comparative simulation. Fig. 6 depicts the range-angle array factors of PA, FDA, MIMO, and FDA-MIMO systems. In all cases, the spacing between adjacent

antenna elements at both the transmitter and receiver is set to  $d_T = d_R = \frac{\lambda}{2}$ . The results reveal that PA and MIMO exhibit range-invariant behavior, as their phase structures depend exclusively on spatial variables. While MIMO enhances the effective aperture through waveform separation and virtual-array synthesis, it does not introduce transmit-side range dependence, since its phase structure remains purely spatial after matched filtering. In contrast, the FDA and FDA-MIMO configurations inherently incorporate range-dependent phase terms due to their frequency-diverse transmissions, leading to tilted interference contours.

Fig. 7 further examines the angular array factor at a fixed range-time slice, offering deeper insight into the DoF governing each paradigm. The results demonstrate that waveform-driven DoF predominantly enhance angular resolution, as they exploit spatial diversity to sharpen the beam pattern. In contrast, frequency-driven DoF fundamentally reshape the propagation-induced interference structure, introducing range-dependent phase variations that enable joint range-angle processing. This distinction underscores the complementary roles of waveform and frequency diversity in FDA-based systems, where the interplay between spatial, frequency, and waveform domains unlocks unique operational capabilities. These observations confirm that the fundamental distinction among array paradigms lies in their propagation-kernel structure.

#### C. Design Variables and DoF: A Physical-Layer Criterion vs. Equivalent-Layer Phenomena

Before examining whether FDA introduces an additional physical DoFs, it is necessary to clarify that the notion of ‘‘frequency diversity’’ has been used in conceptually different ways in the literature.

In some architectures [11]–[14], frequency serves merely as a signal-separation mechanism or an indexing resource, without altering the propagation structure. In contrast, FDA embeds element-dependent frequency offsets directly into the propagation kernel, thereby modifying the range-dependent phase progression itself. Confusing these roles may lead to interpreting equivalent processing-level effects as genuine physical-layer DoF expansion. Therefore, from a signal-processing perspective, frequency can play fundamentally different roles in system design, i.e.,

- Frequency gradient (FDA):  $\Delta f_m$  remains in the propagation-kernel phase and induces inter-channel range-phase-gradient differences. The gradient exists before reception and shapes the interference pattern during propagation.
- Frequency-domain orthogonality (FDMA-style separation): frequency is used solely for channel separation. The propagation kernel is effectively shared at  $f_c$ , and no inter-channel range-gradient difference is introduced.
- Subcarrier structure (e.g., OFDM): frequency acts as an indexing resource for modulation and multiplexing. Although multi-frequency components are

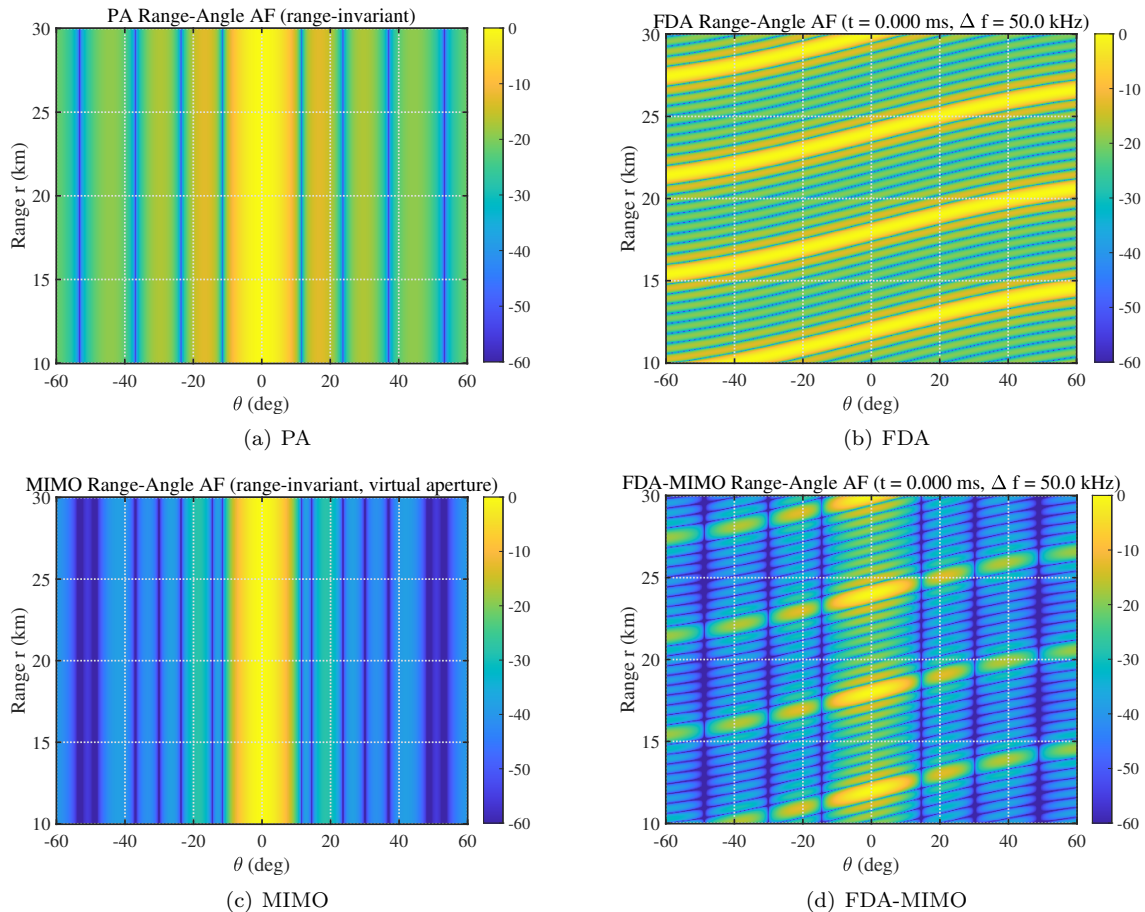


Fig. 6: Range-angle response comparison based on the corresponding array-factor formulations of four array paradigms. PA and MIMO remain range-invariant, whereas FDA introduces range-angle coupling, and FDA-MIMO combines coupling with virtual aperture expansion.

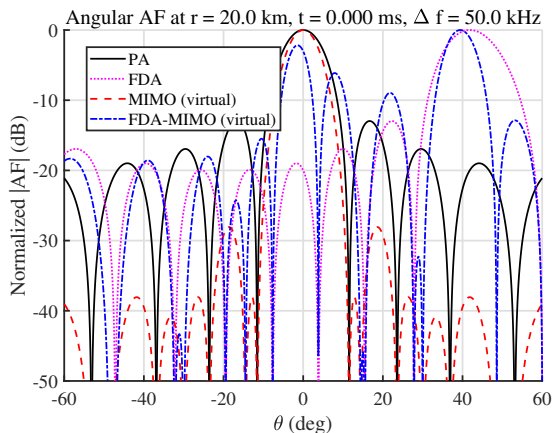


Fig. 7: Angular AF comparison at a fixed range-time slice.

present, they do not necessarily induce element-dependent range-phase gradients.

The above distinction highlights that frequency-driven behavior may arise either from propagation physics or from signal-level multiplexing, and these two mechanisms are fundamentally different in terms of DoF interpretation.

1) Physical Range DoF: A Reducibility/Irreducibility Criterion: The range-dependent component of the propagation kernel for the  $m$ -th channel is

$$e^{-j2\pi(f_c + \Delta f_m) \frac{R_m}{c}}. \quad (21)$$

Define the range-phase gradient of each channel as

$$\nabla_{R_m} \phi_m = -2\pi(f_c + \Delta f_m)/c. \quad (22)$$

All channels share the common baseline gradient  $-2\pi f_c/c$ , similar to PA. However, FDA introduces additional inter-channel gradient differences given by

$$\nabla_{R_m} \phi_m - \nabla_{R_n} \phi_n = -2\pi \frac{\Delta f_m - \Delta f_n}{c}. \quad (23)$$

If  $\nabla_{R_m} \phi_m \neq \nabla_{R_n} \phi_n$  for  $m \neq n$ , the propagation exhibits a multi-gradient structure. This leads to a fundamental question:

Do these additional gradients represent a genuine physical DoF created during wave propagation, or can they be completely removed through independent per-channel linear compensation at the receiver?

Definition 1 (Physical Range DoF – Reducibility Criterion): If there exists a set of operators  $\{\mathcal{L}_m\}$ , one for

each channel  $m$ , such that for all  $R_m$ ,

$$\mathcal{L}_m \left\{ e^{-j\frac{2\pi}{c}(f_c + \Delta f_m)R_m} \right\} = e^{-j\frac{2\pi}{c}f_c R_m}, \quad \forall m, \quad (24)$$

then the system is reducible (or DoF free). Otherwise, if no such operator exist, the system has irreducible physical DoF.

For FDA architectures in which the frequency offsets remain embedded in the propagation kernel and jointly affect the received superposition across channels, per-channel compensation operators generally do not exist without altering the multi-channel interference structure. This is because the additional range-phase gradients are formed prior to reception through wave propagation, thereby shaping the interference geometry itself. Consequently, such gradients constitute an irreducible physical range DoF.

FDA becomes reducible only under degenerate conditions, such as when all frequency offsets are identical, or when compensation is tailored to a single known range point. In general multi-range scenarios, however, the element-dependent range-phase gradients introduce propagation-structural differences that cannot be eliminated by independent per-channel linear operations. In essence, FDA is reducible only when its frequency offsets do not induce inter-channel range-phase curvature differences over the scene of interest.

Hence, the reducibility criterion serves as a physics-grounded boundary that separates true propagation-level DoF creation from equivalent processing-layer reformulation.

#### Remark 2: Physical vs. Equivalent Processing Layer

- The reducibility criterion emphasizes that system taxonomy should be determined by the structure of the propagation kernel, rather than by post-reception signal manipulation. Even if the receiver implements channel-wise compensation, the interference structure has already been formed during propagation.
- Frequency-driven behavior is fundamentally a property of wave physics, not merely a processing-level artifact. The essence of physical DoF lies in whether a dimension is created during propagation, not whether it can be algebraically removed afterward.
- The reducibility criterion provides a physics-grounded boundary between genuine DoF expansion and equivalent signal reparameterization.

#### D. The Answers to Three Major Structural Debates

1) Taxonomy of FDA-MIMO – Orthogonal-Waveforms vs. Orthogonal-Frequency realizations: From a system-design perspective, FDA-MIMO architectures can be more naturally categorized according to how channel

orthogonality is achieved, namely through waveform orthogonality or frequency orthogonality. This classification is particularly relevant for FDA-MIMO, since the orthogonalization strategy not only determines the receiver processing architecture, but also affects whether the propagation-induced range-phase gradients are preserved, suppressed, or re-synthesized in the final range-angle response. Eq.(11) shows that the range-dependent component  $-2\pi\Delta f_m \frac{R_0}{c}$  represents the FDA-induced range-phase gradient. Although this gradient is always embedded in the propagation kernel, its manifestation in the final system response depends strongly on the adopted orthogonality mechanism.

a) Type I - Waveform-Orthogonal FDA-MIMO: In waveform-orthogonal FDA-MIMO, the transmit channels are separated by orthogonal waveforms while the element-dependent carrier offsets remain jointly embedded in the propagation field. As a result, the FDA-induced range-phase gradients coexist during propagation and physically contribute to the transmitted radiation pattern. Therefore, the range-angle coupling is directly preserved in the common propagation field, and the resulting FDA behavior is observed without requiring cross-band reconstruction at the receiver.

b) Type II - Frequency-Orthogonal FDA-MIMO (FDMA Realization): In frequency-orthogonal FDA-MIMO, the frequency offsets are chosen such that the transmitted spectra occupy non-overlapping subbands, for example under FDMA-style multiplexing with  $\Delta f = B$ , where  $B$  is the bandwidth. The transmitted signals are therefore orthogonal in frequency and can be separated at the receiver. Importantly, the element-dependent carrier frequencies  $f_m$  remain embedded in the propagation kernel. Consequently, the radiated field during propagation still exhibits range-angle coupling and forms the characteristic FDA slanted interference structure. However, unlike waveform-orthogonal FDA-MIMO, the final range-angle response is no longer determined solely by propagation. Instead, it depends on how the separated subbands are processed at the receiver.

- Independent Subband Processing. Each frequency channel is matched-filtered (MF) and beamformed independently. In this case the cross-channel phase gradients are not coherently combined, and the system behavior reduces to that of a conventional MIMO radar with virtual spatial aperture expansion.
- Coherent Multiband Synthesis. If the separated subbands are phase-aligned and coherently combined across frequency, the propagation-induced gradients can be jointly exploited. The resulting array response forms a range-dependent virtual beam pattern analogous to that of propagation-coupled FDA structures.

Therefore, frequency-orthogonal FDA-MIMO remains an FDA system at the propagation level, but its final range-angle behavior depends on whether the receiver performs independent subband processing or coherent cross-band synthesis.

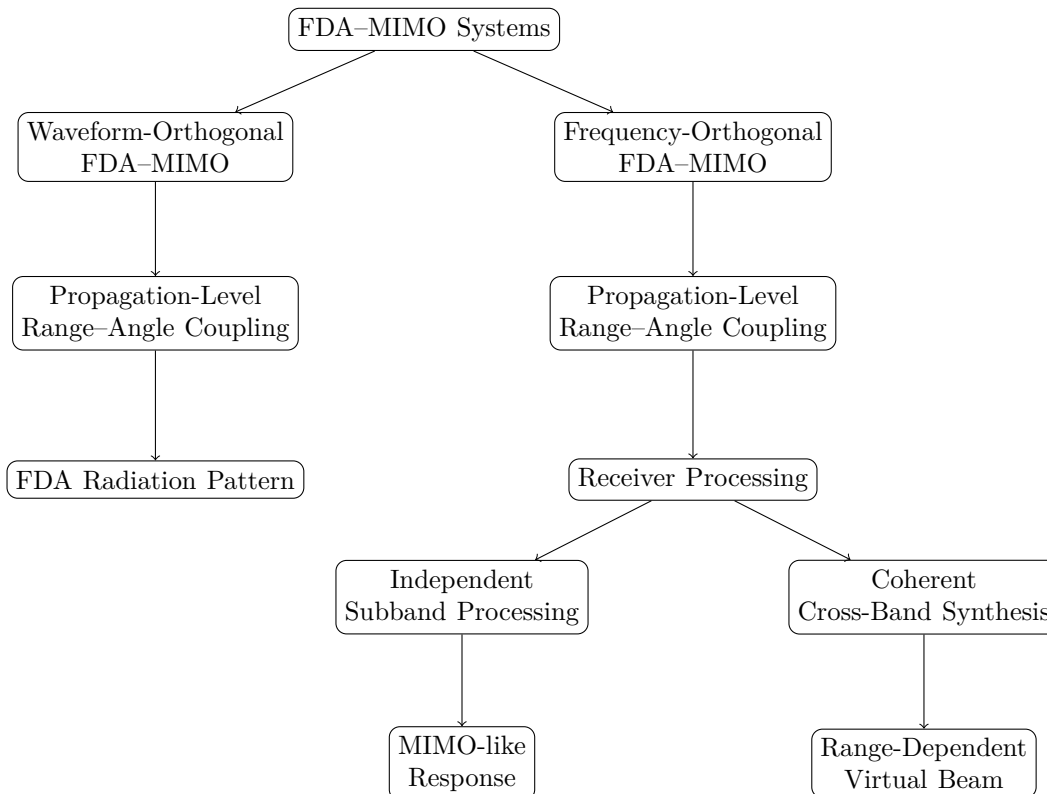


Fig. 8: Taxonomy of FDA-MIMO architectures based on the orthogonality mechanism used to separate transmit channels. Both waveform-orthogonal and frequency-orthogonal FDA-MIMO preserve propagation-level range-angle coupling due to element-dependent carrier offsets. However, in frequency-orthogonal FDA-MIMO the final system response depends on the receiver processing strategy, which may either suppress or exploit the propagation-induced gradients.

The above discussion leads to a conceptual taxonomy of FDA-MIMO architectures, as illustrated in Fig. 8. The classification is based on the orthogonality mechanism used to separate the transmit channels, namely waveform orthogonality and frequency orthogonality. In waveform-orthogonal FDA-MIMO, the element-dependent carrier offsets coexist within a common propagation field, leading to propagation-coupled range-angle interference patterns. In contrast, frequency-orthogonal FDA-MIMO separates the channels spectrally. Although the propagation field still retains the same range-phase gradients, the final range-angle behavior depends on the receiver processing strategy.

To further illustrate the mechanism of frequency-orthogonal FDA-MIMO, Fig. 9 visualizes the propagation field and the corresponding receiver responses under different processing strategies. During propagation, the transmitted field still exhibits the characteristic FDA slanted range-angle interference structure, as shown in Fig. 9(a). If each subband is processed independently, the cross-band gradients are not combined and the resulting response reduces to a conventional MIMO virtual aperture pattern, as shown in Fig. 9(b). In contrast, when coherent cross-band synthesis is performed, the propagation-induced gradients are jointly exploited and a range-dependent

virtual beam is formed, as illustrated in Fig. 9(c).

**Key Insight:** FDA range-angle coupling is fundamentally a propagation phenomenon, while the orthogonality mechanism determines whether the resulting gradients are directly observed or reconstructed through receiver processing.

2) Range-Angle coupling: Redundancy or DoF?: Range-angle coupling [135], [136] arises from the superposition of frequency-gradient terms across the transmit aperture. In conventional PA processing frameworks, where range and angle are typically assumed to be separable parameters, such coupling is often regarded as undesirable. Its practical value, however, depends strongly on the processing framework adopted by the system:

- **Redundancy Viewpoint:** If one insists on PA-style “separable-parameter” processing [6], range-angle coupling manifests as estimation difficulty, beam distortion, and defocusing.
- **DoF Viewpoint:** If joint  $(R_0, \theta)$  filtering, compensation, or coding is employed, the same coupling structure can be exploited to enable range-selective beamforming [137]–[139], interference suppression [140], [141], and ambiguity-function shaping [47], [142], [143].

Therefore, range-angle coupling is neither inherently

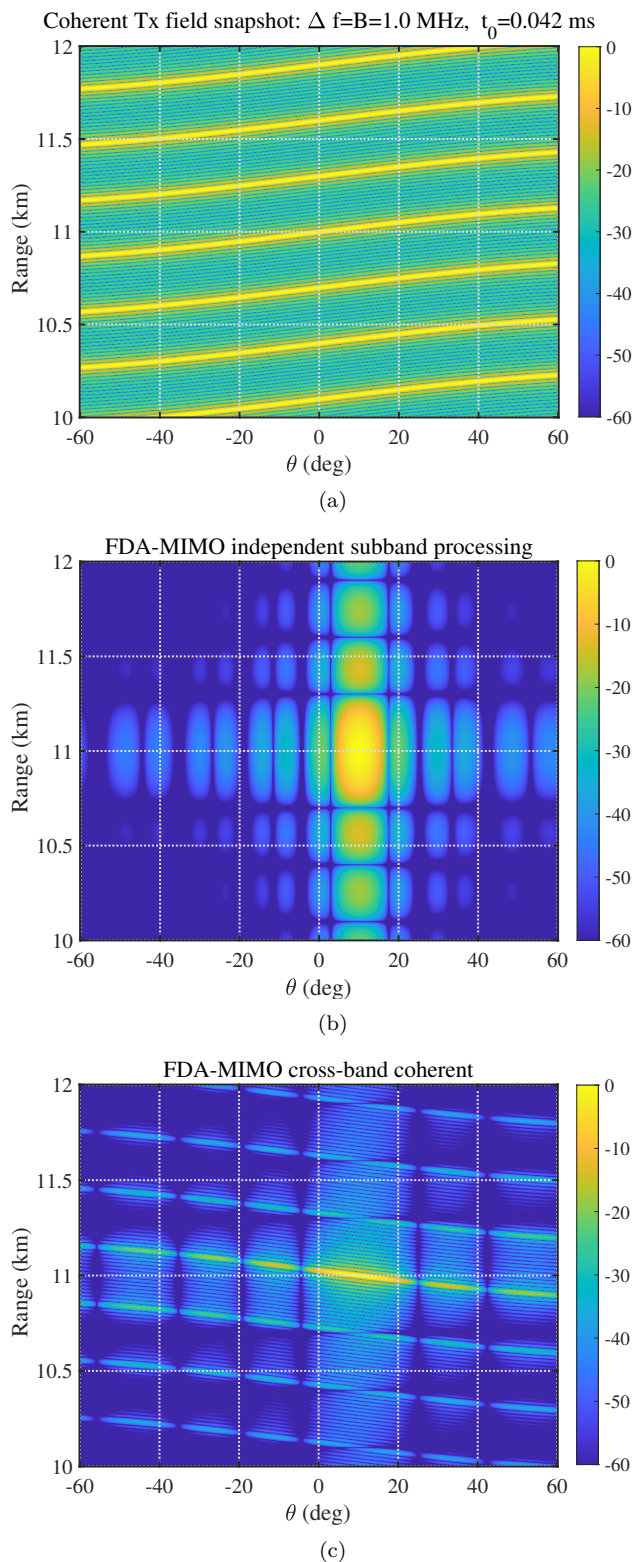


Fig. 9: Mechanism of frequency-orthogonal FDA-MIMO. (a) During propagation the transmitted field still exhibits FDA-type range-angle coupling for an LFM waveform. (b) Independent subband processing leads to a conventional MIMO-like virtual aperture pattern. (c) Coherent cross-band synthesis jointly exploits the propagation-induced gradients and produces a range-dependent virtual beam.

beneficial nor detrimental. Rather, it represents a structured degree of freedom in the range-angle response whose value becomes explicit only under an appropriate joint processing framework.

3) Time-Invariant Spatial Focusing: Physical Infeasibility and “Equivalent Focusing”: At the physical-field or transmit-array-factor level, the FDA response contains an explicit time gradient, i.e.,

$$\nabla_t \phi_m = 2\pi \Delta f_m. \quad (25)$$

Hence, as long as  $\Delta f_m \neq 0$  for some  $m$ ,  $AF(t, R_0, \theta)$  is intrinsically time-varying [95], [144]. The “time-invariant focusing” reported in much of the literature [50], [51], [145]–[149] typically corresponds to two equivalent implementations, namely

- Instantaneous Focusing: achieving local focusing at a particular time instant within a finite time window (or under pulsed operation);
- Post-Processing Equivalent Focusing: constructing a stable peak in the output domain via matched filtering/phase compensation at the receiver.

Because the range gradient and the time gradient originate from the same frequency-offset term, any attempt to remove time variation at the physical-field level would generally suppress the associated range-gradient effect as well, thereby driving the structure toward PA-like degeneration. Therefore, strictly time-invariant spatial focusing at the physical-field level is incompatible with the FDA mechanism. Instead, the time-varying structure should be regarded as an intrinsic feature of FDA arrays and exploited to enhance detection, estimation, and interference suppression.

#### E. A Forward-Looking Answer: Reinterpreting Coherent FDA Beyond Pulse Compression

The above discussions also suggest a potentially important re-evaluation of coherent FDA. Under the conventional pulse-compression framework, coherent FDA is often regarded as difficult to process, since the element-dependent carrier offsets may produce misaligned compressed responses and multiple nonuniform range peaks across channels, as shown in Fig. 10. From this viewpoint, coherent FDA appears incompatible with the standard delay-domain ranging pipeline.

However, this apparent difficulty may stem less from the FDA mechanism itself than from the long-standing assumption that distance must first be recovered through conventional pulse compression. If range in FDA/FDA-MIMO is no longer interpreted exclusively as a delay-domain quantity, but instead as an irreducible parameter embedded in the propagation manifold, then coherent FDA may become a much more meaningful architecture. In that case, its propagation-level phase coupling and coherent field gain need not be treated as processing obstacles, but rather as exploitable structural resources. This perspective opens the possibility of a manifold-based processing framework for coherent FDA. Instead

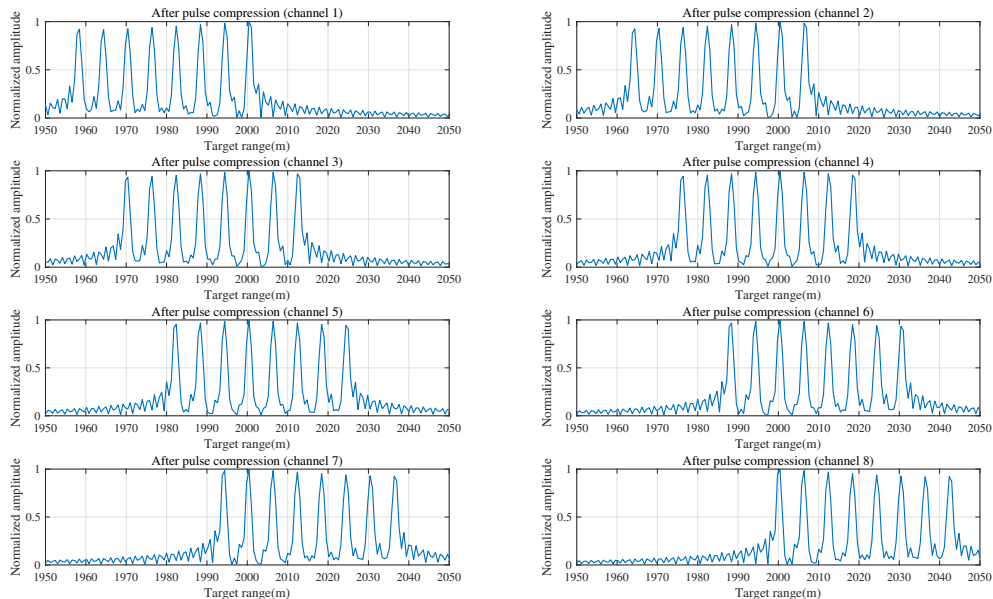


Fig. 10: Pulse-compression outputs for different channels in a coherent FDA system. Because each transmit element operates at a different carrier frequency, conventional pulse compression produces multiple peaks and nonuniform range alignment across channels.

of forcing the received signals into a conventional pulse-compression pipeline, one may directly exploit the joint time–range–angle response through manifold matching, coherent hypothesis testing, joint parameter estimation, or structure-aligned focusing. Under such a viewpoint, coherent FDA may offer a form of coherent gain that is not fully captured by traditional delay-domain processing.

Therefore, an important open question is whether the true value of coherent FDA has been partially obscured by the classical pulse-compression paradigm. Revisiting coherent FDA from a manifold-based ranging and detection perspective may provide a new avenue for unlocking its physical advantages and clarifying its role within future FDA/FDA–MIMO systems.

### III. Fundamental Design Dimensions of FDA: From Mechanism to Structural Abstraction

Having established the propagation-kernel-based taxonomy in the previous section, we now examine the fundamental properties of FDA from an array-manifold perspective. The goal of this section is not simply to enumerate several characteristic FDA phenomena, but to show that they originate from a common structural mechanism: the frequency gradient across the transmit aperture reshapes the array manifold and enlarges the set of controllable dimensions of the radiated field. Under this viewpoint, time variability, beam scanning, and range–angle coupling are direct manifestations of the same underlying expansion, while the integrated transmit beampattern, the ambiguity function, and the scattering response can be understood as higher-level consequences

of this altered manifold structure. This mechanism-to-property perspective helps connect the basic physical behavior of FDA with its broader implications for sensing, imaging, and communication applications.

In conventional phased arrays (PAs), the radiated response depends only on the angular variable, which can be represented as  $\mathcal{A}_{\text{PA}}(\theta)$ . By contrast, FDA introduces element-dependent carrier frequencies, so that the array response becomes a joint function of time, range, and angle,  $\mathcal{A}_{\text{FDA}}(t, R_0, \theta)$ . This expansion from an angle-only response to a time–range–angle-dependent manifold is the fundamental structural distinction between FDA and conventional arrays. We begin with time variability, which is the most immediate consequence of this additional manifold dimension.

#### A. Time Variability as Manifold Expansion

Introducing a frequency gradient  $\Delta f$  fundamentally alters the structure of the array manifold. Unlike conventional PA, whose array responses are independent of time, the FDA manifold explicitly includes time as an intrinsic dimension. Fig. 11 illustrates the fundamental difference between PA and FDA in the range–time plane. For PA, the beam pattern remains stationary because the array response depends only on angle. In contrast, the element-dependent frequency offsets in FDA introduce intrinsic time–range coupling, causing the constructive-interference ridge to propagate along the range direction as time evolves.

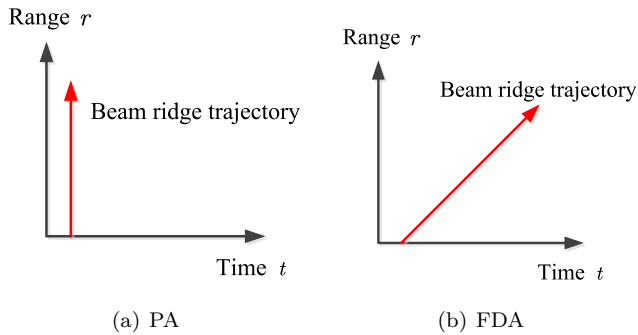


Fig. 11: Comparison of beam behavior in FDA and PA in the range–time plane. The PA beam remains spatially stationary, whereas the FDA beam forms a propagating constructive-interference ridge that moves along the range direction as time increases.

Under far-field conditions, the trajectory of the FDA mainlobe can be approximately described by

$$R_0 = ct - \ell \frac{c}{\Delta f} + \left(1 + \frac{f_c}{\Delta f}\right) d_T \sin \theta, \quad (26)$$

where  $R_0$  is the range,  $t$  is time,  $c$  is the speed of light,  $d_T$  is the transmit element spacing,  $\theta$  is the observation angle, and  $\ell$  denotes the beam index associated with different propagation ridges. This expression reveals an important physical insight: the FDA beam ridge propagates approximately at the speed of light along the range direction. Therefore, the FDA beam pattern is intrinsically time-varying rather than spatially stationary. The above analytical result is further illustrated in Fig. 12.

Because of this inherent beam evolution, many studies have attempted to synthesize time-invariant FDA beam-patterns. One line of research introduces time-varying frequency offsets to compensate for the beam drift. Khan et al. [150] proposed such a time-varying frequency offset strategy. Another line of work relies on time-modulated frequency design. Yao et al. [151] introduced a time-modulated frequency offset scheme for time-invariant spatial focusing, and further extended it to multi-time focusing [152] and near-range multi-point focusing scenarios [153]. In addition, array-structure-based solutions have also been explored. Cheng et al. [146] proposed an array pointing modulation approach, while Yang et al. [52] developed a time-invariant beamforming method based on sparse frequency diverse arrays [154].

Nevertheless, from a physical viewpoint, the time-varying characteristic of FDA beams originates from the outward propagation of electromagnetic energy. Hence, such approaches may reshape or compensate the beam-pattern at selected instants, but they cannot fundamentally force the beam peak to remain permanently at a fixed range. Therefore, the time variability of FDA should not be regarded as a mere modulation artifact. Rather, it is a structural consequence of manifold expansion from the spatial response  $\mathcal{A}_{\text{PA}}(\theta)$  to the joint time–range–angle response  $\mathcal{A}_{\text{FDA}}(t, r, \theta)$ .

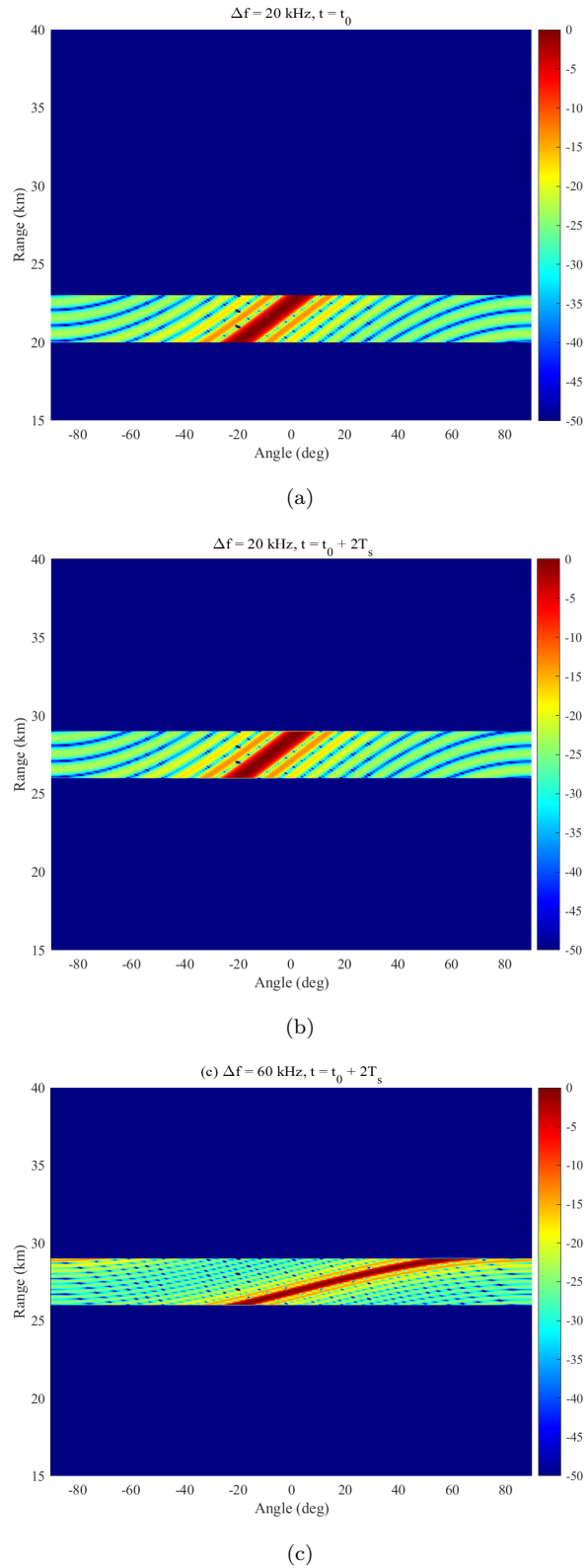


Fig. 12: Time evolution of the FDA transmit beam-pattern under different frequency increments. For a fixed  $\Delta f$ , the mainlobe ridge shifts toward farther ranges as time increases. A larger  $\Delta f$  further strengthens the range–angle–time coupling and changes the ridge trajectory.

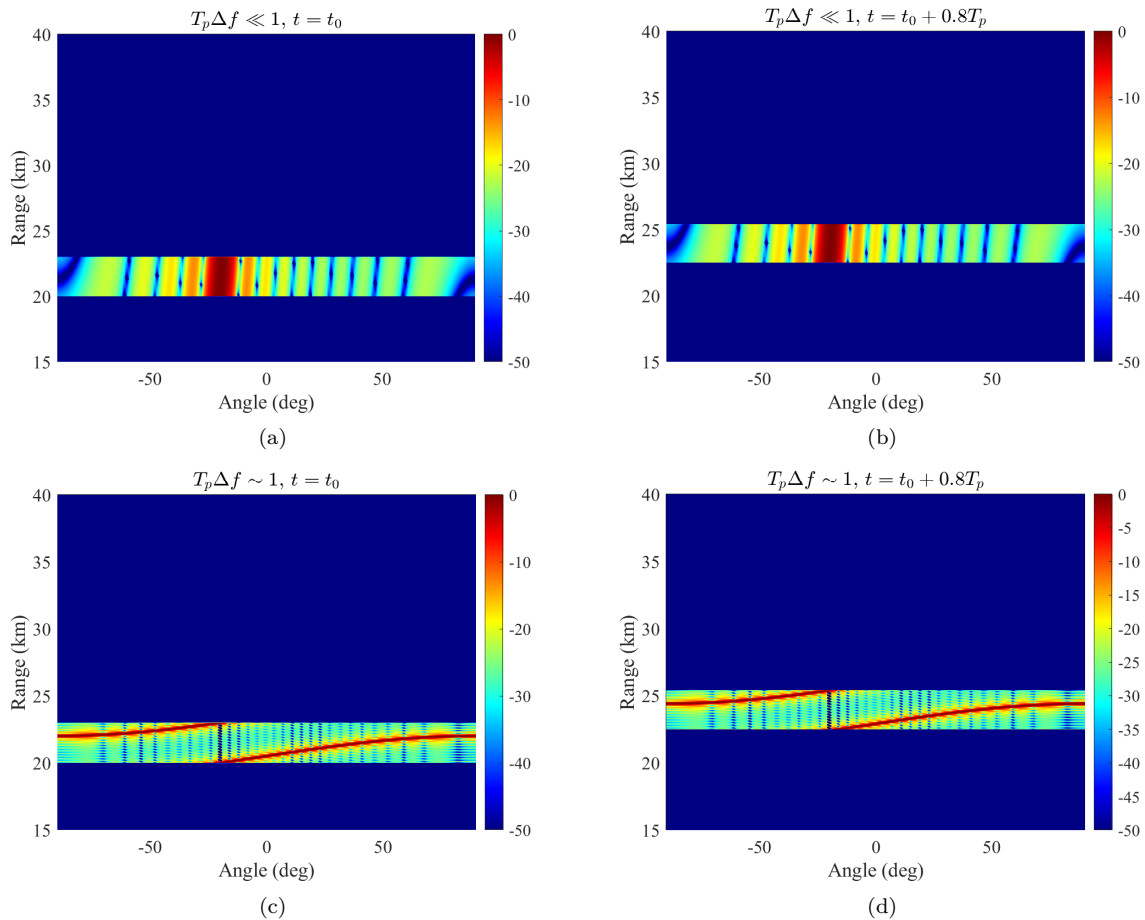


Fig. 13: Illustration of two FDA operating regimes determined by the product  $T_p \Delta f$ . When  $T_p \Delta f \ll 1$ , the beam pattern remains approximately unchanged within a pulse. When  $T_p \Delta f \sim 1$ , the mainlobe ridge evolves significantly within the same pulse duration, resulting in noticeable beam scanning.

## B. Frequency Gradient and Scanning Mechanism

The automatic beam scanning behavior of FDA can be interpreted from the perspective of array manifold evolution. As discussed in the previous subsection, the FDA array response extends from a purely spatial manifold  $\mathcal{A}_{\text{PA}}(\theta)$  to a joint time–range–angle manifold  $\mathcal{A}_{\text{FDA}}(t, r, \theta)$ . Within this expanded manifold, the beam peak corresponds to a constructive-interference ridge rather than a stationary point. As time evolves, this ridge propagates across the manifold, and its projection onto the angular dimension manifests as an apparent beam scanning phenomenon.

From the ridge trajectory derived previously, the temporal variation of the beam pointing direction can be approximated as

$$\frac{\partial \theta}{\partial t} = \frac{-c \Delta f}{(f_c + \Delta f) d_T \cos \theta}, \quad (27)$$

which represents the angular scanning rate of the FDA mainlobe. This expression indicates that the scanning speed is directly controlled by the frequency increment  $\Delta f$ . Therefore, the frequency gradient determines the scale and rate of beam scanning, rather than the existence of

scanning itself.

Two distinct operating regimes can be identified depending on the product  $T_p \Delta f$ , where  $T_p$  denotes the pulse duration. When  $T_p \Delta f \ll 1$ , the phase evolution induced by the frequency gradient is negligible within a single pulse, and the beam can therefore be regarded as approximately stationary. In contrast, when  $T_p \Delta f \sim 1$ , the manifold ridge evolves significantly within one pulse duration, resulting in noticeable beam scanning, as illustrated by the representative beam pattern snapshots in Fig. 13.

## C. Range–Angle Coupling in the FDA Manifold

Another fundamental characteristic introduced by frequency diversity is the coupling between range and angle. In conventional PA, the array manifold depends only on the angular variable, i.e.,  $\mathbf{a}(\theta)$ , and the range parameter affects only the signal delay rather than the spatial phase structure. In FDA systems, however, the element-dependent frequency offsets introduce an additional range-dependent phase term. As a result, the equivalent beam

pointing direction can be expressed as

$$\theta_e = \sin^{-1} \left[ \left( 1 + \frac{\Delta f}{f_c} \right) \sin \theta - \frac{\Delta f}{f_c d_T} R_0 \right], \quad (28)$$

which explicitly depends on both the target angle  $\theta$  and range  $R_0$ .

From the manifold perspective, this implies that the array response is no longer described by the one-dimensional manifold  $\mathbf{a}(\theta)$ , but instead by a two-dimensional manifold  $\mathbf{a}(R_0, \theta)$ . In other words, the parameter space expands from a purely angular dimension to a joint range-angle space. Therefore, the range-angle coupling observed in FDA systems can be interpreted as a parameter-mixing phenomenon caused by this manifold-dimension expansion. In practice, such coupling may degrade the focusing capability of the transmit beam and affect target localization accuracy. Consequently, a number of studies have attempted to mitigate this effect through frequency design. For example, Khan et al. proposed a logarithmic frequency increment scheme to suppress the range-angle coupling effect and generate discrete point-like beams in the propagation space [150]. Subsequent works [155], [156] further explored nonlinear frequency increment strategies, such as exponential [30] and quadratic frequency offsets [157], which improve beam focusing performance. In addition, frequency coding strategies, including Costas frequency coding [36] and random frequency assignments [38], have also been investigated to alleviate the coupling effect in the transmit beampattern.

Despite these efforts, such approaches essentially reshape the frequency distribution rather than eliminating the underlying physical mechanism. From the manifold perspective, the coupling originates from the intrinsic expansion of the array manifold from  $\mathbf{a}(\theta)$  to  $\mathbf{a}(R_0, \theta)$ , and thus cannot be fundamentally removed. Instead of treating range-angle coupling purely as an undesirable artifact, it can also be interpreted as an additional structural degree of freedom introduced by the expanded manifold. Although the coupling complicates conventional separable parameter estimation methods, it can be exploited through coupling-aware joint processing for enhanced sensing and beamforming capabilities.

#### D. Integrated Transmit Beampattern from a Manifold Perspective

From the manifold viewpoint, the instantaneous FDA transmit beampattern can be interpreted as the response of the time-varying array manifold to the transmit signal. When the transmit field is integrated over time, the resulting beampattern corresponds to the statistical average of this manifold response. Specifically, the integrated transmit beampattern can be written as

$$P_{\text{FDA}}(\theta) = \mathbb{E}_t \left[ |\mathbf{a}^H(\theta) \mathbf{s}(t)|^2 \right] = |\mathbf{a}^H(\theta) \mathbf{R}_T \mathbf{a}(\theta)|, \quad (29)$$

where  $\mathbf{s}(t)$  denotes the transmit signal vector and  $\mathbf{R}_T = \mathbb{E}_t[\mathbf{s}(t)\mathbf{s}^H(t)]$  is the transmit signal correlation matrix. From this perspective, the integrated beampattern reflects

the statistical spatial response determined by the correlation structure of the transmitted signals. This expression resembles the conventional MIMO radar beampattern, but here it arises from integrating the time-varying FDA transmit response over time.

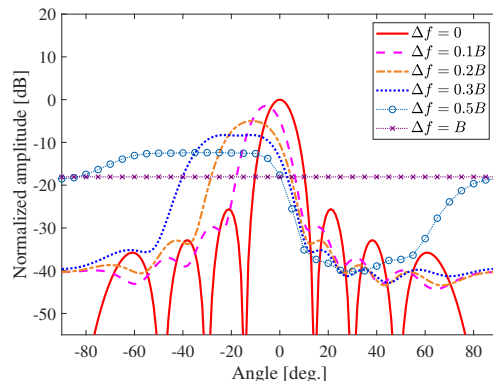


Fig. 14: Integrated transmit beampattern of FDA for different frequency increments [134].

An important transition occurs as the frequency increment  $\Delta f$  increases. As illustrated in Fig. 14, when  $\Delta f$  is much smaller than the signal bandwidth  $B$ , the transmit signals across the array elements remain highly correlated, and the integrated beampattern is approximately consistent with that of a conventional phased array. As  $\Delta f$  increases, the inter-element correlation gradually decreases, leading to a progressive broadening of the integrated beampattern. When  $\Delta f \geq B$ , the transmit signals become nearly orthogonal, and the integrated beampattern approaches an approximately omnidirectional radiation pattern.

These observations highlight that the instantaneous and integrated FDA beampatterns describe two complementary aspects of the same system. The instantaneous beampattern captures the time-varying focusing behavior produced by frequency diversity, whereas the integrated beampattern characterizes the correlation-dependent average radiation pattern of the array.

#### E. Ambiguity-Function Interpretation of the FDA Manifold

The ambiguity function provides a useful framework for characterizing the resolution and parameter separability of radar systems. From a manifold perspective, the ambiguity function can be interpreted as the correlation (inner product) between array responses corresponding to two parameter vectors, i.e.,

$$\chi_{\text{FDA}}(\Theta_1, \Theta_2) = \langle \mathbf{a}(\Theta_1), \mathbf{a}(\Theta_2) \rangle, \quad (30)$$

where  $\Theta$  denotes the parameter vector that may include range, angle, and Doppler variables [134]. In this sense, the ambiguity function reflects the correlation structure of the array manifold in the parameter space.

In FDA systems, the element-dependent frequency offsets modify the phase structure of the array manifold,

which consequently reshapes the multidimensional ambiguity function. Compared with conventional phased arrays, the introduced frequency gradient generates additional coupling among range, angle, and time dimensions, leading to a more intricate ambiguity surface. From the ambiguity-function perspective, the most notable impact of frequency diversity appears in the range dimension. Unlike conventional phased arrays, the effective range resolution of FDA systems is jointly determined by the signal bandwidth and the frequency increment across the transmit array,

$$[\Delta R]_{\text{res}} = \min \left\{ \frac{c}{2B}, \frac{c}{2M\Delta f} \right\}. \quad (31)$$

This result indicates that the additional phase diversity introduced by the frequency gradient can provide an extra range discrimination capability beyond the conventional bandwidth-limited resolution<sup>1</sup>.

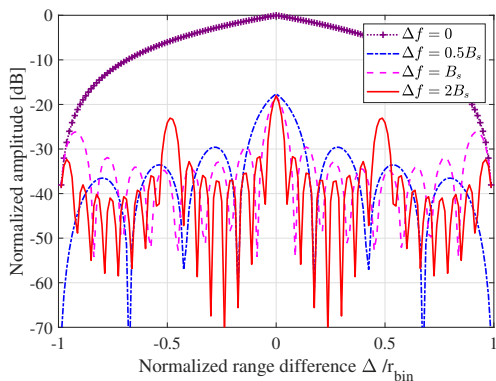


Fig. 15: Range-cut of the FDA ambiguity function for different frequency increments  $\Delta f$  [134].

Fig. 15 shows the range-cut of the FDA ambiguity function for different frequency increments  $\Delta f$ . The conventional range bin size is given by  $R_{\text{bin}} = c/(2B)$ . As  $\Delta f$  increases, the additional phase diversity across the transmit array enhances the range discrimination capability. However, when the frequency increment becomes excessively large, multiple dominant peaks may appear within a single range bin. This phenomenon can be interpreted as the emergence of secondary range cells, which introduce additional range ambiguities in the FDA response. Physically, this behavior originates from the

<sup>1</sup>This observation also raises a broader conceptual question regarding the interpretation of range in FDA systems. If the effective range discrimination is no longer determined solely by the delay-bandwidth relation, but also by the frequency-gradient-induced manifold structure, then the classical pulse-compression-based notion of range resolution may no longer be sufficient to fully characterize the system. In this sense, the role of pulse compression in FDA may need to be reconsidered: rather than serving as the unique mechanism for range acquisition, it may become only one component in a broader ranging framework where distance is also reflected in the distinguishability of range-dependent array responses. Accordingly, whether distance in FDA/FDA-MIMO should still be measured exclusively through propagation delay, or jointly interpreted through delay and manifold discrimination, remains an open but important question.

additional range-dependent phase term induced by the frequency gradient, which creates multiple constructive-interference regions within a single conventional range resolution cell.

In addition to modifying the range resolution, frequency diversity also changes the geometric structure of the ambiguity surface. Eq.(30) shows that the phase difference between two parameter points  $(r_1, \theta_1)$  and  $(r_2, \theta_2)$  becomes

$$\Delta\phi_m = 2\pi \frac{f_c}{c} m d_T (\sin\theta_2 - \sin\theta_1) - 2\pi \frac{\Delta f m}{c} (R_2 - R_1). \quad (32)$$

Constructive interference occurs when the phase difference remains approximately constant across the array aperture, which leads to the approximate relation

$$\Delta R \approx \frac{f_c d_T}{\Delta f} \Delta \sin \theta. \quad (33)$$

This relation indicates that the mainlobe of the ambiguity function forms a slanted ridge in the  $(\Delta R, \Delta \sin \theta)$  plane rather than a separable peak at  $(0, 0)$ . The resulting tilted ambiguity surface directly reflects the intrinsic range-angle coupling induced by the frequency gradient. By contrast, the angular resolution under far-field conditions remains primarily determined by the physical aperture of the array, while the Doppler resolution depends on the coherent observation time, as in conventional radar systems. Therefore, frequency diversity mainly reshapes the ambiguity structure in the range dimension rather than fundamentally altering the angular or Doppler resolution limits.

## F. Scattering Response from a Manifold Perspective

The scattering response of a target can also be interpreted through the array manifold. Consider a target consisting of multiple scattering centers  $\{(R_k, \theta_k)\}$  with complex amplitudes  $\alpha_k$ . The received echo can be expressed as the coherent superposition of the manifold responses associated with these scattering centers, namely [158]

$$y(t) = \sum_k \alpha_k \mathbf{1}^T \mathbf{a}(t, R_k, \theta_k), \quad (34)$$

where  $\mathbf{a}(t, r, \theta)$  denotes the FDA array manifold and  $\mathbf{1}$  denotes the vector whose entries are all equal to one. This expression indicates that the received signal results from the coherent projection of the array manifold responses corresponding to different scattering points.

Expanding the manifold response reveals that each scattering contribution contains a phase term determined by the propagation delay and the element-dependent carrier frequency. In FDA systems, the introduced frequency offsets generate an additional time-dependent phase component, which causes the relative phases among the scattered contributions to evolve continuously. The received signal can therefore be written as  $y(t) = \sum_k \alpha_k e^{-j\phi_k(t)}$ , with

$$\phi_k(t) = 2\pi f_c \tau_k + 2\pi \Delta f_k t, \quad (35)$$

where  $\tau_k$  denotes the propagation delay associated with the  $k$ th scattering center and  $\Delta f_k$  represents the effective frequency offset contributing to the time-varying phase evolution. Besides, the equivalent radar cross section (RCS) is defined as the squared magnitude of the received echo, i.e., [159]

$$\sigma_{\text{FDA}}(t, \Delta f) = |y(t)|^2. \quad (36)$$

Unlike conventional phased arrays, where the relative phases among scattering contributions remain constant for a fixed target geometry, the FDA-induced phase evolution causes the coherent superposition to vary with time, like Fig.16.

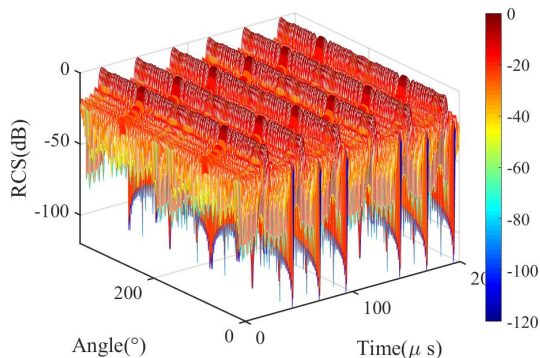


Fig. 16: Time-varying RCS of an FDA radar target as a function of time and observation angle. The periodic fluctuations demonstrate that, due to the element-dependent frequency offsets, the coherent superposition of scattering contributions evolves over time, resulting in a time-varying equivalent RCS even for a static target [159]

However, the aforementioned time-varying RCS behavior relies on the coherence of the scattered echoes across the array elements. If the frequency increment becomes excessively large, the echoes corresponding to different transmit elements may become decorrelated within a single range resolution cell. To preserve the coherent superposition among array elements, the frequency increment must satisfy the approximate constraint [160]

$$\Delta f \leq \frac{c}{4(M-1)\Delta r}, \quad (37)$$

which ensures that the phase variation across the array remains sufficiently small within one range cell. Since the range resolution is given by  $\Delta r = c/(2B)$ , this condition can be equivalently written as [161], [162]

$$(M-1)\Delta f \leq B. \quad (38)$$

When this condition is violated, the scattered echoes from different transmit elements lose their mutual coherence, and the FDA echo model approaches that of a frequency-agile or MIMO radar. In such cases, the coherent scattering mechanism described above no longer holds, and the RCS statistics follow the conventional models used for decorrelated radar returns.

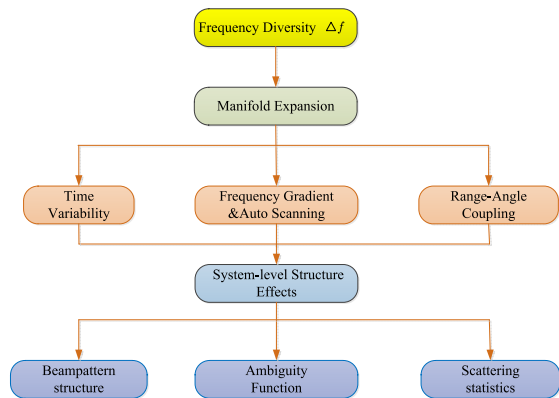


Fig. 17: Unified structural interpretation of FDA from the array manifold perspective. Frequency diversity induces manifold expansion, which gives rise to time variability, automatic scanning, and range-angle coupling, and subsequently manifests in the beampattern structure, ambiguity function, and scattering statistics.

From a statistical viewpoint, this phenomenon indicates that frequency diversity fundamentally reshapes the geometry of the FDA array manifold. Consequently, the transmit beampattern, ambiguity structure, and coherent scattering statistics are all determined by this manifold expansion, as summarized in Fig. 17.

#### IV. Frequency-Gradient and Time-Coding Array Paradigms

In the literature, FDA and FDA-MIMO are often discussed together with other array paradigms capable of producing range-angle dependent responses, such as element-pulse coding (EPC) arrays [108]–[113] and space-time coding arrays (STCA) [114]–[120]. Because these architectures may produce similar output behaviors, they are sometimes interpreted as belonging to the same class of range-angle dependent arrays. However, the mechanisms that generate these behaviors are fundamentally different. To clarify these relationships, this section compares FDA/FDA-MIMO and representative time-coding paradigms from a structural perspective. The comparison focuses on the design variables involved in signal generation, the resulting propagation-phase structures, and the corresponding system DoF. In particular, we distinguish between physical range dependence created directly by carrier-frequency gradients and processing-induced range selectivity obtained through temporal coding and receiver-side reconstruction.

##### A. Propagation Phase and Design Dimensions

To reveal the fundamental differences among array paradigms, it is instructive to examine how the design variables affect the propagation phase of the transmitted signal. Consider the signal transmitted by the  $m$ -th array element and observed at location  $(r, \theta)$ . Under far-field narrowband propagation, its phase can be written as

$$\phi_m(t, R_0, \theta) = 2\pi f_m t - \frac{2\pi f_m}{c} R_0 + \frac{2\pi f_m d_m \sin \theta}{c}. \quad (39)$$

This expression shows that the received phase is determined by three physical quantities: the carrier frequency  $f_m$ , the element position  $x_m$ , and the propagation delay  $R_0/c$ . Consequently, different array paradigms can be interpreted according to which of these variables they manipulate during signal generation. From this viewpoint, several fundamental design dimensions can be identified:

- Spatial dimension: Element positions  $x_m$  determine the spatial phase distribution across the aperture and are responsible for conventional angular selectivity.
- Frequency dimension: Element-dependent carrier frequencies  $f_m$  introduce inter-channel frequency gradients, which directly modify the propagation phase and can produce range-dependent interference structures.
- Temporal coding dimension: Time-domain modulation across pulses or symbols provides structured signal diversity and may generate equivalent range selectivity after matched filtering and receiver-side reconstruction.
- Waveform diversity dimension: Orthogonal waveforms enable channel separability and facilitate virtual-array formation in MIMO-type systems.

Different array paradigms activate different subsets of these dimensions. As will be discussed in the following subsections, this distinction is particularly important for understanding the fundamental difference between frequency-gradient arrays (e.g., FDA) and time-coding-based arrays including EPC and STCA, since only the former directly modify the propagation phase associated with range. Among the design dimensions discussed above, the frequency dimension plays a unique role because it directly modifies the carrier-dependent propagation phase. This property gives rise to the class of frequency-gradient arrays, represented by FDA and FDA-MIMO.

## B. Frequency-Driven Paradigm: FDA and FDA-MIMO

Frequency diverse arrays introduce element-dependent carrier frequencies  $f_m$  across the transmit aperture, which fundamentally modifies the propagation-phase structure of the transmitted field. Substituting  $f_m = f_c + \Delta f_m$  reveals that the element-dependent frequency offsets introduce additional phase terms proportional to both time and range. In particular, the range-phase gradient becomes (22). Since  $\Delta f_m$  varies across array elements, different transmit channels exhibit different range-phase gradients, i.e.,

$$\Delta(\nabla_R \phi_m) = -\frac{2\pi \Delta f_m}{c}. \quad (40)$$

This inter-channel gradient difference creates range-dependent interference directly during electromagnetic propagation. As a result, FDA is able to generate transmit-side range-angle dependent responses without relying on receiver-side temporal reconstruction. From a system-design perspective, the introduction of element-dependent

carrier frequencies therefore expands the design space of the array manifold Eq.(12). When orthogonal waveforms are further transmitted across array elements (FDA-MIMO), waveform diversity provides an additional signal-space dimension, leading to Eq.(19).

The key characteristic of this paradigm is that range-dependent behavior is embedded directly in the propagation phase through carrier-frequency gradients, rather than being reconstructed through temporal coding or receiver-side processing.

## C. Time-Coding-Driven Paradigm I: EPC

EPC arrays [163]–[166] represent a class of transmit architectures that synthesize structured transmit diversity by applying coding weights jointly across array elements and pulses. Instead of transmitting identical pulses from all elements, EPC introduces element-dependent coding coefficients across successive pulse repetition intervals, thereby coupling the spatial dimension (array aperture) with the slow-time dimension (pulse index).

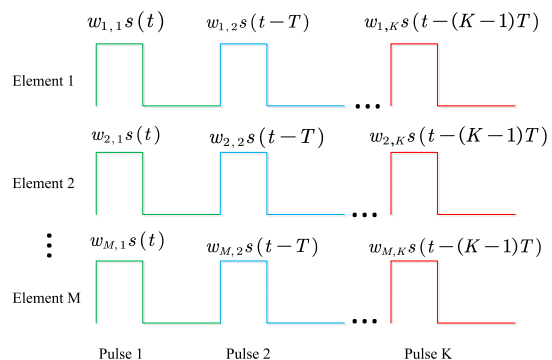


Fig. 18: Illustration of the EPC structure. Each array element transmits a sequence of coded pulses across successive pulse repetition intervals. The coding weights  $w_{m,p}$  form an element-pulse coding matrix that couples the spatial and slow-time dimensions.

As shown in Fig.18, in EPC architectures, the signal transmitted by the  $m$ -th element can be written as

$$s_m(t) = \sum_p w_{m,p} s(t - pT), \quad (41)$$

where  $p$  denotes the pulse index,  $T$  is the pulse repetition interval, and  $w_{m,p}$  represents the coding weight applied to the  $p$ -th pulse at the  $m$ -th element. The coefficients  $\{w_{m,p}\}$  form an element-pulse coding matrix that jointly controls the spatial and temporal structure of the transmitted signals. As a result, different array elements transmit differently weighted pulse sequences over time. This structure effectively expands the design space of the transmit array beyond the purely spatial aperture.

After propagation, the echoes corresponding to different pulses arrive at the receiver with different time delays. When matched filtering is applied with respect to the transmitted waveform  $s(t)$ , the echoes associated with

different pulses are separated in the range domain. By properly designing the coding matrix  $\{w_{m,p}\}$ , the receiver can combine these delayed echoes to synthesize transmit responses that depend on both angle and range. From a system-design viewpoint, EPC introduces an additional temporal degree of freedom beyond the spatial dimension, leading to the effective system DoF, namely

$$\text{DoF}_{\text{EPC}} = \text{Space} \oplus \text{Time}. \quad (42)$$

It is important to emphasize that all transmit elements share the same carrier frequency. Consequently, the propagation kernel  $e^{-j2\pi f_c r/c}$  remains identical across array channels. No inter-element range-phase gradient difference is introduced during propagation. Therefore, the range-dependent behavior observed in EPC arrays arises primarily from pulse-domain processing and temporal reconstruction at the receiver rather than from transmit-side propagation-phase gradients.

#### D. Time-Coding-Driven Paradigm II: STCA

STCA represent another class of transmit architectures capable of producing range-angle dependent responses. Unlike FDA, STCA introduces element-dependent time delays across the transmit aperture, thereby coupling the spatial and temporal dimensions of the transmitted signals.

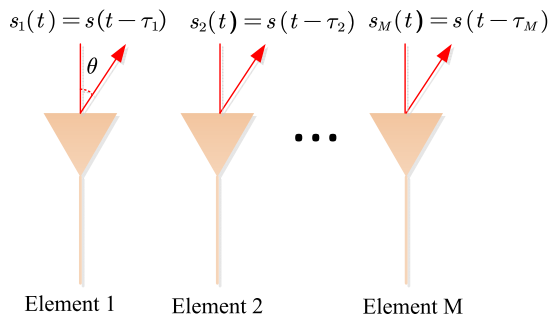


Fig. 19: Illustration of the STCA structure. Each transmit element radiates a delayed replica of the same waveform,  $s_m(t) = s(t - \tau_m)$ , where  $\tau_m$  denotes the element-dependent time delay. Unlike FDA that employ carrier-frequency offsets, STCA introduces coupling between space and time through relative time delays across the transmit aperture.

As illustrated in Fig. 19, the signal transmitted by the  $m$ -th element can be expressed as

$$s_m(t) = s(t - \tau_m), \quad (43)$$

where  $\tau_m$  denotes the relative time delay applied to the  $m$ -th array element. Through these element-dependent delays, the transmitted waveform across the array aperture becomes jointly structured in the spatial and temporal

domains. More generally, STCA can also be described using a space-time coding formulation

$$s_m(t) = \sum_p a_{m,p} s_p(t), \quad (44)$$

where  $a_{m,p}$  denotes the space-time coding coefficient applied at the  $p$ -th time slot and  $s_p(t)$  represents the transmitted waveform during that slot. This formulation highlights that STCA jointly exploits spatial weighting, temporal coding, and waveform diversity within a unified transmit framework.

Due to the element-dependent time delays, the transmitted steering vector becomes dependent on both range and angle. Consequently, STCA can produce range-angle coupled responses in the transmitted field. From a system-design perspective, STCA introduces additional temporal and waveform dimensions beyond the spatial aperture, leading to the effective degrees of freedom, namely

$$\text{DoF}_{\text{STCA}} = \text{Space} \oplus \text{Time} \oplus \text{Waveform}. \quad (45)$$

It is worth noting that all transmit elements typically share the same carrier frequency. Therefore, the propagation kernel  $e^{-j2\pi f_c r/c}$  remains identical across array channels. As a result, the range-dependent behavior observed in STCA systems primarily originates from space-time signal processing rather than from propagation-phase gradients across the transmit aperture.

#### E. Structural Comparison of Array Paradigms

Although FDA, EPC, and STCA may produce similar range-angle dependent responses in certain signal-processing frameworks, the mechanisms that generate these behaviors originate from fundamentally different design dimensions. A structural comparison can therefore be made in terms of the design variables that shape the transmitted field.

Table I summarizes the representative paradigms and the corresponding design dimensions they activate. FDA introduces element-dependent carrier offsets, which create range-dependent phase gradients directly during electromagnetic propagation. As a result, the transmitted steering vector inherently depends on both range and angle. In contrast, time-coding-based architectures such as EPC and STCA rely on temporal modulation across the transmit array. EPC achieves this through coding weights applied to successive pulses, while STCA introduces relative time delays or more general space-time coding structures across the array aperture. These mechanisms enable structured transmit diversity and can synthesize range-angle dependent responses after signal processing. However, since all transmit elements typically share the same carrier frequency in these architectures, the propagation kernel remains identical across channels. Consequently, the observed range selectivity arises primarily from temporal coding and receiver-side reconstruction rather than from transmit-side propagation-phase gradients.

TABLE I: Structural comparison of representative array paradigms in terms of their activated design variables.

Paradigm	Frequency gradient	Temporal modulation	Waveform orthogonal	Physical range dependence
FDA	✓	×	×	✓
FDA-MIMO	✓	×	✓	✓
EPC	×	✓	×	Processing-induced
STCA	×	✓	✓	Processing-induced

Therefore, among the paradigms summarized above, only frequency-gradient arrays (e.g., FDA and FDA-MIMO) introduce range-dependent structure directly in the physical propagation phase.

### V. FDA System Capability Mapping Framework

While the previous sections focus on the structural properties of FDA, this section interprets these properties in terms of system capabilities. Building upon the unified signal model and the manifold-expansion theory developed in the previous sections, this section establishes a capability mapping framework for FDA systems. The objective is to relate the underlying design variables of the transmit architecture to the system-level capabilities enabled by the expanded array manifold. In particular, we interpret FDA capabilities through the structural relationship between design variables, the resulting propagation-phase structure, the physical degrees of freedom introduced in the array manifold, and the system capabilities that these degrees of freedom enable.

Under the unified signal representation, the phase of the  $m$ -th transmit channel can be written as

$$\phi_m(t, r, \theta) = \phi_m^{\text{space}} + \phi_m^{\text{freq}} + \phi_m^{\text{time}} + \phi_m^{\text{waveform}}, \quad (46)$$

where each component corresponds to a different design dimension of the transmit architecture. Different array paradigms activate different phase-gradient components, which determine how the transmit manifold expands in the joint space of range, angle, and time.

For FDA systems, the introduction of element-dependent carrier frequencies creates additional propagation-phase gradients that expand the array manifold along new physical dimensions. As a result, several distinctive capabilities emerge beyond those of conventional phased arrays. In the following subsections, we analyze three representative capabilities enabled by this manifold expansion: range-angle selectivity, time-evolving beam control, and frequency-domain diversity.

#### A. Range-Angle Selectivity

A fundamental capability introduced by FDA is the ability to generate transmit responses that depend jointly on range and angle. In conventional PA, the transmit steering vector depends only on the spatial direction, i.e.,  $\mathbf{a}(\theta)$ , which leads to a one-dimensional angular response. In contrast, FDA introduces element-dependent carrier frequencies, which expand the transmit manifold into a joint range-angle domain,  $\mathbf{a}_{\text{FDA}}(r, \theta)$ . As a result, the

array response becomes inherently two-dimensional in  $(r, \theta)$ , enabling selective focusing or interference control across both dimensions.

The origin of this capability lies in the range-dependent propagation phase associated with element-dependent carrier frequencies. When frequency offsets  $\Delta f_m$  are introduced across array elements, the propagation phase exhibits different range-phase gradients across channels. These gradient differences produce controllable interference structures along the range dimension during electromagnetic propagation. Consequently, the transmitted field no longer forms a purely angular beam pattern, but instead generates a range-angle dependent response whose structure can be shaped through the frequency-gradient design.

An additional consequence of this frequency-gradient structure is the emergence of a finer discrimination scale along the range dimension. When multiple transmit elements operate with slightly different carrier frequencies, the superposition of their radiated fields forms a periodic interference pattern in range. Under coherent conditions, this structure can provide a secondary range discrimination capability beyond the conventional bandwidth-limited resolution [167], [168]. For example, when a uniform frequency increment  $\Delta f$  is applied across  $M$  transmit elements, the effective sub-range discrimination scale can be approximated as [134], [169], [170]

$$\Delta r_{\text{sub}} \approx \frac{c}{2M\Delta f}, \quad (47)$$

which corresponds to the spacing between adjacent constructive interference regions generated by the multi-frequency transmit aperture.

In practice, the effectiveness of this range-angle selectivity depends on several factors. First, excessively large frequency offsets may introduce inter-element decorrelation or violate the narrowband assumption. Second, coherent combination of the multi-frequency components is required in order to preserve the interference structure. Finally, propagation environments with strong multipath or heterogeneous clutter may distort the range-angle coupling pattern.

Overall, range-angle selectivity represents one of the most fundamental capabilities enabled by the frequency-gradient architecture of FDA, reflecting the expansion of the array manifold into the joint range-angle domain.

#### B. Time-Evolving Beam Control

Another distinctive capability of FDA is the ability to generate transmit responses that evolve over time.

In conventional PA, the transmit beampattern is typically time-invariant once the spatial weights are fixed. In contrast, FDA introduces element-dependent carrier frequencies, which cause the relative phases across the array aperture to change continuously with time. As a result, the resulting beampattern becomes inherently time-varying, producing dynamic beam trajectories in the joint range–angle domain. The time evolution of the FDA beampattern originates from the temporal phase gradient introduced by the frequency offsets across array elements. Because each element transmits with a slightly different carrier frequency, the inter-element phase differences vary continuously with time. This temporal phase evolution modifies the interference structure of the transmitted field, leading to dynamic redistribution of radiated energy in space.

Consequently, time becomes an intrinsic dimension of the transmit manifold, and the resulting beam structure can evolve along both the range and angular directions. The apparent beam dynamics depend on the relationship between the pulse duration and the frequency offsets applied across the array.

- **Small Frequency Offsets:** When the product of pulse duration and frequency offset is small, the beampattern can be regarded as approximately static within a single pulse.
- **Larger Frequency Offsets:** When the temporal phase evolution becomes significant over the pulse duration, the beam structure may vary noticeably within a pulse, leading to continuous scanning or drifting effects in the range–angle domain.

The time-varying nature of FDA beams also introduces several practical considerations:

- Perfect time-invariant focusing cannot be maintained when nonzero frequency offsets are present.
- The apparent beam trajectory depends on both waveform duration and frequency-gradient design.
- Receiver-side processing is often required to reconstruct stationary responses for parameter estimation.

Overall, the time-evolving beam behavior reflects the intrinsic temporal phase gradients introduced by frequency diversity, distinguishing FDA from conventional arrays with static spatial beampatterns.

### C. Frequency-Domain Diversity

Another important capability introduced by frequency diverse arrays is frequency-domain diversity. Because different transmit elements operate at slightly different carrier frequencies, the radiated field can be interpreted as a superposition of multiple narrowband components distributed across the frequency domain. Compared with conventional phased arrays, where all elements share a common carrier frequency, FDA effectively creates a distributed multi-frequency transmit aperture. This structure introduces additional diversity in the frequency domain and expands the available signal space for sensing and communication tasks. The origin of this capability lies

in the element-dependent carrier frequencies  $f_m$  which produce distinct spectral components across the transmit aperture. As a result, the transmitted field contains multiple frequency-dependent responses that propagate simultaneously through the environment.

These frequency components experience different propagation phases and scattering responses, providing additional diversity beyond the purely spatial domain. The frequency diversity introduced by FDA enables several useful signal-processing mechanisms:

- **Multi-Frequency Observation:** Different carrier frequencies probe the scene with slightly different propagation characteristics, providing additional independent observations.
- **Frequency-Dependent Interference Shaping:** The superposition of multiple frequency components allows the spatial–spectral structure of the transmitted field to be adjusted through the design of frequency offsets.
- **Enhanced Parameter Discrimination:** Frequency diversity improves the separability of targets or channels that may be indistinguishable in purely spatial processing.

The additional diversity provided by multiple carrier frequencies can be exploited in several system-level tasks, such as enhanced parameter estimation, interference mitigation, and joint sensing–communication waveform design. However, the achievable benefits depend on maintaining coherence across the array elements and on the appropriate selection of frequency offsets relative to the system bandwidth and propagation conditions.

Overall, frequency-domain diversity represents another fundamental capability enabled by the frequency-gradient architecture of FDA, complementing the range–angle selectivity and time-evolving beam behaviors discussed in the previous subsections. This capability plays an important role in modern sensing and integrated sensing–communication (ISAC) systems where multi-frequency observations provide additional information for joint environment perception and data transmission.

### D. Capability Mapping Summary

The above discussions reveal that the distinctive capabilities of FDA systems originate from the additional phase gradients introduced by element-dependent carrier frequencies. These gradients expand the array manifold beyond the purely spatial dimension, enabling new forms of signal diversity and beam control. The capability mapping discussed above can be summarized in Table II. The key contribution of FDA is not merely the introduction of frequency offsets, but the expansion of the array manifold through additional propagation-phase gradients. These gradients create new physical degrees of freedom that enable capabilities beyond those of conventional phased arrays.

In practice, these capabilities are realized through concrete signal and array design strategies, including frequency-offset optimization, subarray architectures, and

TABLE II: Capability mapping of FDA systems based on propagation phase gradients and manifold expansion.

Capability	Design Variable	Phase-Gradient Origin	Manifold Expansion
Range–Angle Selectivity	Frequency offsets $\Delta f_m$	Range phase gradient	Range–angle manifold
Time-Evolving Beam Control	Frequency offsets $\Delta f_m$	Temporal phase gradient	Time–range manifold
Frequency-Domain Diversity	Multi-frequency transmit aperture	Spectral diversity	Spectral manifold

array-geometry design. A large portion of the FDA literature has approached the problem from the perspective of transmit beampattern synthesis, with the goal of shaping the range–angle-dependent radiation pattern induced by the frequency-gradient structure. From this viewpoint, such design methods form the mechanism-level bridge between the physical capabilities summarized above and the radar task families discussed next.

## VI. FDA Applications Across Radar Task Families

Building on the capability mapping developed in the previous section, we now examine how the structural properties of FDA translate into performance gains across representative radar task families. Rather than reviewing the literature chronologically, we adopt a task-oriented perspective and focus on the relationship among the task objective, the required physical degrees of freedom, the structural mechanisms introduced by FDA, and the practical conditions under which these mechanisms can be effectively exploited.

The applications discussed in this section can be interpreted through three core FDA capabilities established earlier: range–angle manifold expansion, time-evolving beam behavior, and multi-frequency transmit diversity. Different radar tasks draw on one or more of these capabilities in different ways. This perspective helps clarify not only where FDA can provide genuine advantages, but also why such advantages may disappear when the underlying structural effects cannot be coherently preserved or effectively utilized.

### A. Parameter Estimation and Target Localization

Target parameter estimation and localization represent one of the most fundamental tasks in radar systems. In conventional PA radar, the transmit steering vector depends only on the angular direction, and range estimation is typically performed independently through matched filtering. In contrast, FDA introduces element-dependent carrier frequencies, which expand the transmit manifold into a joint range–angle domain. This capability corresponds to the range–angle manifold expansion identified in the capability mapping framework, and provides a structural basis for joint parameter estimation and target localization. As a result, the received signal model can be written as

$$\mathbf{y} = \alpha \mathbf{a}_{\text{FDA}}(R_0, \theta) + \mathbf{n}. \quad (48)$$

This additional manifold dimension provides new opportunities for joint parameter estimation and improved target localization performance [46], [65], [171], [172]. However,

the range–angle coupling introduced by FDA also complicates parameter estimation, since the conventional separation between range processing and spatial processing no longer strictly holds. To address this challenge, a variety of signal processing strategies have been developed to either decouple the parameters or directly perform joint estimation [173], [174].

One representative class of approaches exploits cooperative or hybrid architectures that combine conventional PA signals with FDA signals. For example, dual-pulse schemes have been proposed in which one pulse operates in the conventional PA mode to estimate the target angle, while the other pulse employs FDA signals to estimate range using the known angular information [46]. This idea has been further extended to FDA–MIMO radar configurations to improve parameter identifiability [66]. Related cooperative schemes have also been proposed where different portions of the transmit array operate in PA and FDA modes, enabling sequential estimation of angle and range parameters [175].

Another widely studied class of approaches relies on subarray-based FDA structures. In such architectures, coherent signals are transmitted within each subarray while different subarrays employ distinct frequency offsets or orthogonal waveforms. By exploiting the resulting spatial–frequency diversity, joint range–angle estimation can be performed using beamforming or subspace-based signal processing techniques [54], [55], [65], [176]. Analytical studies have also investigated the theoretical estimation performance of FDA–MIMO systems in terms of the Cramér–Rao lower bound (CRLB) and mean-square error (MSE) properties [67].

Despite the large number of algorithms proposed in the literature, several challenges remain. First, the parameter coupling introduced by frequency offsets increases computational complexity and may degrade the performance of classical subspace estimators when the frequency gradient becomes large. Second, many existing algorithms rely on multiple snapshots or high signal-to-noise ratios, which may not always be available in practical scenarios. To address these limitations, recent research has explored more robust estimation frameworks, including compressive sensing and tensor-decomposition-based approaches, which can reduce the required number of snapshots and improve robustness to noise and model mismatch [177]–[179]. Furthermore, extending FDA parameter estimation frameworks to more complex array configurations, such as planar arrays, coprime arrays, conformal arrays, multi-static radar systems, or polarization-diverse systems, introduces additional parameters and coupling relationships

that remain active research topics [58], [59], [180], [181].

Overall, although a large number of algorithms have been developed for FDA parameter estimation [172], [182], [183], most existing studies focus on linear array configurations and idealized signal models. Extending these techniques to more practical scenarios therefore remains an important direction for future research.

## B. Target Detection in Complex Environments

1) **Detection Model and FDA Structural Effect:** Target detection is one of the most fundamental functions of radar systems. The detection problem is commonly formulated as a binary hypothesis test, namely

$$\begin{cases} \mathcal{H}_0 : \mathbf{y} = \mathbf{n}, \\ \mathcal{H}_1 : \mathbf{y} = \alpha \mathbf{a}(R_0, \theta) + \mathbf{n}, \end{cases} \quad (49)$$

where  $\mathbf{y}$  denotes the received signal vector,  $\alpha$  is the target reflection coefficient, and  $\mathbf{n}$  denotes disturbance including thermal noise, clutter, and interference.

For multichannel radar systems, target detection is commonly addressed within the framework of binary hypothesis testing, where classical detectors such as the generalized likelihood ratio test (GLRT), adaptive matched filter (AMF), Rao test, and Wald test have been extensively studied [77], [184]–[189]. In conventional adaptive radar, many detectors rely on secondary or training data to estimate the disturbance covariance matrix and achieve constant false alarm rate (CFAR) performance in unknown environments [190]. At the same time, training-free or reduced-training detection strategies [191]–[193] have also been developed for scenarios where homogeneous secondary data are unavailable or insufficient. Overall, detection performance depends not only on the detector structure itself, but also on the availability of prior information [194], [195], training support, and the accuracy of the assumed signal model [196]–[198].

When FDA is introduced, the received signal structure becomes explicitly range-dependent due to the element-dependent carrier frequencies. This property is consistent with the range–angle manifold expansion discussed in the previous section and fundamentally modifies the statistical structure of the received data. Meanwhile, the use of multiple carrier frequencies across the transmit aperture introduces an inherent multi-frequency transmit diversity, which provides additional spectral degrees of freedom beyond conventional spatial processing.

As a result, the clutter and interference characteristics observed by FDA radar can differ from those of conventional arrays, creating new opportunities for target detection in complex environments such as range-ambiguous clutter, deceptive jamming, and high-speed target scenarios where Doppler–frequency coupling can be effectively exploited.

2) **Detection in Range-Ambiguous Clutter:** In high-PRF airborne radar systems, clutter echoes from different range intervals may fold into the same observation cell, resulting in range-ambiguous clutter. Conventional PA

radar mainly relies on angular discrimination or space–time adaptive processing (STAP) to suppress such clutter [69], [199], [200]. However, these approaches operate primarily in the spatial or space–time domain and do not explicitly exploit range-dependent structure. In contrast, FDA enables joint range–angle beam pattern shaping due to its element-dependent carrier frequencies, allowing the radiated field to exhibit controllable gain variations across range. This additional degree of freedom can be exploited to suppress ambiguous clutter originating from undesired range regions by placing nulls or low-gain zones at specific ranges [78], [201].

Building upon this property, FDA–MIMO systems further extend the processing capability by employing orthogonal transmit waveforms, which enable reconstruction of the transmit aperture at the receiver. This facilitates joint space–time–range adaptive processing for clutter suppression and target detection [68]–[70], [202], [203]. Moreover, several studies have demonstrated that FDA-based processing can significantly improve the detection performance of moving targets in range-ambiguous clutter environments [204]–[206], highlighting the effectiveness of exploiting range-dependent diversity in challenging scenarios.

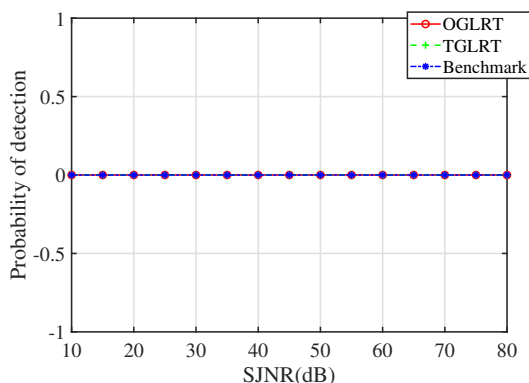
3) **Detection Under Deceptive Jamming:** FDA radar exhibits inherent advantages in countering deceptive jamming, particularly in mainlobe scenarios where conventional angle-domain discrimination becomes ineffective. In classical PA radar, deceptive signals generated by repeaters can closely match the spatial steering vector of the true target, making them difficult to distinguish and suppress using spatial processing alone. In contrast, due to the element-dependent carrier frequencies, FDA introduces a range-dependent phase structure, leading to a range–angle coupled manifold. As a result, false targets generated by repeaters generally cannot simultaneously match both the range and angle characteristics of the true FDA echo, unless precise knowledge of the frequency offsets and target parameters is available. This inherent mismatch provides an additional discrimination mechanism beyond conventional spatial processing.

Moreover, the multi-frequency transmit diversity of FDA further enhances robustness against deceptive jamming. Specifically, the frequency-dependent echo structure introduces additional constraints on the jammer, making it difficult to coherently replicate the full signal model across the aperture, especially under dynamic or partially known conditions [207]. As such, FDA transforms the deceptive jamming suppression problem from a purely spatial discrimination task into a joint range–angle–frequency inference problem.

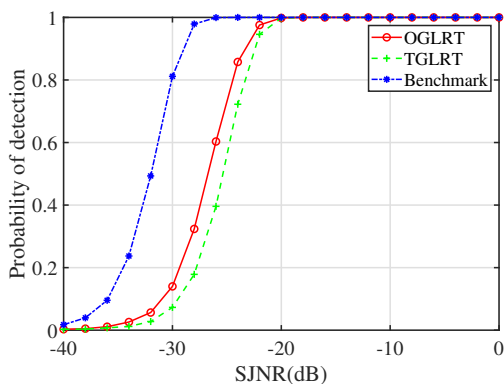
Building upon these properties, adaptive detection schemes based on GLRT, Rao, and Wald tests have been extended to FDA–MIMO systems under deceptive and suppression jamming scenarios [75], [76], [208]. In particular, GLRT-based adaptive detectors have been developed for FDA–MIMO radar operating in mainlobe

deceptive jamming environments, where the jammer and target share similar angular signatures but differ in their range-dependent structures [209], [210]. Extensions to partially homogeneous noise environments have also been investigated, demonstrating robustness under practical conditions [211]. To further highlight the fundamental role of frequency diversity, we consider the limiting case where  $\Delta f = 0$ , under which waveform-orthogonality FDA-MIMO degenerates to conventional MIMO radar. The corresponding detection performance under mainlobe deceptive jamming is illustrated in Fig. 20. It is observed that, when  $\Delta f = 0$ , all detectors fail to achieve reliable detection, whereas when  $\Delta f \neq 0$ , FDA enables effective target detection by exploiting range-dependent diversity.

This result clearly indicates that FDA does not merely improve detection performance, but fundamentally enables reliable target detection in scenarios where conventional MIMO radar becomes ineffective. Furthermore,



(a) MIMO ( $\Delta f = 0$ )



(b) FDA-MIMO ( $\Delta f \neq 0$ )

Fig. 20: Detection performance under mainlobe deceptive jamming [209]. When  $\Delta f = 0$ , corresponding to conventional MIMO radar, all detectors fail to achieve reliable detection. In contrast, when  $\Delta f \neq 0$ , FDA enables effective target detection by exploiting range-dependent diversity, even in the presence of strong mainlobe deceptive jamming.

joint target-jammer detection frameworks have been proposed to simultaneously identify desired targets and de-

ceptive signals within the mainlobe [212]. These methods exploit the additional degrees of freedom introduced by FDA to enable more effective separation of target and jammer components, further improving detection performance in challenging electronic countermeasure scenarios.

4) Detection for High-Speed Target : High-speed or maneuvering targets introduce significant challenges for radar detection due to Doppler ambiguity, Doppler spreading, and range migration effects. In conventional radar systems, target motion induces a Doppler shift  $f_d = \frac{2v}{c} f_c$ , which can be effectively handled when the velocity is moderate. However, for high-speed targets, Doppler ambiguity and spectral spreading degrade coherent integration performance and reduce detection sensitivity. In FDA radar, the presence of element-dependent carrier frequencies introduces an additional Doppler-related component. Specifically, the Doppler shift becomes

$$f_{\text{obs}} = \frac{2v}{c} (f_c + \Delta f_m), \quad (50)$$

which can be decomposed as a conventional Doppler term plus an FDA-induced Doppler expansion term. Although  $\Delta f_m \ll f_c$ , these additional Doppler components introduce phase accumulation errors across pulses and array elements. As pointed out in [213], neglecting these effects leads to defocusing of the target response in the range-angle-Doppler domain, thereby degrading detection performance.

Unlike conventional systems where Doppler effects are treated purely as impairments, FDA provides an additional degree of freedom to exploit these frequency-dependent Doppler variations. The induced Doppler expansion and phase diversity can be leveraged to enhance target identifiability and improve detection performance, especially for high-speed or maneuvering targets. Building upon this property, several FDA-based detection frameworks have been developed. For example, Doppler-spread-aware detection methods have been proposed to account for motion-induced spectral broadening [214]. Long-time coherent integration and joint range-angle beamforming techniques have been designed to compensate for motion-induced phase errors and improve detection sensitivity [213]. FDA has also been applied to resolve Doppler ambiguity of high-speed targets by exploiting its multi-frequency structure [215].

To illustrate the impact of Doppler ambiguity in high-speed target detection, Fig. 21(a) shows the SCNR loss versus normalized Doppler frequency. It can be observed that conventional MIMO and PA radar suffer from severe SCNR degradation around the Doppler-ambiguous region (i.e.,  $f_d \approx \text{PRF}$ ), where deep notches appear due to blind Doppler. In contrast, FDA-MIMO effectively mitigates this degradation and maintains a relatively stable SCNR level, demonstrating its inherent robustness against Doppler ambiguity. This advantage directly translates into improved detection performance. As shown in Fig. 21(b), FDA-MIMO achieves a significantly higher detection probability than conventional MIMO and PA, especially in

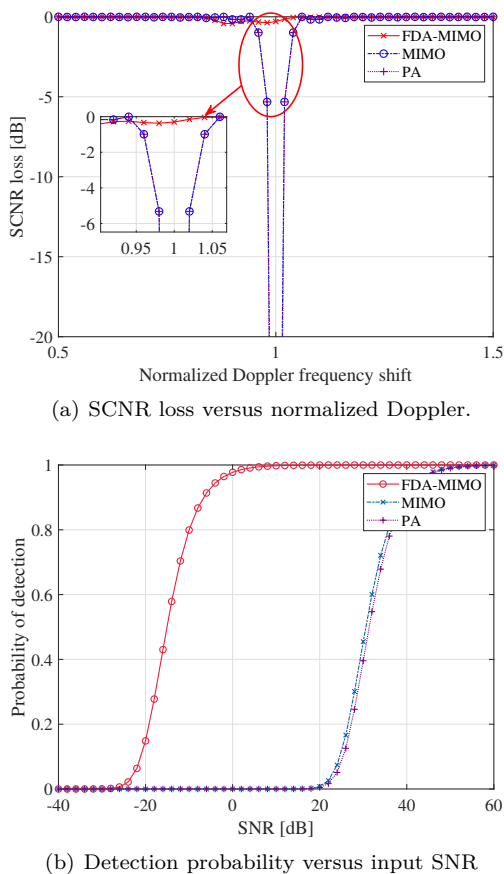


Fig. 21: High-speed target detection performance under Doppler spreading [216].

low-SNR regimes. Furthermore, FDA enables effective detection of maneuvering targets in complex environments. Detection frameworks incorporating Doppler spread and range migration have been developed for FDA-MIMO radar systems [217]. In the presence of mainlobe clutter or deceptive jamming, FDA-based methods can jointly exploit frequency diversity and motion-induced signatures to improve detection robustness [216].

Overall, FDA transforms high-speed target detection from a conventional Doppler processing problem into a joint range-angle-frequency-Doppler inference problem. This additional structural diversity provides new opportunities for detecting high-speed and maneuvering targets in challenging scenarios.

5) Detection in Secondary Range Cells: A fundamental yet often overlooked phenomenon in FDA systems stems from the inherent range-frequency coupling introduced by element-dependent frequency offsets. From the perspective of the ambiguity function, FDA does not produce a single dominant range mainlobe as in conventional phased-array radar. Instead, it generates a set of periodic range responses, with peaks located at

$$\Delta R_{\text{peak}} = \ell \frac{c}{2\Delta f}, \quad (51)$$

where  $\ell$  is an integer index. This periodic structure reflects a transmit-induced range super-resolution capability, whereby multiple distinguishable responses can be formed across different range locations. As a consequence, the effective degrees of freedom in the range domain are no longer solely limited by the signal bandwidth, but are further enriched by the frequency diversity across the transmit aperture.

From a detection perspective, however, this structural property fundamentally alters the conventional interpretation of a range cell. In classical radar systems, each range cell is typically modeled as containing a single dominant scatterer. In contrast, due to the presence of secondary peaks, an FDA range cell may correspond to multiple effective scattering components, which can be viewed as a distributed target structure induced by the waveform [218]. This shift in the signal model has two important implications. First, the coexistence of multiple peaks may introduce ambiguities, especially when secondary responses overlap with clutter or interference. To address this issue, various ambiguity mitigation strategies have been developed, including the use of nonlinear frequency offsets, multi-pulse diversity, and adaptive processing techniques, which aim to decorrelate or suppress undesired secondary peaks [219]–[221]. Second, and more importantly, these multiple responses can be actively exploited to enhance detection performance. By interpreting the secondary range peaks<sup>2</sup> as structured multi-component signals, recent works have developed distributed detection frameworks that leverage the additional degrees of freedom provided by FDA. Such approaches enable the detection of multiple targets within a single conventional range cell, or equivalently, improve detection performance in scenarios where the target exhibits extended or multi-scattering characteristics [85], [87], [167], [170], [222].

To illustrate this effect, Fig. 22 shows the detection probability as a function of the signal-to-clutter ratio (SCR) for different numbers of scattering components within a single range cell. Here,  $H$  represents the number of effective scatterers, which can be interpreted as the number of FDA-induced peaks contributing to the received signal. It can be observed that increasing  $H$  leads to improved detection performance, as multiple components contribute constructively to the received energy. This observation highlights a key distinction between FDA and conventional radar systems: while secondary range responses are traditionally regarded as ambiguity, in FDA they constitute a structured source of diversity that enables a transition from single-target detection to distributed detection. As such, the secondary range cells in FDA should not be viewed solely as a limitation, but rather as a fundamental structural feature that can be

<sup>2</sup>A broader open issue concerns whether the conventional range-cell model should continue to serve as the primary interpretive framework for FDA/FDA-MIMO systems. If secondary range peaks are directly incorporated into target detection rather than regarded merely as byproducts of range compression, it remains unclear whether they may support a different form of range discrimination beyond the classical resolution limit.

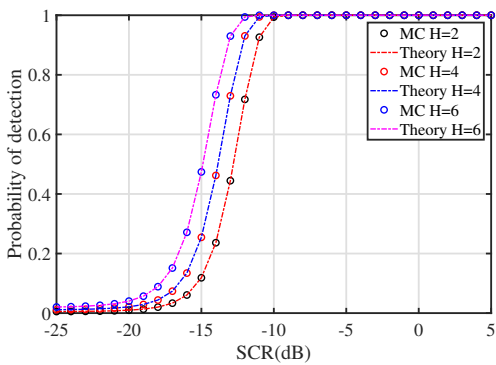


Fig. 22: Probability of detection versus SCR for different numbers of scattering components within a single range cell [85]. Here,  $H$  denotes the number of scatterers (i.e., effective peaks) within the cell, and “MC” represents Monte Carlo simulations. The results show that the detection performance is strongly affected by the intra-cell scattering structure, highlighting the impact of distributed targets in FDA secondary range cell detection.

either mitigated or exploited depending on the system design objective.

6) Challenges and Opportunities: Despite its significant potential, FDA-based detection also faces several fundamental challenges that stem from its range–angle–time coupled signal structure.

1) Non-stationary and range-dependent environments: The range-dependent and non-stationary nature of clutter in FDA systems complicates the construction of homogeneous training data, which is critical for conventional adaptive detection. The violation of the stationarity assumption poses a major challenge for covariance estimation and limits the effectiveness of classical STAP-like methods.

2) High-dimensional signal processing: The expanded signal dimensionality introduced by FDA, while beneficial for detection performance, leads to increased computational complexity. Joint processing across range, angle, and Doppler dimensions requires high-dimensional matrix operations, which may hinder real-time implementation.

3) Hardware and synchronization constraints: FDA relies on precise control of element-dependent frequency offsets and strict phase coherence across transmit channels. Hardware impairments and synchronization mismatches may distort the intended interference structure, degrading performance.

4) Ambiguity–diversity trade-off: The secondary range responses in FDA introduce an inherent trade-off between ambiguity suppression and diversity exploitation, making system design more challenging.

Opportunities:

While these challenges present practical limitations, they also reveal several promising research opportunities.

1) Exploiting Doppler–frequency coupling for high-speed targets: FDA inherently couples Doppler and fre-

quency, providing a new mechanism to mitigate Doppler ambiguity and Doppler spreading. Fully exploiting this property for maneuvering and high-speed targets, especially under range migration, remains an open direction.

2) Detection in heterogeneous and non-Gaussian environments: The non-stationary nature of FDA signals suggests that conventional homogeneous Gaussian assumptions are insufficient. Developing detection frameworks for non-homogeneous clutter, range-dependent interference, and non-Gaussian disturbances is a critical research direction.

3) Distributed detection and structured signal modeling: The secondary range responses in FDA can be interpreted as structured multi-component signals within a single range cell. This enables a transition from single-target detection to distributed detection, opening new possibilities for exploiting intra-cell diversity.

4) Emerging applications in low-altitude scenarios: FDA provides additional degrees of freedom for distinguishing targets in complex environments, which is particularly promising for low-altitude economy (LAE) scenarios involving low-slow-small (LSS) targets. Leveraging FDA for reliable detection in such highly dynamic and cluttered environments is an important future direction.

Overall, these observations suggest that FDA not only introduces new challenges, but also fundamentally expands the design space of radar detection, calling for a unified co-design of waveform, hardware, and signal processing tailored to application-specific requirements.

7) Summary of FDA Detection Advantages: In summary, FDA introduces a fundamentally different detection paradigm by extending the conventional spatial processing framework to a joint range–angle–time domain. Compared with traditional phased-array and MIMO radar systems, FDA offers several distinctive advantages:

- Expanded Degrees of Freedom: The introduction of frequency diversity enables additional controllable dimensions in the transmit signal, providing enhanced capability for clutter and interference suppression.
- Intrinsic discrimination capability: The range-dependent phase structure allows FDA to distinguish targets from deceptive jamming and interference that share similar angular signatures but differ in range characteristics.
- Robustness in ambiguous environments: FDA can effectively mitigate performance degradation in range-ambiguous or Doppler-spread scenarios by exploiting its structured signal diversity.
- Distributed detection capability: The presence of secondary range responses enables a transition from single-target detection to distributed detection, allowing multiple scattering components to be resolved and exploited within a single conventional range cell.

Overall, FDA shifts the role of ambiguity from a limiting factor to a structured source of diversity, thereby opening new opportunities for target detection in complex and contested environments. This paradigm shift positions

FDA as a promising candidate for next-generation radar systems.

### C. Anti-Deception and Anti-Jamming

Electronic counter-countermeasure (ECCM) is one of the most compelling application domains of FDA and FDA-MIMO radar. In particular, FDA exhibits a fundamental advantage in countering mainlobe deceptive jamming, a scenario where conventional phased-array and MIMO radars are known to fail.

**Mainlobe Deceptive Jamming:** Moreover, the robustness of FDA against mainlobe deceptive jamming can be understood from the perspective of signal separability at the receiver. Unlike conventional radar systems, where target and jammer signals share the same angle-dependent steering vector within the mainlobe, FDA introduces an additional range-dependent dimension into the signal manifold. As a result, even when a jammer lies within the mainlobe and matches the angular signature of the target, the corresponding received signals remain distinguishable due to their different ranges. This range-dependent structure enables joint range-angle processing, allowing the receiver to separate or suppress deceptive signals that would otherwise be indistinguishable in conventional systems [83], [113], [119], [223].

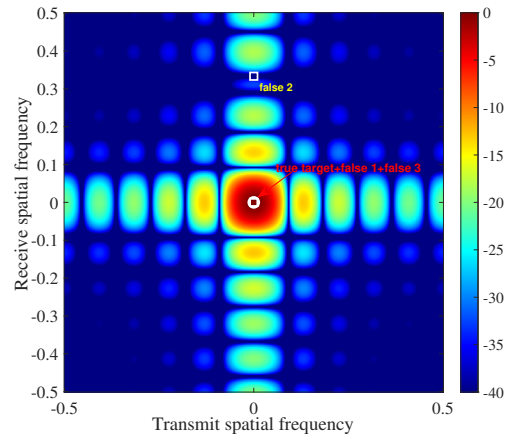
From a structural viewpoint, this separability originates from the range-dependent phase gradient induced by the element-dependent carrier frequencies. Specifically, the propagation-induced phase exhibits a range derivative that varies across the array, and any mismatch between the target and jammer can be characterized as

$$\Delta(\nabla_R \phi_m)_{\text{jam}} \neq \Delta(\nabla_R \phi_m)_{\text{radar}}, \quad (52)$$

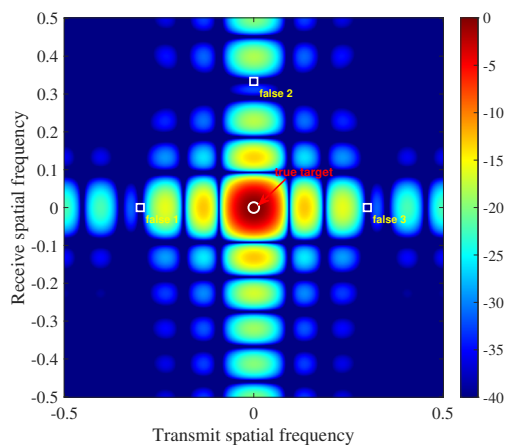
which prevents the jammer from aligning with the target in the joint range-angle domain [224]–[231].

Fig. 23 illustrates the fundamental difference between conventional MIMO and FDA-MIMO in handling deceptive targets. In Fig. 23(a), target separability relies solely on the receive spatial-frequency dimension. While false target 2 can be distinguished from the true target, false targets 1 and 3 fall within the same mainlobe region and remain inseparable, leading to strong ambiguity. In contrast, Fig. 23(b) shows that FDA-MIMO introduces an additional degree of freedom through range-dependent transmit spatial frequencies. Although false targets 1 and 3 still overlap with the true target in the receive domain, they become separable in the transmit dimension. This joint-domain separability enables effective suppression of deceptive targets located within the mainlobe. These results highlight that the key advantage of FDA-MIMO lies in its ability to break the mainlobe ambiguity inherent in conventional MIMO systems by exploiting transmit-side range dependence. In practical terms, FDA does not prevent the generation of deceptive signals, but instead enables the receiver to discriminate them by leveraging the intrinsic range-dependent structure.

Furthermore, the multi-frequency transmit mechanism provides additional diversity across the array, which en-



(a) MIMO



(b) FDA-MIMO

Fig. 23: Comparison of the joint transmit–receive spatial-frequency responses for MIMO and FDA-MIMO. The true target and three deceptive false targets are indicated. In the MIMO case, false target 2 is separable from the true target in the receive spatial-frequency domain and can therefore be suppressed, whereas false targets 1 and 3 lie within the same mainlobe region as the true target and are indistinguishable using receive-domain processing alone. In contrast, FDA-MIMO introduces range-dependent transmit spatial frequencies, which enable additional separation in the transmit dimension, allowing effective suppression of mainlobe deceptive interference.

hances robustness against model mismatch and improves reliability in challenging deceptive jamming scenarios.

**Range-Ambiguous Clutter and General ECCM:** Beyond deceptive jamming, FDA also provides additional degrees of freedom for suppressing range-ambiguous clutter, which is a critical issue in high-PRF airborne radar systems. In such scenarios, clutter from different range intervals may fold into the same observation cell, severely degrading detection performance.

FDA-MIMO radar enables joint range-angle beam-pat-

tern shaping, allowing clutter from different ambiguous regions to be separated or suppressed. Early studies demonstrated that the range-dependent transmit beam pattern can be used to mitigate range ambiguities [232], and subsequent works extended this concept to adaptive space-time-range processing frameworks for improved clutter suppression and target detection [68]–[70]. Existing ECCM approaches can be broadly categorized into three groups. The first exploits range-dependent transmit beam pattern shaping to place nulls at interference locations [71], [82]. The second combines FDA-MIMO with adaptive space-time-range processing to separate target, clutter, and jammer components in a higher-dimensional domain [72], [233]. The third focuses on robust processing strategies, including interference-aware training data selection and optimization-based beamforming [73], [74], [234]. Recent works have also explored hybrid coding schemes, such as quadratic phase coding (QPC) and EPC-assisted FDA, to further enhance robustness in severe interference environments [80], [81], [83], [235].

Discussion: Overall, the key advantage of FDA in ECCM does not merely lie in improved suppression capability, but in its ability to fundamentally reshape the signal manifold. In particular, the range-dependent phase structure introduces a new discrimination dimension that makes coherent deceptive reconstruction significantly more difficult. This capability is especially critical in mainlobe jamming scenarios, where conventional radars lack effective countermeasures. Nevertheless, practical deployment remains challenging. Reliable target-jammer discrimination, robust covariance estimation under range-dependent clutter, and the high computational complexity of space-time-range processing remain open problems. These challenges indicate that the full potential of FDA-based ECCM can only be realized through joint waveform, hardware, and signal processing design.

#### D. Low-Probability-of-Intercept Radar

FDA architectures provide a fundamentally new mechanism for low-probability-of-intercept (LPI) radar design by introducing spatio-temporal energy dispersion at the waveform propagation level. Unlike conventional PA, whose radiation pattern is stationary once the steering direction is fixed, FDA produces a time-varying and range-dependent field distribution. As a result, the instantaneous spatial power density

$$P(t, R_0, \theta) = |\mathcal{A}_{\text{FDA}}(t, R_0, \theta)|^2, \quad (53)$$

becomes inherently non-stationary, exhibiting dynamic evolution over the coupled range-angle-time domain. From a structural perspective, this behavior can be interpreted as a spatio-temporal energy dispersion mechanism, where transmit energy is redistributed across multiple dimensions rather than concentrated at a fixed spatial location. This fundamentally alters the interceptability of the emitted signal, as passive receivers can no longer rely on persistent high-power observations.

To quantitatively characterize this effect, we define the detection persistence ratio as

$$\eta = \frac{1}{T} \int_0^T \mathbb{I}(P(t, R_0, \theta_0) > P_{\text{th}}) dt, \quad (54)$$

where  $\mathbb{I}(\cdot)$  is the indicator function,  $P_{\text{th}}$  denotes the interception threshold, and  $(R_0, \theta_0)$  represents the location of a passive interceptor. This metric captures the fraction of time during which the signal remains detectable and directly reflects the feasibility of interception and coherent integration.

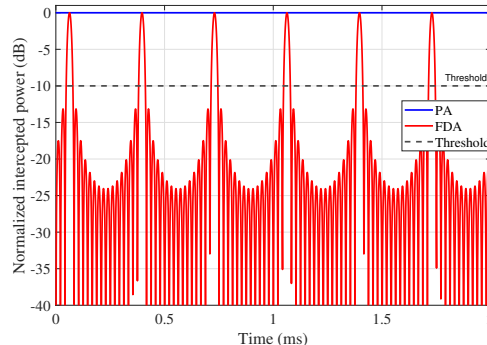


Fig. 24: Intercepted power trajectories at a passive receiver for PA and FDA. A detection threshold is introduced to characterize interceptability. While PA maintains a nearly constant received power above the threshold, FDA exhibits strong temporal fluctuations due to its range-dependent and time-varying radiation structure. Consequently, the FDA signal achieves a significantly reduced detection persistence ratio (approximately 9.25%), compared to 100% for PA, indicating substantially lower interceptability.

Fig. 24 illustrates the intercepted power trajectories at a passive receiver for both PA and FDA. For PA, the received power remains almost constant and continuously exceeds the detection threshold, leading to  $\eta \approx 1$ . This enables stable interception and facilitates long-time coherent integration at the receiver. In contrast, FDA produces a highly time-varying received power due to its intrinsic range-angle-time coupling. As shown in Fig. 24, the received power intermittently crosses the detection threshold, resulting in a much smaller detection persistence ratio (e.g.,  $\eta \approx 9.25\%$  in this example).

This observation reveals that FDA-enabled LPI is fundamentally achieved not by reducing the instantaneous transmit power, but by suppressing the temporal persistence of detectability. The intermittent nature of the received signal prevents reliable energy accumulation and disrupts coherent processing at passive interceptors. From a physical standpoint, the reduction of  $\eta$  can be directly attributed to the additional time and range phase gradients induced by frequency offsets across the array elements. These gradients continuously reshape the interference pattern in space, causing the high-energy regions to drift over time and preventing sustained illumination of any fixed location.

Existing studies have explored several design strategies to exploit this property. One line of work leverages FDA-induced range–angle coupling and temporal variability to introduce ambiguity or deception in passive localization [236], [237]. Another direction focuses on joint transmit–receive optimization, where adaptive beam pattern shaping is employed to balance detection performance and LPI requirements [96]. This concept has also been extended to integrated radar–communication systems, where LPI-oriented waveform design is jointly optimized with communication signaling to ensure coexistence and interference mitigation [107]. In addition, cognitive FDA frameworks have been proposed, in which frequency offsets and array phases are dynamically adapted to enhance radio-frequency stealth in complex environments [238].

Overall, FDA provides a promising pathway for LPI radar by transforming interceptability from a static power-level problem into a dynamic spatio-temporal behavior. The introduced detection persistence ratio serves as a unifying metric that links transmit-side waveform design to receiver-side detectability. However, the actual LPI performance depends not only on the transmit strategy but also on the interception capability of adversarial receivers, suggesting that receiver-aware and scenario-dependent design remains an important open research direction.

### E. Imaging and Wide-Area Surveillance

Building upon the capability-mapping framework established in the previous section, FDA-enabled imaging can be interpreted as a direct consequence of range–angle selectivity and frequency-domain diversity. These capabilities fundamentally reshape the signal formation process in radar imaging, providing new mechanisms for resolution enhancement, ambiguity suppression, and scene reconstruction. In contrast to conventional PA-based imaging systems, where the transmit response depends primarily on angle, FDA introduces explicit range-dependent propagation characteristics. As a result, the imaging process is no longer governed solely by receiver-side aperture synthesis, but also by the transmit-side manifold expansion.

**Range-Domain Resolution and Multi-Frequency Synthesis:** From the perspective of frequency-domain diversity, FDA can be viewed as a distributed multi-frequency transmit aperture. Each array element radiates at a slightly different carrier frequency, leading to a composite spectrum that spans a wider frequency range. Under ideal coherent synthesis across frequency channels, the composite spectrum spans a frequency range approximately given by

$$B_{\text{eff}} \approx B + (M - 1) \Delta f. \quad (55)$$

However, it should be noted that this extended bandwidth can only translate into improved range resolution if coherent processing across different frequency components is properly achieved.

More fundamentally, this effect originates from the range-phase gradients introduced by frequency offsets, which create additional interference structures along the range dimension. Compared with conventional SAR, where range resolution is determined solely by signal bandwidth, FDA introduces a secondary range discrimination mechanism associated with the multi-frequency transmit aperture [239]–[241].

**Ambiguity Suppression via Range–Angle Coupling:** Beyond resolution enhancement, FDA also provides new mechanisms for ambiguity suppression through its intrinsic range–angle selectivity. Because the transmit response depends jointly on range and angle, echoes originating from different ambiguous regions may exhibit distinguishable signatures even when they overlap in conventional SAR processing.

This property is particularly beneficial for high-resolution wide-swath (HRWS) SAR systems [243]–[247], where range and azimuth ambiguities pose fundamental limitations. By exploiting the range-dependent transmit field, FDA enables additional separation mechanisms that can be leveraged through adaptive beamforming or spectral reconstruction techniques. Similarly, in forward-looking SAR configurations, where Doppler diversity is inherently limited, the range-dependent transmit structure provides an alternative source of diversity, thereby improving imaging performance in scenarios where conventional approaches are constrained [232], [248]–[250].

**Imaging Manipulation and Electronic Countermeasures:** In addition to performance enhancement, the same multi-dimensional characteristics of FDA can also be exploited in electronic countermeasure (ECM) scenarios. One representative line of work employs scene-template-based deceptive jamming, in which a desired false target template is first constructed and then embedded into the SAR echo formation process to manipulate the final reconstructed image. An example is shown in Fig. 25, where an aircraft template is injected into a real GF-3 runway scene, resulting in structured false targets appearing in the final SAR image. From a system perspective, FDA-induced range–angle coupling enables more flexible control over the spatial and spectral distribution of transmitted signals. In SAR deception scenarios, this flexibility can be used to generate artificial scatterers or manipulate reconstructed images by injecting multi-frequency and spatially distributed interference [242], [251]–[258]. Compared with conventional jamming techniques, FDA-based approaches provide additional degrees of freedom for shaping false targets and distributed interference patterns in the image domain.

Overall, despite these potential advantages, the practical realization of FDA-based imaging remains challenging. On the one hand, multi-frequency synthesis requires strict phase coherence across transmit channels, imposing demanding hardware synchronization and calibration requirements. On the other hand, the range–angle coupling introduced by FDA breaks the separability assumptions underlying conventional SAR processing, thereby neces-

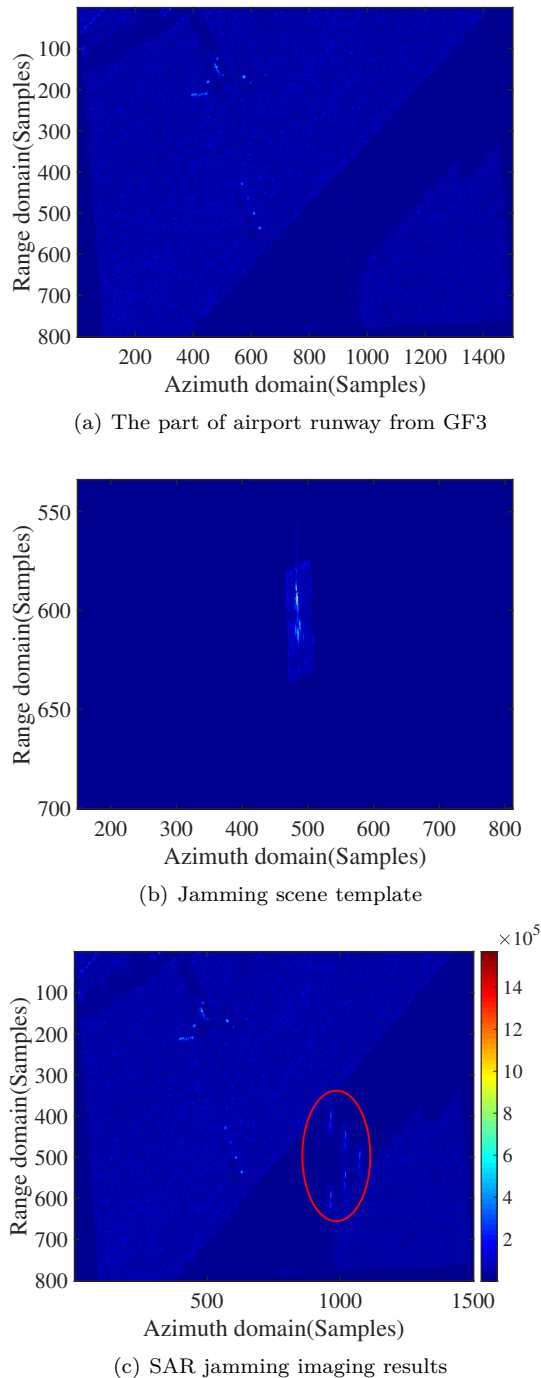


Fig. 25: Example of scene-template-based deceptive jamming in SAR using FDA [242]. This example illustrates that FDA can be exploited not only for sensing and imaging enhancement, but also for image-domain manipulation and electronic countermeasures through controllable range-angle-dependent signal synthesis.

sitating new reconstruction algorithms that explicitly account for the expanded transmit manifold.

Beyond these fundamental issues, most existing FDA imaging studies remain largely theoretical. Practical challenges such as bandwidth constraints, computational complexity, and robustness in heterogeneous environments have yet to be fully addressed. While the time-evolving beam property may offer additional diversity in dynamic scenarios, its role in imaging is not yet well established and remains an open topic for future investigation. A further open issue arises if FDA-based SAR imaging moves beyond the conventional pulse-compression-based treatment of the range dimension. In that case, classical SAR imaging algorithms and processing chains may no longer be directly applicable, and it remains an open question how HRWS SAR imaging should be reformulated under an FDA-oriented imaging framework.

#### F. Target Tracking and Adaptive Sensing

Target tracking requires radar systems to continuously estimate the kinematic state of a target while maintaining sufficient illumination and measurement quality over time. In conventional phased-array systems, beam steering is achieved through spatial phase control, resulting in angle-focused but range-invariant transmit beampatterns that remain essentially static once configured. By contrast, the element-dependent carrier frequencies of FDA introduce explicit time-range phase gradients across the transmit aperture, leading to inherently time-varying and range-angle-coupled transmit responses. This structural property provides additional flexibility for shaping the spatiotemporal distribution of radiated energy, and has motivated a series of studies on FDA-based target tracking.

A central line of work focuses on exploiting the range-angle-dependent beampattern of FDA for tracking purposes. However, the intrinsic time-variant and range-periodic characteristics of conventional FDA beampatterns significantly limit their direct applicability, as targets are only intermittently illuminated with sufficient energy. To overcome this limitation, several studies have proposed the synthesis of time-invariant and range-angle-focused beampatterns through nonlinear or time-dependent frequency offset designs, as well as multicarrier FDA architectures [259]–[263]. These approaches enable the formation of pencil-shaped beams that remain concentrated at a desired range-angle location over time, thereby improving energy accumulation and facilitating more reliable tracking. Extensions to multi-target scenarios have also been investigated, primarily through time-division-based beam synthesis approaches, where multiple focused beams are sequentially formed within a pulse duration to enable multi-target tracking [264].

Beyond transmit beampattern synthesis, FDA has also been explored from the perspective of adaptive sensing. By dynamically adjusting the frequency offsets based on prior observations, the transmit field can be reconfigured to emphasize specific range regions where targets are

likely to appear. This capability is closely related to the concept of cognitive radar [265]–[269], in which waveform parameters are adaptively updated in a closed-loop manner according to the estimated target state. In this sense, FDA provides a form of range-aware adaptive illumination that is not directly available in conventional phased-array systems. Nevertheless, existing works in this direction are still primarily focused on transmit-side design, and the integration with complete tracking frameworks, such as Kalman or particle filtering with FDA, specific measurement models—remains relatively limited.

Despite these developments, the practical use of FDA in target tracking still faces several fundamental challenges. First, tracking-oriented FDA designs usually rely on carefully engineered nonlinear or time-dependent frequency offsets, which increase waveform design complexity and make real-time implementation more difficult. Second, even when approximately time-invariant focusing is synthesized, residual range–angle coupling and inherent range periodicity may still undermine stable target illumination, especially in cluttered or multi-target scenarios. Third, because FDA signals are intrinsically time-varying and structurally coupled, it remains difficult to formulate measurement models that are both physically consistent and convenient for recursive tracking algorithms. Finally, most existing studies remain focused on transmit-side beampattern synthesis, whereas the end-to-end advantages of FDA in complete tracking pipelines, including detection, association, filtering, and robustness analysis, are still far from fully established.

Overall, FDA introduces a distinctive mechanism for range–angle-dependent beam control and adaptive illumination, which may provide additional flexibility for target tracking. However, compared with its more mature applications in interference suppression and range-aware sensing, the role of FDA in target tracking is still in an early stage and requires further systematic investigation.

### G. Summary and Key Insight

The above analysis reveals that the performance gains of FDA radar are not determined by individual signal processing techniques, but by whether the underlying phase-gradient structure induced at the propagation level can be effectively aligned with the requirements of a given task. This relationship is summarized in Table III, which provides a mapping between FDA physical degrees of freedom, their induced structural mechanisms, and the corresponding radar task capabilities. From this perspective, different radar tasks exploit fundamentally different manifestations of FDA-induced diversity. Estimation and localization primarily benefit from range–angle manifold expansion, detection in complex environments relies on range diversity for clutter suppression, while anti-deception capability arises from joint range–angle separability that prevents coherent matching by deceptive signals. LPI performance is enabled by spatio-temporal energy dispersion, whereas imaging and tracking tasks

depend on virtual aperture extension and dynamic range-aware beam control, respectively.

These observations indicate that FDA does not provide a uniform improvement over conventional radar systems. Instead, its effectiveness is fundamentally governed by a structure–task matching principle: performance gains can only be realized when the FDA-induced structural properties remain physically irreducible and can be coherently exploited under given processing and environmental conditions. Otherwise, the additional degrees of freedom collapse into equivalent conventional representations, yielding limited or no practical advantage.

## VII. Extensions Toward Communications and Integrated Sensing and Communications (ISAC)

Beyond conventional radar applications, FDA has also attracted increasing attention in communication and integrated sensing and communication (ISAC) systems. This extension naturally raises a fundamental question: whether the frequency-gradient-induced range dependence introduces genuinely new communication-theoretic capabilities, or simply reshapes existing spatial resources in a different form. To address this question, FDA-enabled communication and ISAC systems can be interpreted from a structural perspective. Specifically, the frequency offsets at the transmit side modify the propagation kernel, which in turn reshapes the channel structure and influences the resulting information-theoretic performance metrics, ultimately leading to new sensing–communication trade-offs. From this viewpoint, the role of FDA in communication is not merely to provide an additional design parameter, but to alter the geometry of the underlying channel representation. This perspective enables a interpretation of FDA-based secure transmission, index modulation (IM), and ISAC waveform design within a common analytical framework.

### A. Physical-Layer Secure Communications

Physical-layer security is one of the earliest and most extensively investigated application directions of FDA in communication systems. By introducing element-dependent frequency offsets, FDA generates range-dependent beampatterns, enabling selective signal focusing in both angle and range domains. This allows FDA to distinguish users that are closely aligned in angle but separated in range, thereby providing a fundamental mechanism for enhancing secrecy performance beyond conventional angle-only beamforming.

At a more fundamental level, such security capability originates from the irreducible range-phase gradient introduced by FDA across the transmit aperture, given by

$$\nabla_R \phi_m = -\frac{2\pi(f_c + \Delta f_m)}{c}. \quad (56)$$

This gradient induces intrinsic differences in the propagation responses toward users located at different ranges, resulting in a range–angle-dependent channel structure

TABLE III: Mapping between FDA physical degrees of freedom, underlying mechanisms, and radar task capabilities.

Task	Primary FDA DoF	Underlying Mechanism
Parameter Estimation & Localization	Frequency	Range–angle manifold expansion
Detection in Complex Environments	Frequency	Range diversity for clutter suppression
Anti-Deception & Anti-Jamming	Frequency + Space	Joint range–angle separability
Low-Probability-of-Intercept (LPI)	Time + Frequency	Spatio-temporal energy dispersion
Imaging & Wide-Area Surveillance	Frequency + Space	Virtual bandwidth and aperture extension
Target Tracking & Adaptive Sensing	Time + Frequency	Dynamic range-aware beam control

that cannot be replicated by conventional PA systems. Consequently, FDA enables physical-layer security through propagation-layer differentiation, rather than relying solely on signal-domain processing.

From a communication-theoretic perspective, consider a legitimate user located at  $(R_L, \theta_L)$  and an eavesdropper at  $(R_E, \theta_E)$ . Under FDA transmission, the effective channels can be expressed as

$$h_L = \mathbf{w}^H \mathbf{a}(R_L, \theta_L), \quad h_E = \mathbf{w}^H \mathbf{a}(R_E, \theta_E), \quad (57)$$

where  $\mathbf{a}(R_0, \theta)$  denotes the FDA array manifold. Unlike conventional phased-array systems with  $h(\theta)$ , the FDA channel explicitly depends on both range and angle. The resulting secrecy rate is given by

$$C_s = [\log_2(1 + \gamma_L) - \log_2(1 + \gamma_E)]^+, \quad (58)$$

which is fundamentally governed by the separability of  $\mathbf{a}(r, \theta)$  in the joint range–angle domain. In particular, secure transmission becomes feasible when

$$\mathbf{a}(R_L, \theta_L) \neq \mathbf{a}(R_E, \theta_E), \quad (59)$$

even if  $\theta_L \approx \theta_E$  but  $R_L \neq R_E$ , highlighting the role of range-dependent channel discrimination.

Motivated by this structural property, existing FDA-based physical-layer security techniques can be broadly categorized into two main paradigms: artificial noise (AN) injection and directional modulation (DM). The AN-based approach enhances secrecy by projecting interference into the orthogonal range–angle subspace of the legitimate user, thereby degrading the reception quality of potential eavesdroppers [97]–[99]. In contrast, DM-based schemes directly manipulate the transmitted constellation in a location-dependent manner, such that only the intended receiver can correctly demodulate the signal, while distorted constellations are observed at other locations [100]–[102], [270], [271]. These two paradigms exploit the range–angle-dependent transmission property of FDA from complementary perspectives and have been further extended to more complex scenarios. For example, Jian et al. [104] investigated multi-hop FDA systems and jointly exploited AN and DM to enhance secrecy performance across multiple transmission stages. Beyond these canonical paradigms, FDA has also been integrated with advanced modulation schemes to further improve both security and spectral efficiency. For instance, Basit et al. [272] combined FDA with quadrature spatial modulation (QSM), enabling information embedding through

frequency offsets. This line of work further suggests that FDA extends secure transmission from angle-only to joint range–angle domains.

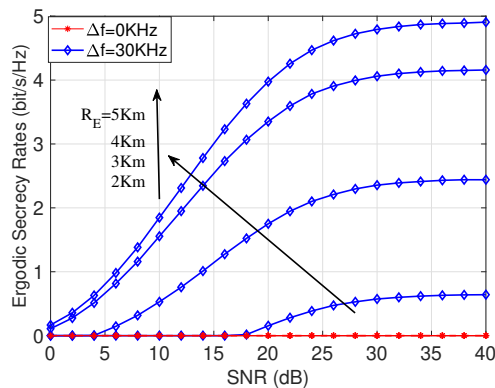


Fig. 26: Ergodic secrecy rate versus SNR for PA ( $\Delta f = 0$ ) and FDA ( $\Delta f = 30$  kHz) under different eavesdropper distances  $R_E$  [104]. While PA yields nearly zero secrecy rate, FDA achieves significant secrecy gains that increase with SNR and improve as the eavesdropper moves farther away, demonstrating its inherent range-dependent security capability.

Fig. 26 demonstrates the secrecy performance difference between PA and FDA systems. Due to the lack of range selectivity, the PA scheme fails to provide positive secrecy rate, as both the legitimate user and the eavesdropper experience similar channel gains. In contrast, FDA introduces a frequency-induced range–angle coupling, which enables spatially selective energy focusing not only in angle but also in range. As a result, FDA effectively suppresses signal leakage toward the eavesdropper, leading to a significant secrecy rate improvement. Furthermore, as the eavesdropper moves away from the intended range, the mismatch in the FDA beam pattern becomes more pronounced, yielding higher secrecy gains.

Despite these advantages, such gains are not universally guaranteed and depend on several practical conditions. First, the achievable secrecy gain strongly relies on accurate range information, and the advantage diminishes when the eavesdropper is located close to the legitimate user. Second, if the frequency offsets are known and can be compensated, the range-dependent structure may be weakened, reducing the security benefit. Finally, practical issues such as time-varying beam patterns, synchronization

requirements, and hardware complexity further constrain real-world deployment.

## B. Index Modulation and Hybrid Transmission Schemes

Index modulation (IM) improves spectral efficiency (SE) by encoding information into transmission resource indices, antennas, subcarriers, time slots, carrier frequencies, or channel states [273]–[276]. In FDA systems, element-dependent frequency offsets introduce a fundamentally new indexing mechanism, where information can be embedded directly into the frequency-gradient domain. From a physical perspective, this capability originates from the frequency-gradient structure of FDA. By assigning  $f_m = f_c + \Delta f_m(b)$ , the transmitted waveform becomes dependent on the selected frequency-offset pattern indexed by  $b$ . Unlike conventional IM schemes that rely on discrete antenna or subcarrier selection, FDA enables indexing through structured frequency variations, thereby introducing a propagation-level signaling dimension.

From a signal representation viewpoint, classical IM can be expressed as

$$\mathbf{s} = \mathbf{e}_k x, \quad (60)$$

where  $\mathbf{e}_k \in \mathbb{C}^{N_t}$  denotes the  $k$ -th canonical basis vector (i.e., the  $k$ -th transmit antenna or subcarrier is activated), and  $x \in \mathbb{C}$  is the modulated symbol drawn from a given constellation. FDA-based IM extends this principle by mapping information bits to frequency-offset configurations. Consequently, the effective signaling space can be characterized as

$$\text{DoF}_{\text{IM-FDA}} = \text{Space} \oplus \text{Frequency}, \quad (61)$$

indicating that FDA expands the index domain beyond conventional spatial or subcarrier-based schemes. This additional degree of freedom enables more flexible information embedding and provides new opportunities for SE enhancement.

From a design perspective, existing FDA-based IM schemes can be interpreted as progressively exploiting this frequency-gradient-induced dimension. Early works focus on frequency-offset-only indexing, where information is conveyed by selecting or rearranging frequency offsets [277]–[279]. Subsequent approaches introduce joint space–frequency indexing, combining antenna selection with frequency offsets to improve SE [280]. More recent studies further integrate FDA-based IM with system-level functionalities, such as receiver-efficient designs and multi-user security-oriented transmission [281], [282]. Overall, this evolution reflects a transition from single-domain indexing to multi-domain joint modulation across space, frequency, and system dimensions. Motivated by this expanded signaling space, FDA has also been combined with various communication frameworks to form hybrid transmission schemes. Typical examples include integration with OFDM for joint subcarrier–frequency indexing, space-time coding for diversity enhancement, artificial-noise-aided transmission for secure IM [283]–[287]. These

designs exploit multiple domains jointly to further enhance flexibility and performance [288].

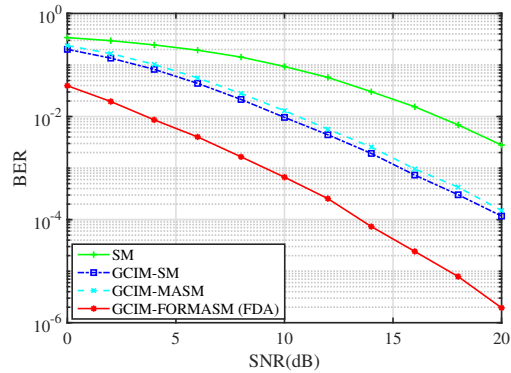


Fig. 27: BER performance of index modulation schemes with different indexing domains [288].

Fig. 27 shows the BER performance of different IM schemes with increasing indexing dimensions. Conventional schemes such as spatial modulation (SM) [289], generalized code index modulation-SM (GCIM-SM) [290], and generalized CM modulation-aided multiple-antenna SM (GCIM-MASM) [288] exploit spatial and coding domains for information embedding. In contrast, the proposed FDA-based scheme introduces the frequency-offset dimension as an additional index domain. The inclusion of this frequency index increases the overall indexing dimensionality, resulting in a larger set of distinguishable transmission states. Consequently, the receiver can better differentiate between index combinations, leading to improved detection reliability and reduced BER.

From a broader perspective, a fundamental question remains: whether FDA-based IM introduces genuinely new physical degrees of freedom, or merely redistributes existing signaling resources across spatial and frequency domains. Answering this question is essential for understanding the ultimate performance limits of FDA-enabled communication systems.

## C. FDA-Enabled ISAC Systems

Motivated by the unique physical-layer characteristics of FDA-MIMO, recent studies have begun to explore its integration into ISAC systems. Although this research direction is still in its early stage, accumulating works suggest that FDA-MIMO introduces fundamentally new design opportunities beyond conventional ISAC paradigms. Unlike conventional PA or MIMO-based ISAC systems, where sensing and communication primarily share spatial (angle-domain) resources, FDA-MIMO introduces a frequency-gradient-induced propagation structure, which gives rise to an additional range-dependent degree of freedom. Specifically, by assigning element-dependent carrier frequencies, the resulting transmit field becomes inherently dependent on time, range, and angle. This leads to a range-selective propagation kernel, enabling the transmit energy distribution to be jointly controlled over

both angle and range dimensions. As a result, range is no longer merely an observable parameter for sensing, but becomes a controllable resource that can be actively exploited for joint sensing and communication design.

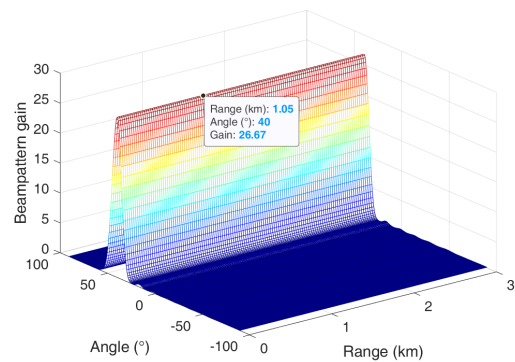
From this perspective, existing FDA-MIMO-based ISAC schemes can be reinterpreted under a unified framework, where both sensing and communication functionalities are realized through range-dependent signal shaping.

1) Communication-oriented designs: Several works embed communication information into FDA-MIMO radar waveforms by exploiting the frequency-offset dimension. For instance, information bits can be conveyed through the sign or configuration of frequency offsets [291], or embedded via time-modulated spreading sequences [292]. More advanced designs further improve communication rate by dividing pulses into multiple chips carrying PSK symbols [293], or by introducing index modulation over waveform selection and frequency-offset patterns [294], [295]. These approaches effectively utilize the range-dependent channel variations induced by FDA to realize communication signaling.

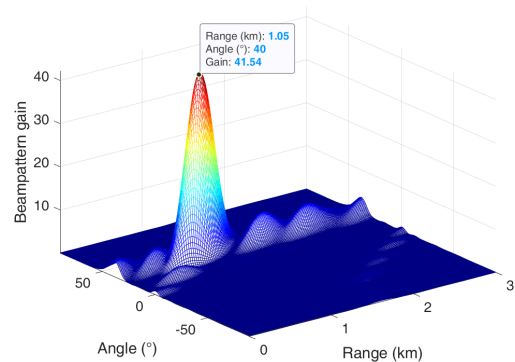
2) Sensing-oriented enhancements: On the sensing side, FDA-MIMO enables improved robustness against interference and ambiguity. For example, frequency-offset design can mitigate range ambiguities and facilitate multi-target parameter estimation [296]. Furthermore, FDA's range-dependent beam pattern provides inherent capability to suppress mainlobe deceptive jamming and clutter [297], which are difficult to handle using conventional angle-only beamforming.

3) Joint ISAC optimization: Beyond isolated designs, several works explicitly exploit FDA-MIMO for joint sensing-communication optimization. These include transmit waveform and receive filter co-design for LPI communication [107], region-focused sensing with multi-user communication via joint beamforming [298], and RIS-assisted FDA-MIMO ISAC systems for clutter suppression and rate maximization [299]. These studies demonstrate the flexibility of FDA in balancing sensing and communication performance.

Figs. 28-29 illustrate the fundamental difference between conventional MIMO and FDA-MIMO in ISAC systems. As shown in Fig. 28, conventional MIMO exhibits angle-only beamforming, where the transmit energy is distributed uniformly along the range dimension and thus cannot selectively focus on a specific spatial region. In contrast, FDA-MIMO enables joint angle-range focusing due to its frequency-gradient-induced propagation structure, allowing energy to be concentrated within a desired range-angle region for area-selective surveillance. This structural capability directly impacts the communication performance. As shown in Fig. 29, FDA-MIMO achieves higher communication sum rates compared to MIMO under multi-user scenarios. By properly designing the frequency offsets and transmit strategy, FDA-MIMO can exploit the range-dependent channel variations to improve user separability and enhance communication efficiency. More importantly, these gains are not independent im-



(a) MIMO



(b) FDA-MIMO

Fig. 28: Comparison of area surveillance performance between MIMO [300] and FDA-MIMO [298]. MIMO provides angle-only beamforming, while FDA-MIMO achieves joint angle-range focusing for area-selective surveillance.

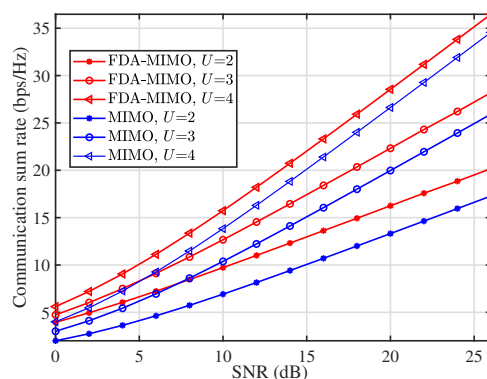


Fig. 29: Communication sum rate versus SNR, showing that FDA-MIMO outperforms MIMO under multi-user transmission.

provements in sensing and communication. Instead, both the area-selective sensing capability and the communication rate enhancement originate from the same underlying mechanism, namely the range-dependent signal shaping enabled by the frequency gradient. This demonstrates that FDA-MIMO does not merely provide additional functionality, but fundamentally enables a new ISAC operating paradigm in which sensing and communication are jointly controlled through the propagation structure.

Despite their diverse implementations, the aforementioned works share a common underlying principle: both communication and sensing functionalities are enabled by the same range-dependent propagation mechanism introduced by FDA. From a communication perspective, techniques such as IM and waveform embedding exploit the distinguishability of range-dependent channel responses, while from a sensing perspective, interference suppression and ambiguity mitigation arise from the ability to shape the transmit energy distribution across range. Therefore, these seemingly different functionalities can be interpreted as different manifestations of a unified concept, namely range-selective signal shaping.

This unified mechanism also leads to a fundamental sensing-communication trade-off governed by the frequency gradient. On one hand, increasing the frequency offset enhances the range-dependent phase variation across the array, improving the sensitivity of the signal with respect to range and angle parameters and thus boosting sensing performance. On the other hand, the same mechanism introduces channel decorrelation and phase dispersion, which reduces the coherence of the effective communication channel and degrades communication reliability. As a result, the frequency offset acts as a shared structural variable that couples sensing and communication, giving rise to a Pareto frontier between sensing accuracy and communication efficiency.

From a higher-level perspective, the key contribution of FDA to ISAC is not merely the introduction of an additional range dimension, but the transformation of how sensing and communication are fundamentally coupled. In conventional ISAC systems, sensing and communication primarily share spatial resources, leading to an angle-centric design paradigm in which the two functionalities inevitably compete for the same degrees of freedom. As a result, the sensing-communication trade-off is largely determined by resource allocation strategies. In contrast, FDA introduces a frequency-gradient-induced propagation structure that jointly governs both the sensing signal manifold and the communication channel. Under this mechanism, sensing and communication are no longer independent functionalities sharing common resources, but are intrinsically coupled through the same range-dependent propagation process.

Consequently, the sensing-communication trade-off in FDA-enabled ISAC systems is not resource-driven but structure-induced. The frequency gradient simultaneously controls the sensitivity of the signal with respect to environmental parameters and the coherence properties of

the communication channel, thereby shaping both sensing and communication performance in a unified manner. This reveals a fundamental paradigm shift: FDA transforms ISAC design from resource sharing to structure coupling, enabling sensing and communication to be coordinated through the same physical mechanism rather than balanced through resource partitioning.

## VIII. Limitations, Misconceptions, and Future Research Directions

While FDA introduces a structurally enriched propagation model with expanded manifold degrees of freedom, its advantages are neither universal nor unconditional. Many reported gains rely on idealized assumptions regarding coherence, linear phase gradients, and hardware realizability, which may not hold in practical scenarios. More importantly, several commonly cited properties of FDA, such as time-invariant focusing or arbitrary range-angle decoupling, are often misunderstood or overstated. A rigorous examination reveals that these behaviors are intrinsically constrained by the underlying frequency-gradient mechanism and its interaction with propagation physics. In this section, we revisit these issues from a unified perspective, aiming to (i) clarify prevalent misconceptions, (ii) identify the fundamental conditions under which FDA provides meaningful gains, and (iii) outline key research directions for bridging the gap between theoretical potential and practical deployment.

### A. On the Feasibility of Time-Invariant Focusing

A recurring claim in parts of the early FDA literature is that time-invariant spatial focusing can be achieved through appropriate frequency design. However, as discussed earlier, the frequency-gradient mechanism of FDA inherently introduces temporal phase evolution into the transmit manifold. As a result, strict time-invariant focusing is not physically compatible with the basic FDA operating principle: once nonzero frequency offsets are used to create range-dependent behavior, the corresponding array response necessarily evolves with time.

From this perspective, the notion of time-invariant focusing should be interpreted with caution. What many existing studies actually realize is not a truly time-invariant FDA field, but rather one of several practical approximations, such as instantaneous focusing at selected snapshots, receive-side compensation, or multi-pulse synthesis that stabilizes the apparent focusing effect over a longer observation interval.

The key structural point is that time invariance and frequency-gradient-induced range selectivity arise from conflicting requirements. The former requires suppressing temporal phase evolution, whereas the latter fundamentally depends on it. Therefore, strict time-invariant focusing and genuine FDA range selectivity cannot be simultaneously achieved within the same single-transmit physical mechanism. This distinction is important for avoiding overstatement in the interpretation of FDA beampattern design results.

## B. Near-Field and Far-Field Applicability Boundary

Most existing FDA analyses are established under the far-field approximation, where the propagation distance of the  $m$ -th element is linearized as

$$R_m \approx R_0 - d_m \sin \theta. \quad (62)$$

Under this assumption, the FDA-induced phase variation can be interpreted as a linear gradient over range and angle, forming the basis of the commonly adopted range-angle coupling model. However, in near-field regimes, the exact propagation distance follows

$$R_m = \sqrt{R_0^2 + d_m^2 - 2R_0d_m \sin \theta}, \quad (63)$$

which introduces intrinsic spherical-wave effects that fundamentally alter the signal structure.

In the near-field, range and angle are inherently coupled by geometry, independent of any frequency offset. As a result, the coupling induced by FDA is no longer the sole source of range-angle dependence, but instead interacts with the natural spherical-wave coupling. This leads to two key consequences:

- The classical interpretation of FDA as a frequency-gradient-induced linear coupling becomes invalid,
- The overall signal manifold is governed by a superposition of geometric coupling and frequency-induced effects.

The far-field FDA model remains valid only when the linear approximation holds, i.e.,

$$\frac{D^2}{\lambda_0} \ll R_0, \quad (64)$$

where  $D$  denotes the array aperture. When this condition is violated, near-field effects dominate, and the FDA signal model must be reformulated based on spherical-wave propagation. FDA does not introduce range-angle coupling in isolation; rather, it modifies an existing propagation structure. In the far-field, this structure is approximately separable and can be shaped by frequency gradients, whereas in the near-field, the intrinsic geometric coupling becomes dominant. Consequently, the role of FDA shifts from creating range-angle coupling to modulating an already coupled propagation manifold.

## C. Frequency-Offset Constraints under Wideband Conditions

Most FDA analyses are derived under the narrowband assumption

$$B \ll f_c, \quad (65)$$

which ensures that the propagation-induced phase can be approximated as a linear function of the frequency offset. Under this condition, the frequency gradient  $\Delta f$  induces a well-defined and coherent phase structure across array elements. However, practical radar and communication systems often operate in wideband regimes, where this

assumption no longer holds. To preserve the linear phase-gradient interpretation, the frequency offset must satisfy

$$\Delta f \ll B. \quad (66)$$

This condition ensures that the frequency diversity across array elements remains small relative to the signal bandwidth, thereby maintaining inter-element coherence.

When  $\Delta f \sim B$ , the FDA structure undergoes a qualitative change:

- Inter-element signals become partially decorrelated,
- The linear phase-gradient model breaks down,
- The resulting ambiguity function becomes distorted and irregular.

The frequency offset is further constrained by hardware limitations, typically requiring

$$\Delta f \leq \min(B, f_c/Q), \quad (67)$$

where  $Q$  characterizes oscillator stability and frequency accuracy. These constraints reveal an inherent trade-off: increasing  $\Delta f$  enhances range-dependent discrimination, but simultaneously weakens coherence and violates the assumptions underlying FDA modeling.

Wideband signaling and frequency-gradient design impose conflicting structural requirements. The former relies on frequency diversity across the signal spectrum, while the latter requires coherence across array elements with controlled frequency offsets. Consequently, the benefits of FDA cannot be arbitrarily amplified by increasing either bandwidth or frequency gradient alone. Effective system design must balance these two factors to preserve both gradient interpretability and signal coherence.

## D. Experimental Validation and Dataset Challenges

A major limitation of current FDA research lies in the lack of large-scale, reproducible, and systematically calibrated experimental validation. Although a substantial body of work has reported promising analytical and simulation-based results, the extent to which these gains can be sustained under realistic operating conditions remains largely unclear. At present, most FDA studies still rely on numerical simulations or small-scale laboratory prototypes, while publicly available benchmark datasets and broadly accessible experimental platforms remain extremely limited.

This gap is particularly critical because FDA is more sensitive to implementation imperfections than many conventional array architectures. Its expected behavior depends on the accurate preservation of frequency-gradient-induced phase structures across the transmit aperture. Consequently, practical FDA systems impose stringent requirements on inter-channel phase calibration, frequency synchronization, and environmental stability. Even small mismatches in phase, timing, oscillator stability, or channel responses may distort the intended range-dependent interference structure, thereby weakening or even obscuring the very effects that FDA is expected to provide.

From this perspective, the experimental challenge in FDA is not merely one of hardware scale or engineering complexity. More fundamentally, it concerns whether the frequency-gradient structure can be generated, maintained, and measured with sufficient fidelity for the claimed physical mechanisms to remain observable. This also explains why direct comparison across different FDA designs is currently difficult: without common datasets, standardized calibration procedures, and shared evaluation protocols, it remains hard to determine whether performance differences are caused by algorithmic improvements or by differences in hardware assumptions and implementation conditions.

Dataset construction is equally challenging. Unlike conventional radar benchmarks, FDA-oriented datasets must preserve not only target and clutter information, but also detailed calibration metadata associated with frequency offsets, phase alignment, synchronization quality, and scene stability. Without such information, many FDA-specific phenomena cannot be reliably reproduced or fairly evaluated. As a result, the absence of open and standardized datasets has become a significant bottleneck for reproducibility, cross-comparison, and data-driven FDA research.

Future progress therefore requires more than isolated hardware demonstrations. It calls for a broader validation ecosystem, including scalable multi-channel FDA testbeds, open benchmark datasets with explicit calibration and synchronization records, and standardized evaluation protocols that enable fair comparison across different array architectures, signal designs, and processing methods. Only through such efforts can the field move from proof-of-concept demonstrations toward robust and reproducible experimental evidence.

Overall, the challenge of experimental validation in FDA should be viewed as a structural issue rather than a purely engineering one. Because the core FDA mechanism is highly sensitive to implementation fidelity, robustness, repeatability, and calibration transparency are central to translating FDA from theoretical promise into practically credible systems.

### E. Future Research Directions

Building upon the aforementioned limitations, future FDA research should move beyond incremental algorithm design toward a deeper understanding of its structural properties and practical realizability. Several key research directions are outlined as follows.

(1) **Coherent FDA Modeling and Processing:** A fundamental challenge lies in maintaining and exploiting coherence in FDA systems. Future work should investigate coherent FDA frameworks, including phase-consistent waveform design, coherent accumulation strategies, and the impact of frequency offsets on coherent integration. In particular, understanding how coherence can be preserved or reconstructed across time, frequency, and array elements remains an open problem.

(2) **Hybrid FDA–PA and Multi-Mode Architectures:** Rather than viewing FDA as a standalone paradigm, hybrid architectures that combine FDA and conventional PA offer a promising direction for balancing flexibility and stability. Such designs enable controlled cooperation between angle-dominant (PA-like) and range–angle coupled (FDA-like) transmission modes. In hybrid FDA–PA architectures, only a subset of array elements employ frequency offsets, while the remaining elements operate at a common carrier frequency. By properly selecting the number and placement of frequency-offset elements, the strength of range–angle coupling can be regulated, allowing the system to retain part of the additional degrees of freedom introduced by FDA while mitigating excessive coupling and instability.

Beyond spatial hybridization, multi-mode transmission strategies can also be realized in the temporal domain. In particular, multi-pulse FDA schemes introduce diversity across pulses by allowing the frequency offsets to vary over time:

$$\Delta f^{(p)}, \quad p = 1, \dots, P. \quad (68)$$

Such frequency scheduling mechanisms effectively reshape the transmit response across pulses, providing additional control over the resulting signal structure. These approaches have been shown to improve ambiguity characteristics, mitigate secondary range ambiguities, and enhance robustness in detection and estimation tasks.

Hybrid FDA–PA architectures and multi-pulse frequency scheduling can be viewed as two complementary mechanisms for controlling FDA-induced coupling. The former regulates coupling in the spatial domain by partially introducing frequency diversity, while the latter redistributes coupling in the temporal domain through pulse-to-pulse variation. Together, they provide a flexible framework for trading off range selectivity, stability, and robustness in practical FDA systems.

(3) **Space–Time–Range Joint Design:** FDA inherently extends the signal model to a joint space–time–range domain. Future research should systematically investigate joint design across these dimensions, including waveform synthesis, beamforming, and resource allocation. This direction also calls for new analytical tools to characterize the expanded signal manifold and its associated degrees of freedom.

(4) **Fundamental Channel Modeling and Information Theory:** The introduction of frequency gradients fundamentally alters the communication channel structure. Key open questions include:

- What is the canonical form of the FDA communication channel matrix?
- How does range-dependent coupling affect channel rank, capacity, and identifiability?
- What are the fundamental limits of FDA-enabled secure communication?

Establishing rigorous channel models and information-theoretic limits is essential for moving beyond heuristic designs.

(5) FDA-Enabled ISAC and Secure Transmission: While FDA has shown potential in ISAC, its unique role in joint sensing–communication remains underexplored. Future research should clarify how range-dependent propagation can be leveraged for:

- Interference-aware communication,
- Physical-layer security via spatial–range selectivity,
- Joint sensing–communication resource allocation.

In particular, experimentally validating FDA-based secure communication schemes remains an open challenge.

(6) Retrofitting Existing Radar Platforms for FDA Realization: A practically important open question is how FDA functionality can be realized by modifying existing radar hardware rather than developing entirely new platforms from scratch. In many scenarios, it may be more realistic to retrofit current phased-array, MIMO radar, or software-defined radio infrastructures through partial frequency-offset control, subarray-level frequency scheduling, multi-pulse transmission strategies, or digital compensation frameworks. Such an approach could significantly lower the barrier to experimental validation and practical deployment.

This direction raises several fundamental questions. First, which FDA capabilities genuinely require element-level frequency offsets at the hardware level, and which can be approximated through hybrid architectures or signal processing? Second, what are the performance limits of FDA-like operation when implemented on legacy platforms with restricted frequency agility and synchronization accuracy? Third, how should existing transmit–receive chains, local oscillators, and calibration procedures be modified to preserve the intended frequency-gradient structure without compromising coherence? Addressing these questions is essential for translating FDA from a conceptually attractive array model into a practically deployable architecture.

(7) Large-Scale Experimental Platforms and Benchmarking: Next, bridging theory and practice requires the development of scalable FDA testbeds, open datasets, and standardized evaluation protocols. This includes multi-channel calibration, synchronization frameworks, and reproducible experimental setups for fair comparison across studies.

(8) FDA and Near-Field / Holographic MIMO Integration: Recent advances in near-field and holographic MIMO systems have highlighted the importance of spherical-wave propagation, where range-dependent effects arise naturally from geometry. This raises a fundamental question regarding the role of FDA in such regimes. In conventional near-field MIMO, range–angle coupling is inherently induced by spherical-wave propagation, without requiring frequency diversity. In contrast, FDA introduces range dependence through frequency-gradient-induced phase modulation, even under far-field conditions.

This distinction suggests that FDA and near-field MIMO provide two different mechanisms for achieving range-dependent channel structures:

- Geometric Coupling: Induced by spherical-wave propagation in near-field systems,
- Frequency-Induced Coupling: Introduced by element-dependent frequency offsets in FDA.

Understanding the interaction between these two mechanisms is an open research problem. In particular, key questions include:

- Whether FDA provides additional degrees of freedom in near-field regimes where coupling already exists,
- How frequency-gradient design interacts with spherical-wave channel models,
- Whether hybrid designs can jointly exploit geometric and frequency-induced coupling for enhanced sensing and communication.

This direction is closely related to emerging 6G concepts such as holographic MIMO and extremely large-scale antenna arrays, where spatial and range-domain effects become tightly intertwined.

## F. Concluding Perspective

FDA is neither a universal replacement for conventional phased arrays nor merely a theoretical construct. Its true significance lies in introducing a new form of propagation-embedded design, where frequency gradients reshape the array manifold beyond purely spatial dimensions.

This structural expansion, however, is fundamentally conditional. Its effectiveness depends critically on the ability to preserve a coherent and irreducible frequency-gradient structure under practical constraints. When this structure is distorted, decorrelated, or averaged out, the system behavior collapses toward conventional array paradigms. In this sense, FDA should not be interpreted as simply adding an additional degree of freedom, but as redefining how degrees of freedom are embedded within the propagation process itself. The practical value of FDA therefore hinges on three intertwined factors:

- Preserving gradient irreducibility in the presence of temporal, spectral, and geometric constraints,
- Maintaining coherence under hardware imperfections and synchronization limitations,
- Aligning the resulting structural degrees of freedom with task-specific objectives in sensing and communication.

Future progress will likely emerge from a deeper integration of propagation theory, hardware-aware design, and information-theoretic analysis. More broadly, FDA highlights a paradigm shift from spatial-domain beamforming to structure-aware signal design, where waveform, array, and channel are no longer separable components but jointly shape system capability.

## IX. Conclusion

This paper presented a unified structural perspective on FDA, connecting design variables, manifold expansion, physical degrees of freedom, and system-level capabilities within a coherent analytical framework. Rather than treating FDA as a collection of application-specific techniques,

we reformulated it through a generalized phase-gradient viewpoint. From this perspective, the defining feature of FDA is not merely frequency diversity, but the introduction of inter-element frequency gradients that embed range dependence directly into the propagation process. This mechanism extends the array manifold from  $\mathbf{a}(\theta)$  to  $\mathbf{a}(t, R_0, \theta)$ , thereby enabling new forms of structural degrees of freedom.

A key insight established in this work is that frequency diversity alone does not guarantee a new physical degree of freedom. The decisive factor is irreducibility: only when the gradient-induced range-phase structure cannot be removed through linear compensation does a genuine range-domain DoF emerge. Otherwise, the system effectively collapses to conventional phased-array or waveform-equivalent models. Within this unified framework, we linked FDA-induced structural DoF to a range of capabilities, including range-angle selectivity, time-varying beam evolution, anti-deception performance, and sensing-communication coupling. At the same time, we emphasized that these gains are inherently conditional. Their realization depends on maintaining coherence, preserving gradient structure, and operating within the validity bounds of underlying modeling assumptions.

We further clarified several common misconceptions. In particular, strict time-invariant focusing is physically infeasible under nonzero frequency gradients, while near-field and wideband regimes fundamentally alter the validity of classical FDA interpretations. These observations highlight that FDA performance must be evaluated in conjunction with propagation conditions and hardware constraints. Ultimately, FDA should be understood not as a universal replacement for phased arrays, but as a propagation-embedded design paradigm that reshapes how degrees of freedom are created and utilized. Its significance lies in redefining the interaction between signal design and propagation physics, rather than simply increasing system dimensionality.

Looking forward, the evolution of FDA will depend on advancing coherent and robust gradient design, extending manifold theory to near-field and wideband regimes, establishing rigorous channel and information-theoretic models, and developing large-scale experimental platforms. More broadly, FDA points toward a shift from spatial-domain beamforming to structure-aware system design, where waveform, array, and channel are jointly optimized to meet task-specific objectives in radar and ISAC systems.

## X. Acknowledgment

The authors would like to sincerely thank all the reviewers for their valuable comments and constructive suggestions, which have helped improve the quality of this manuscript. The authors also gratefully acknowledge Dr. Jiangwei Jian from the University of Electronic Science and Technology of China for his valuable suggestions on the secure communication and ISAC applications covered in this paper.

## References

- [1] H. Rahman, *Fundamental principles of radar*. CRC Press, 2019.
- [2] T. S. Rappaport, "Wireless communications—principles and practice, (the book end)." *Microwave Journal*, vol. 45, no. 12, pp. 128–129, 2002.
- [3] H. Lütkepohl, *Handbook of matrices*. John Wiley & Sons, 1997.
- [4] J. Eaves and E. Reedy, *Principles of modern radar*. Springer Science & Business Media, 2012.
- [5] M. Skolnik, *Introduction to Radar Systems*. New York, NY: McGrawHill, 2001.
- [6] R. J. Mailloux, *Phased array antenna handbook*. Artech house, 2017.
- [7] P. Stoica, R. L. Moses et al., *Spectral analysis of signals*. Pearson Prentice Hall Upper Saddle River, NJ, 2005, vol. 452.
- [8] D. K. Barton, "Modern radar system analysis," Norwood, 1988.
- [9] R. M. Buehrer, *Code division multiple access (CDMA)*. Springer Nature, 2022.
- [10] K. S. Zigangirov, *Theory of code division multiple access communication*. John Wiley & Sons, 2004.
- [11] S. Faruque, "Frequency division multiple access (FDMA)," in *radio frequency multiple access techniques made easy*. Springer, 2018, pp. 21–33.
- [12] R. Saadia and N. M. Khan, "Single carrier-frequency division multiple access radar: Waveform design and analysis," *IEEE Access*, vol. 8, pp. 35 742–35 751, 2020.
- [13] Y. G. Li and G. L. Stuber, *Orthogonal frequency division multiplexing for wireless communications*. Springer Science & Business Media, 2006.
- [14] S. B. Weinstein, "The history of orthogonal frequency-division multiplexing [history of communications]," *IEEE Communications Magazine*, vol. 47, no. 11, pp. 26–35, 2009.
- [15] J. R. Hampton, *Introduction to MIMO communications*. Cambridge university press, 2013.
- [16] A. B. Gershman and N. D. Sidiropoulos, *Space-time processing for MIMO communications*. Wiley Online Library, 2005.
- [17] T. M. Duman and A. Ghayeb, *Coding for MIMO communication systems*. John Wiley & Sons, 2008.
- [18] F. De Flaviis, *Multiantenna systems for MIMO communications*. Morgan & Claypool Publishers, 2008, vol. 7.
- [19] A. Basit, W. Khan, S. Khan, and I. M. Qureshi, "Development of frequency diverse array radar technology: a review," *IET Radar, Sonar & Navigation*, vol. 12, no. 2, pp. 165–175, 2018.
- [20] W.-Q. Wang, "Frequency diverse array antenna: New opportunities," *IEEE Antennas and Propagation Magazine*, vol. 57, no. 2, pp. 145–152, 2015.
- [21] P. Antonik, M. Wicks, H. Griffiths, and C. Baker, "Frequency diverse array radars," in *2006 IEEE Conference on Radar*, Verona, NY, USA, 2006, pp. 3 pp.–.
- [22] P. Antonik, "An investigation of a frequency diverse array," Ph.D. dissertation, UCL (University College London), London, 2009.
- [23] J. Xu, S. Zhu, G. Liao, and Y. Zhang, "An overview of frequency diverse array radar technology," *Journal of Radars*, vol. 7, no. 2, pp. 167–182, 2018. (Chinese).
- [24] W.-Q. Wang, H. C. So, and A. Farina, "An overview on time/frequency modulated array processing," *IEEE Journal of Selected Topics in Signal Processing*, vol. 11, no. 2, pp. 228–246, 2016.
- [25] C. Fulton, M. Yearly, D. Thompson, J. Lake, and A. Mitchell, "Digital phased arrays: Challenges and opportunities," *Proceedings of the IEEE*, vol. 104, no. 3, pp. 487–503, 2016.
- [26] H. J. Visser, *Array and phased array antenna basics*. John Wiley & Sons, 2006.
- [27] W. Khan, I. M. Qureshi, and S. Saeed, "Frequency diverse array radar with logarithmically increasing frequency offset," *IEEE Antennas and Wireless Propagation Letters*, vol. 14, pp. 499–502, 2015.
- [28] B. Wang, J. Xie, J. Zhang, and H. Zhang, "Dot-shaped beamforming analysis based on osb log-FDA," *Journal of Systems Engineering and Electronics*, vol. 31, no. 2, pp. 312–320, 2020.

- [29] Y. Liao, W.-Q. Wang, and Z. Zheng, "Frequency diverse array beampattern synthesis using symmetrical logarithmic frequency offsets for target indication," *IEEE Transactions on Antennas and Propagation*, vol. 67, no. 5, pp. 3505–3509, 2019.
- [30] K. Gao, W.-Q. Wang, J. Cai, and J. Xiong, "Decoupled frequency diverse array range-angle-dependent beampattern synthesis using non-linearly increasing frequency offsets," *IET Microwaves, Antennas & Propagation*, vol. 10, no. 8, pp. 880–884, 2016.
- [31] X. Shao, T. Hu, Z. Xiao, and J. Zhang, "Frequency diverse array beampattern synthesis with modified sinusoidal frequency offset," *IEEE Antennas and Wireless Propagation Letters*, vol. 20, no. 9, pp. 1784–1788, 2021.
- [32] A. Basit, I. M. Qureshi, W. Khan, S. ur Rehman, and M. M. Khan, "Beam pattern synthesis for an FDA radar with hamming window-based nonuniform frequency offset," *IEEE Antennas and Wireless Propagation Letters*, vol. 16, pp. 2283–2286, 2017.
- [33] Y. Liao, H. Tang, X. Chen, and W.-Q. Wang, "Frequency diverse array beampattern synthesis with Taylor windowed frequency offsets," *IEEE Antennas and Wireless Propagation Letters*, vol. 19, no. 11, pp. 1901–1905, 2020.
- [34] Y. Liao, H. Tang, X. Chen, W.-Q. Wang, M. Xing, Z. Zheng, J. Wang, and Q. H. Liu, "Antenna beampattern with range null control using weighted frequency diverse array," *IEEE Access*, vol. 8, pp. 50 107–50 117, 2020.
- [35] S. Saeed, I. M. Qureshi, W. Khan, and A. Salman, "Tangent hyperbolic circular frequency diverse array radars," *the Journal of Engineering*, vol. 2016, no. 3, pp. 23–28, 2016.
- [36] Z. Wang, W.-Q. Wang, and H. Shao, "Range-azimuth decouple beamforming for frequency diverse array with Costas-sequence modulated frequency offsets," *EURASIP Journal on Advances in Signal Processing*, vol. 2016, no. 1, p. 124, 2016.
- [37] W. Choi, A. Georgiadis, M. M. Tentzeris, and S. Kim, "Analysis of exponential frequency-diverse array for short-range beam-focusing technology," *IEEE Transactions on Antennas and Propagation*, vol. 71, no. 2, pp. 1437–1447, 2023.
- [38] Y. Liu, H. Ruan, L. Wang, and A. Nehorai, "The random frequency diverse array: A new antenna structure for uncoupled direction-range indication in active sensing," *IEEE Journal of Selected Topics in Signal Processing*, vol. 11, no. 2, pp. 295–308, 2016.
- [39] G. Huang, Y. Ding, S. Ouyang, and V. Fusco, "Frequency diverse array with random logarithmically increasing frequency offset," *Microwave and Optical Technology Letters*, vol. 62, no. 7, pp. 2554–2561, 2020.
- [40] J. Xiong, W.-Q. Wang, H. Shao, and H. Chen, "Frequency diverse array transmit beampattern optimization with genetic algorithm," *IEEE Antennas and Wireless Propagation Letters*, vol. 16, pp. 469–472, 2017.
- [41] S. Yaw Nusenu and A. Basit, "Frequency-modulated diverse array transmit beamforming with bat metaheuristic optimization," *IET Radar, Sonar & Navigation*, vol. 14, no. 9, pp. 1338–1342, 2020.
- [42] J. Ge, J. Xie, B. Wang, and C. Chen, "Fuzzy entropy for frequency diverse array beampattern synthesis," *IEEE Transactions on Antennas and Propagation*, vol. 70, no. 11, pp. 11 172–11 176, 2022.
- [43] M. C. Wicks and P. Antonik, "Frequency diverse array with independent modulation of frequency, amplitude, and phase," Patent.
- [44] —, "Method and apparatus for a frequency diverse array," Patent.
- [45] A. Aytun, "Frequency diverse array radar," Ph.D. dissertation, Monterey, California, 2010.
- [46] W.-Q. Wang and H. Shao, "Range-angle localization of targets by a double-pulse frequency diverse array radar," *IEEE Journal of Selected Topics in Signal Processing*, vol. 8, no. 1, pp. 106–114, 2013.
- [47] Y. Wang, W.-Q. Wang, and H. Chen, "Linear frequency diverse array manifold geometry and ambiguity analysis," *IEEE Sensors Journal*, vol. 15, no. 2, pp. 984–993, 2014.
- [48] T. Liao, Y. Pan, and W.-Q. Wang, "Generalized linear frequency diverse array manifold curve analysis," *IEEE Signal Processing Letters*, vol. 25, no. 6, pp. 768–772, 2018.
- [49] B. Chen, X. Chen, Y. Huang, and J. Guan, "Transmit beampattern synthesis for the FDA radar," *IEEE Antennas and Wireless Propagation Letters*, vol. 17, no. 1, pp. 98–101, 2017.
- [50] K. Chen, S. Yang, Y. Chen, and S.-W. Qu, "Accurate models of time-invariant beampatterns for frequency diverse arrays," *IEEE Transactions on Antennas and Propagation*, vol. 67, no. 5, pp. 3022–3029, 2019.
- [51] Y. Liao, G. Zeng, Z. Luo, and Q. H. Liu, "Time-variance analysis for frequency-diverse array beampatterns," *IEEE Transactions on Antennas and Propagation*, vol. 71, no. 8, pp. 6558–6567, 2023.
- [52] Y.-Q. Yang, H. Wang, H.-Q. Wang, S.-Q. Gu, D.-L. Xu, and S.-L. Quan, "Optimization of sparse frequency diverse array with time-invariant spatial-focusing beampattern," *IEEE Antennas and Wireless Propagation Letters*, vol. 17, no. 2, pp. 351–354, 2018.
- [53] S. Gong, S. Wang, S. Chen, C. Xing, and X. Wei, "Time-invariant joint transmit and receive beampattern optimization for polarization-subarray based frequency diverse array radar," *IEEE Transactions on Signal Processing*, vol. 66, no. 20, pp. 5364–5379, 2018.
- [54] W.-Q. Wang and H.-C. So, "Transmit subaperturing for range and angle estimation in frequency diverse array radar," *IEEE Transactions on Signal Processing*, vol. 62, no. 8, pp. 2000–2011, 2014.
- [55] W.-Q. Wang, "Subarray-based frequency diverse array radar for target range-angle estimation," *IEEE Transactions on Aerospace and Electronic Systems*, vol. 50, no. 4, pp. 3057–3067, 2014.
- [56] Y. Xu, X. Shi, W. Li, and J. Xu, "Flat-top beampattern synthesis in range and angle domains for frequency diverse array via second-order cone programming," *IEEE Antennas and Wireless Propagation Letters*, vol. 15, pp. 1479–1482, 2015.
- [57] Y. Xu, X. Shi, J. Xu, L. Huang, and W. Li, "Range-angle-decoupled beampattern synthesis with subarray-based frequency diverse array," *Digital Signal Processing*, vol. 64, pp. 49–59, 2017.
- [58] S. Qin, Y. D. Zhang, M. G. Amin, and F. Gini, "Frequency diverse coprime arrays with coprime frequency offsets for multitarget localization," *IEEE Journal of Selected Topics in Signal Processing*, vol. 11, no. 2, pp. 321–335, 2016.
- [59] T. Ni, S. Liu, Z. Mao, and Y. Huang, "Range-dependent beamforming using space-frequency virtual difference coarray," in *2021 IEEE Radar Conference (RadarConf21)*, Atlanta, GA, USA, 2021, pp. 1–5.
- [60] M. Mahmood and H. Mir, "Frequency diverse array beamforming using nonuniform logarithmic frequency increments," *IEEE Antennas and Wireless Propagation Letters*, vol. 17, no. 10, pp. 1817–1821, 2018.
- [61] Y. Xu, A. Wang, and J. Xu, "Range-angle transceiver beamforming based on semicircular-FDA scheme," *IEEE Transactions on Aerospace and Electronic Systems*, vol. 58, no. 2, pp. 834–843, 2022.
- [62] M. Ulrich and B. Yang, "Wavelength-diverse mimo radar: parameter-coupling, array-carrier optimization and direction-of-arrival estimation," *IEEE Transactions on Aerospace and Electronic Systems*, vol. 55, no. 4, pp. 1920–1932, 2018.
- [63] M. Tan, C. Wang, and Z. Li, "Correction analysis of frequency diverse array radar about time," *IEEE Transactions on Antennas and Propagation*, vol. 69, no. 2, pp. 834–847, 2021.
- [64] P. F. Sammartino, C. J. Baker, and H. D. Griffiths, "Frequency diverse MIMO techniques for radar," *IEEE Transactions on Aerospace and Electronic Systems*, vol. 49, no. 1, pp. 201–222, 2013.
- [65] J. Xu, G. Liao, S. Zhu, L. Huang, and H. C. So, "Joint range and angle estimation using MIMO radar with frequency diverse array," *IEEE Transactions on Signal Processing*, vol. 63, no. 13, pp. 3396–3410, 2015.
- [66] W. Khan, I. M. Qureshi, A. Basit, and M. Zubair, "A double pulse MIMO frequency diverse array radar for improved range-angle localization of target," *Wireless Personal Communications*, vol. 82, pp. 2199–2213, 2015.
- [67] J. Xiong, W.-Q. Wang, and K. Gao, "FDA-MIMO radar range-angle estimation: CRLB, MSE, and resolution analysis," *IEEE Transactions on Aerospace and Electronic Systems*, vol. 54, no. 1, pp. 284–294, 2018.

- [68] J. Xu, S. Zhu, and G. Liao, "Range ambiguous clutter suppression for airborne FDA-STAP radar," *IEEE Journal of Selected Topics in Signal Processing*, vol. 9, no. 8, pp. 1620–1631, 2015.
- [69] J. Xu, G. Liao, and H. C. So, "Space-time adaptive processing with vertical frequency diverse array for range-ambiguous clutter suppression," *IEEE Transactions on Geoscience and Remote Sensing*, vol. 54, no. 9, pp. 5352–5364, 2016.
- [70] J. Xu, G. Liao, Y. Zhang, H. Ji, and L. Huang, "An adaptive range-angle-doppler processing approach for FDA-MIMO radar using three-dimensional localization," *IEEE Journal of Selected Topics in Signal Processing*, vol. 11, no. 2, pp. 309–320, 2017.
- [71] J. Xu, G. Liao, S. Zhu, and H. C. So, "Deceptive jamming suppression with frequency diverse MIMO radar," *Signal Processing*, vol. 113, pp. 9–17, 2015.
- [72] J. Xu, S. Zhu, and G. Liao, "Space-time-range adaptive processing for airborne radar systems," *IEEE Sensors Journal*, vol. 15, no. 3, pp. 1602–1610, 2015.
- [73] L. Lan, G. Liao, J. Xu, Y. Zhang, and F. Fioranelli, "Suppression approach to main-beam deceptive jamming in FDA-MIMO radar using nonhomogeneous sample detection," *IEEE Access*, vol. 6, pp. 34582–34597, 2018.
- [74] C. Wen, J. Peng, J. Zhou, and J. Wu, "Enhanced three-dimensional joint domain localized STAP for airborne FDA-MIMO radar under dense false-target jamming scenario," *IEEE Sensors Journal*, vol. 18, no. 10, pp. 4154–4166, 2018.
- [75] R. Gui, W. Wang, and Z. Zheng, "Low-complexity GLRT for FDA radar without training data," *Digital Signal Processing*, vol. 107, 2020.
- [76] B. Huang, A. Basit, R. Gui, and W.-Q. Wang, "Adaptive moving target detection without training data for FDA-MIMO radar," *IEEE Transactions on Vehicular Technology*, vol. 71, no. 1, pp. 220–232, 2022.
- [77] L. Lan, A. Marino, A. Aubry, A. De Maio, G. Liao, J. Xu, and Y. Zhang, "GLRT-based adaptive target detection in FDA-MIMO radar," *IEEE Transactions on Aerospace and Electronic Systems*, pp. 1–1, 2020.
- [78] Y. Wang and S. Zhu, "Range ambiguous clutter suppression for FDA-MIMO forward looking airborne radar based on main lobe correction," *IEEE Transactions on Vehicular Technology*, vol. 70, no. 3, pp. 2032–2046, 2021.
- [79] —, "Range ambiguous clutter suppression for FDA-MIMO forward looking airborne radar based on main lobe correction," *IEEE Transactions on Vehicular Technology*, vol. 70, no. 3, pp. 2032–2046, 2021.
- [80] Z. Liu, S. Zhu, J. Xu, X. He, K. Duan, and L. Lan, "Range-ambiguous clutter suppression for STAP-based radar with vertical coherent frequency diverse array," *IEEE Transactions on Geoscience and Remote Sensing*, vol. 61, pp. 1–17, 2023.
- [81] Z. Qiu, Z. Liao, J. Xu, and K. Duan, "Range-ambiguous clutter suppression for space-based early warning radar using vertical FDA and horizontal EPC," *IEEE Geoscience and Remote Sensing Letters*, vol. 20, pp. 1–5, 2023.
- [82] Y. Wang and S. Zhu, "Main-beam range deceptive jamming suppression with simulated annealing FDA-MIMO radar," *IEEE Sensors Journal*, vol. 20, no. 16, pp. 9056–9070, 2020.
- [83] L. Lan, J. Xu, G. Liao, Y. Zhang, F. Fioranelli, and H. C. So, "Suppression of mainbeam deceptive jammer with FDA-MIMO radar," *IEEE Transactions on Vehicular Technology*, vol. 69, no. 10, pp. 11584–11598, 2020.
- [84] R. Gui, W.-Q. Wang, C. Cui, and H. C. So, "Coherent pulsed-FDA radar receiver design with time-variance consideration: SINR and CRB analysis," *IEEE Transactions on Signal Processing*, vol. 66, no. 1, pp. 200–214, 2018.
- [85] B. Huang, J. Jian, A. Basit, R. Gui, and W.-Q. Wang, "Adaptive distributed target detection for FDA-MIMO radar in Gaussian clutter without training data," *IEEE Transactions on Aerospace and Electronic Systems*, vol. 58, no. 4, pp. 2961–2972, 2022.
- [86] B. Huang, A. Basit, W.-Q. Wang, and S. Zhang, "Adaptive detection with Bayesian framework for FDA-MIMO radar," *IEEE Geoscience and Remote Sensing Letters*, vol. 19, pp. 1–5, 2022.
- [87] B. Huang, D. Orlando, W.-Q. Wang, W. Liu, and L. Lan, "Adaptive multiple targets detection for FDA-MIMO radar with gaussian clutter," *Signal Processing*, vol. 205, p. 108893, 2023. [Online]. Available: <https://www.sciencedirect.com/science/article/pii/S0165168422004327>
- [88] H. Chen, R. Li, H. Chen, Q. Qu, B. Zhou, B. Li, and Y. Wang, "Monopulse parameter estimation for FDA-MIMO radar under mainlobe deception jamming," *Remote Sensing*, vol. 15, no. 16, p. 3947, 2023.
- [89] J. Farooq, M. A. Temple, and M. A. Saville, "Application of frequency diverse arrays to synthetic aperture radar imaging," in *2007 International Conference on Electromagnetics in Advanced Applications*. Turin, Italy: IEEE, 2007, pp. 447–449.
- [90] —, "Exploiting frequency diverse array processing to improve sar image resolution," in *2008 IEEE Radar Conference*. Rome, Italy: IEEE, 2008, pp. 1–5.
- [91] C. Wang, J. Xu, G. Liao, X. Xu, and Y. Zhang, "A range ambiguity resolution approach for high-resolution and wide-swath SAR imaging using frequency diverse array," *IEEE Journal of Selected Topics in Signal Processing*, vol. 11, no. 2, pp. 336–346, 2017.
- [92] C. Lin, P. Huang, W. Wang, Y. Li, and J. Xu, "Unambiguous signal reconstruction approach for sar imaging using frequency diverse array," *IEEE Geoscience and Remote Sensing Letters*, vol. 14, no. 9, pp. 1628–1632, 2017.
- [93] Y. Zhou, W. Wang, Z. Chen, Q. Zhao, H. Zhang, Y. Deng, and R. Wang, "High-resolution and wide-swath SAR imaging mode using frequency diverse planar array," *IEEE Geoscience and Remote Sensing Letters*, vol. 18, no. 2, pp. 321–325, 2021.
- [94] M. Zhang, G. Liao, J. Xu, X. He, Q. Liu, L. Lan, and S. Li, "High-resolution and wide-swath SAR imaging with sub-band frequency diverse array," *IEEE Transactions on Aerospace and Electronic Systems*, vol. 59, no. 1, pp. 172–183, 2023.
- [95] L. Wang, W.-Q. Wang, H. Guan, and S. Zhang, "LPI property of FDA transmitted signal," *IEEE Transactions on Aerospace and Electronic Systems*, vol. 57, no. 6, pp. 3905–3915, 2021.
- [96] P. Gong, Z. Zhang, Y. Wu, and W.-Q. Wang, "Joint design of transmit waveform and receive beamforming for LPI FDA-MIMO radar," *IEEE Signal Processing Letters*, vol. 29, pp. 1938–1942, 2022.
- [97] S. Ji, W. Wang, H. Chen, and Z. Zheng, "Secrecy capacity analysis of an-aided FDA communication over nakagami- $m$  fading," *IEEE Wireless Communications Letters*, vol. 7, no. 6, pp. 1034–1037, 2018.
- [98] B. Qiu, J. Xie, L. Wang, and Y. Wang, "Artificial-noise-aided secure transmission for proximal legitimate user and eavesdropper based on frequency diverse arrays," *IEEE Access*, vol. 6, pp. 52531–52543, 2018.
- [99] J. Hu, S. Yan, F. Shu, J. Wang, J. Li, and Y. Zhang, "Artificial-noise-aided secure transmission with directional modulation based on random frequency diverse arrays," *IEEE Access*, vol. 5, pp. 1658–1667, 2017.
- [100] Q. Cheng, S. Wang, V. Fusco, F. Wang, J. Zhu, and C. Gu, "Physical-layer security for frequency diverse array-based directional modulation in fluctuating two-ray fading channels," *IEEE Transactions on Wireless Communications*, pp. 1–1, 2021.
- [101] S. Wang, S. Yan, J. Zhang, N. Yang, R. Chen, and F. Shu, "Secrecy zone achieved by directional modulation with random frequency diverse array," *IEEE Transactions on Vehicular Technology*, vol. 70, no. 2, pp. 2001–2006, 2021.
- [102] B. Qiu, M. Tao, L. Wang, J. Xie, and Y. Wang, "Multi-beam directional modulation synthesis scheme based on frequency diverse array," *IEEE Transactions on Information Forensics and Security*, vol. 14, no. 10, pp. 2593–2606, 2019.
- [103] J. Jian, B. Huang, and W.-Q. Wang, "Physical-layer security with frequency diverse array for DF multi-antenna relaying SWIPT system," *International Journal of Electronics Letters*, pp. 1–9, 2022.
- [104] J. Jian, W.-Q. Wang, A. Basit, and B. Huang, "Physical layer security for frequency diverse array-based dual-hop spatial modulation," *IEEE Transactions on Wireless Communications*, pp. 1–1, 2023.
- [105] S. Y. Nusenu and W.-Q. Wang, "Dual-function FDA MIMO radar-communications system employing costas signal waveforms," in *2018 IEEE Radar Conference (RadarConf18)*, Oklahoma City, OK, USA, 2018, pp. 0033–0038.
- [106] M. Li and W.-Q. Wang, "Joint radar-communication system design based on FDA-MIMO via frequency index modulation," *IEEE Access*, vol. 11, pp. 67722–67736, 2023.

- [107] P. Gong, K. Xu, Y. Wu, J. Zhang, and H. C. So, "Optimization of LPI-FDA-MIMO radar and MIMO communication for spectrum coexistence," *IEEE Wireless Communications Letters*, vol. 12, no. 6, pp. 1076–1080, 2023.
- [108] J. Xu, Y. Zhang, G. Liao, and H. C. So, "Resolving range ambiguity via multiple-input multiple-output radar with element-pulse coding," *IEEE Transactions on Signal Processing*, vol. 68, pp. 2770–2783, 2020.
- [109] Y. Liu, L. Lan, J. Xu, G. Liao, and Y. Zhang, "Resolving range ambiguity in EPC SAR based on beam pattern precise control," in *IET Conference Proceedings CP874*, vol. 2023, no. 47. IET, 2023, pp. 3324–3330.
- [110] F. Liu, S. Zhu, J. Xu, X. Li, L. Lan, and G. Liao, "Range ambiguity mitigation and range-angle estimation with EPC-FDA-MIMO radar," *IEEE Transactions on Aerospace and Electronic Systems*, vol. 61, no. 3, pp. 6280–6294, 2025.
- [111] L. Lan, Y. Zhang, R. Liao, G. Liao, J. Xu, and H. C. So, "Mainlobe deceptive jammer mitigation with multipath in EPC-MIMO radar exploiting matrix decomposition," *IEEE Transactions on Vehicular Technology*, vol. 73, no. 10, pp. 14 674–14 688, 2024.
- [112] J. Zhu, X. Zhang, L. Lan, R. Ma, L. Cui, G. Chen, J. Xu, and G. Liao, "Simultaneous detection and estimation with distributed FDA-MIMO and EPC-MIMO radars," in *2024 IEEE International Conference on Signal, Information and Data Processing (ICSIDP)*. IEEE, 2024, pp. 1–6.
- [113] L. Lan, G. Liao, J. Xu, and Y. Zhang, "Mainlobe deceptive jammer suppression with mimo radar using element-pulse coding," in *2020 IEEE Radar Conference (RadarConf20)*. IEEE, 2020, pp. 1–6.
- [114] L. Lan, G. Liao, J. Xu, S. Zhu, and Z. Wang, "Subarray-based time-delay low sidelobes methods for space-time coding array," *IET Radar, Sonar & Navigation*, vol. 12, no. 8, pp. 807–814, 2018.
- [115] Y. Liu, P. Wang, Z. Men, Y. Guo, T. He, R. Bao, and L. Cui, "A signal model based on the space-time coding array and a novel imaging method based on the hybrid correlation algorithm for F-SCAN SAR," *Remote Sensing*, vol. 15, no. 17, p. 4276, 2023.
- [116] H. Wang, G. Liao, Y. Zhang, J. Xu, S. Zhu, and L. Huang, "Transmit beam pattern synthesis for chirp space-time coding array by time delay design," *Digital Signal Processing*, vol. 110, p. 102901, 2021.
- [117] S. Wang, F. He, and Z. Dong, "A sidelobe optimization method using spatial code based on space-time coding array," in *2024 IEEE International Conference on Signal, Information and Data Processing (ICSIDP)*. IEEE, 2024, pp. 1–5.
- [118] H. Wang, S. Li, G. Liao, and Y. Quan, "Range-ambiguous clutter modeling, separation, and reduced-dimensional stap for MIMO-STCA radar," *IEEE Transactions on Aerospace and Electronic Systems*, 2025.
- [119] H. Wang, B. Cai, and G. Liao, "Mainlobe jamming suppression using MIMO-STCA radar," *arXiv preprint arXiv:2505.09112*, 2025.
- [120] H. Wang, D. Zhang, G. Liao, and Y. Quan, "Monopulse parameter estimation based on MIMO-STCA radar in the presence of multiple mainlobe jammings," *IEEE Transactions on Aerospace and Electronic Systems*, 2025.
- [121] T. Eker, S. Demir, and A. Hizal, "Exploitation of linear frequency modulated continuous waveform (lfmcw) for frequency diverse arrays," *IEEE Transactions on Antennas and Propagation*, vol. 61, no. 7, pp. 3546–3553, 2013.
- [122] W.-Q. Wang and H. C. So, "Transmit subaperturing for range and angle estimation in frequency diverse array radar," *IEEE Transactions on Signal Processing*, vol. 62, no. 8, pp. 2000–2011, 2014.
- [123] Y. Liao, W.-Q. Wang, and Z. Zheng, "Frequency diverse array beam pattern synthesis using symmetrical logarithmic frequency offsets for target indication," *IEEE Transactions on Antennas and Propagation*, vol. 67, no. 5, pp. 3505–3509, 2019.
- [124] Y. Liao, H. Tang, X. Chen, and W. Q. Wang, "Frequency diverse array beam pattern synthesis with Taylor windowed frequency offsets," *IEEE Antennas and Wireless Propagation Letters*, vol. 19, no. 11, pp. 1901–1905, 2020.
- [125] M. Richards, *Fundamentals of Radar Signal Processing*, 2005.
- [126] D. H. Johnson and D. E. Dudgeon, *Array signal processing: concepts and techniques*. Simon & Schuster, Inc., 1992.
- [127] M. Secmen, S. Demir, A. Hizal, and T. Eker, "Frequency diverse array antenna with periodic time modulated pattern in range and angle," in *2007 IEEE Radar Conference*. IEEE, 2007, pp. 427–430.
- [128] X. Liu, T. Huang, N. Shlezinger, Y. Liu, J. Zhou, and Y. C. Eldar, "Joint transmit beamforming for multiuser MIMO communications and mimo radar," *IEEE Transactions on Signal Processing*, vol. 68, pp. 3929–3944, 2020.
- [129] G. San Antonio, D. R. Fuhrmann, and F. C. Robey, "MIMO radar ambiguity functions," *IEEE Journal of Selected Topics in Signal Processing*, vol. 1, no. 1, pp. 167–177, 2007.
- [130] C.-Y. Chen and P. Vaidyanathan, "MIMO radar ambiguity properties and optimization using frequency-hopping waveforms," *IEEE Transactions on signal processing*, vol. 56, no. 12, pp. 5926–5936, 2008.
- [131] J. Li and P. Stoica, *MIMO Radar Signal Processing*. New York, USA: John Wiley & Sons, Inc, 2009.
- [132] M. Akcakaya and A. Nehorai, "MIMO radar sensitivity analysis for target detection," *IEEE Transactions on Signal Processing*, vol. 59, no. 7, pp. 3241–3250, 2011.
- [133] J. Xu, G. Liao, S. Zhu, and H. C. So, "Deceptive jamming suppression with frequency diverse mimo radar," *Signal Processing*, vol. 113, pp. 9–17, 2015.
- [134] R. Gui, B. Huang, W.-Q. Wang, and Y. Sun, "Generalized ambiguity function for FDA radar joint range, angle and doppler resolution evaluation," *IEEE Geoscience and Remote Sensing Letters*, vol. 19, pp. 1–5, 2020.
- [135] W.-G. Tang, H. Jiang, and Q. Zhang, "Range-angle decoupling and estimation for FDA-MIMO radar via atomic norm minimization and accelerated proximal gradient," *IEEE Signal Processing Letters*, vol. 27, pp. 366–370, 2020.
- [136] W. Wang, "Range-angle dependent transmit beam pattern synthesis for linear frequency diverse arrays," *IEEE Transactions on Antennas and Propagation*, vol. 61, no. 8, pp. 4073–4081, 2013.
- [137] Y. Xu, X. Shi, J. Xu, and P. Li, "Range-angle-dependent beamforming of pulsed frequency diverse array," *IEEE Transactions on Antennas and Propagation*, vol. 63, no. 7, pp. 3262–3267, 2015.
- [138] M. Mahmood and H. Mir, "Frequency diverse array beamforming using nonuniform logarithmic frequency increments," *IEEE Antennas and Wireless Propagation Letters*, vol. 17, no. 10, pp. 1817–1821, 2018.
- [139] H. S. Mir, L. Albasha, and K. T. Wong, "Frequency diverse array using equivalent transmit beamforming: Array factor for multiple receive-antennas," *IEEE Wireless Communications Letters*, vol. 14, no. 10, pp. 3259–3263, 2025.
- [140] Y. Liao, H. Tang, W.-Q. Wang, and M. Xing, "A low sidelobe deceptive jamming suppression beamforming method with a frequency diverse array," *IEEE Transactions on Antennas and Propagation*, vol. 70, no. 6, pp. 4884–4889, 2022.
- [141] M. Tan, C. Wang, B. Xue, and J. Xu, "A novel deceptive jamming approach against frequency diverse array radar," *IEEE Sensors Journal*, vol. 21, no. 6, pp. 8323–8332, 2021.
- [142] M. Liu, C. Wang, J. Gong, M. Tan, L. Bao, and C. Zhou, "Ambiguity function analysis and optimization of coherent fda radar," *IEEE Geoscience and Remote Sensing Letters*, vol. 21, pp. 1–5, 2024.
- [143] W.-Q. Wang, M. Dai, and Z. Zheng, "FDA radar ambiguity function characteristics analysis and optimization," *IEEE Transactions on Aerospace and Electronic Systems*, vol. 54, no. 3, pp. 1368–1380, 2017.
- [144] M. Liao and Y. Zakharov, "Estimation of time-varying channels in virtual angular domain for massive mimo systems," *IEEE Access*, vol. 11, pp. 1923–1933, 2023.
- [145] S. Gong, S. Wang, S. Chen, C. Xing, and X. Wei, "Time-invariant joint transmit and receive beam pattern optimization for polarization-subarray based frequency diverse array radar," *IEEE Transactions on Signal Processing*, vol. 66, no. 20, pp. 5364–5379, 2018.
- [146] Q. Cheng, J. Zhu, T. Xie, J. Luo, and Z. Xu, "Time-invariant angle-range dependent directional modulation based on time-modulated frequency diverse arrays," *IEEE access*, vol. 5, pp. 26 279–26 290, 2017.
- [147] Y. Q. Hei, X. Y. Ju, L. Y. Ma, W. T. Li, and X. W. Shi, "ANN-assisted quasi-time-invariant beamforming for retrodirective

- frequency diverse array," *IEEE Transactions on Antennas and Propagation*, vol. 72, no. 5, pp. 4271–4282, 2024.
- [148] W. Zhai, X. Wang, M. S. Greco, and F. Gini, "Joint optimization of sparse FDAs for time invariant transmit beampattern synthesis," *IEEE Signal Processing Letters*, vol. 29, pp. 110–114, 2021.
- [149] A. Bilal, Y. H. Shah, A. Hadee, S. Bhattacharjee, P. Srihari, and C. S. Cho, "Measurement of time-invariant range-angle maps in frequency diverse array radar using USRP," *IEEE Sensors Journal*, 2026.
- [150] W. Khan, I. M. Qureshi, and S. Saeed, "Frequency diverse array radar with logarithmically increasing frequency offset," *IEEE antennas and wireless propagation letters*, vol. 14, pp. 499–502, 2014.
- [151] A.-M. Yao, W. Wu, and D.-G. Fang, "Frequency diverse array antenna using time-modulated optimized frequency offset to obtain time-invariant spatial fine focusing beampattern," *IEEE Transactions on Antennas and Propagation*, vol. 64, no. 10, pp. 4434–4446, 2016.
- [152] —, "Single-sideband time-modulated phased array," *IEEE Transactions on Antennas and Propagation*, vol. 63, no. 5, pp. 1957–1968, 2015.
- [153] —, "Solutions of time-invariant spatial focusing for multi-targets using time modulated frequency diverse antenna arrays," *IEEE Transactions on Antennas and Propagation*, vol. 65, no. 2, pp. 552–566, 2016.
- [154] H. Chen, H. Shao, and W. Wang, "Sparse reconstruction based frequency diverse array transmit beampattern synthesis," in *2015 3rd International Workshop on Compressed Sensing Theory and its Applications to Radar, Sonar and Remote Sensing (CoSeRa)*. IEEE, 2015, pp. 253–257.
- [155] H. Shao, J. Dai, J. Xiong, H. Chen, and W.-Q. Wang, "Dot-shaped range-angle beampattern synthesis for frequency diverse array," *IEEE antennas and wireless propagation letters*, vol. 15, pp. 1703–1706, 2016.
- [156] J. Xiong, W.-Q. Wang, H. Shao, and H. Chen, "Frequency diverse array transmit beampattern optimization with genetic algorithm," *IEEE Antennas and Wireless Propagation Letters*, vol. 16, pp. 469–472, 2016.
- [157] W. Xu, L. Zhang, H. Bi, P. Huang, and W. Tan, "FDA beampattern synthesis with both nonuniform frequency offset and array spacing," *IEEE Antennas and Wireless Propagation Letters*, vol. 20, no. 12, pp. 2354–2358, 2021.
- [158] C. Cetintepe and S. Demir, "Examination of target RCS characteristics in FDA radars," in *2014 IEEE Antennas and Propagation Society International Symposium (APSURSI)*. IEEE, 2014, pp. 1754–1755.
- [159] B. Huang, Y. Yan, A. Basit, W.-Q. Wang, and J. Cheng, "Radar cross section characterization of frequency diverse array radar," *IEEE Transactions on Aerospace and Electronic Systems*, pp. 1–11, 2022.
- [160] R. Gui, W.-Q. Wang, H.-C. So, and C. Cui, "Target reflectivity characterization for fda radar," in *2020 IEEE 11th Sensor Array and Multichannel Signal Processing Workshop (SAM)*. IEEE, 2020, pp. 1–5.
- [161] R. Gui, "Research on adaptive processing technology for frequency diverse array radar," Ph.D. dissertation, University of Electronic Science and Technology of China, Chengdu, China, 2020,(Chinese).
- [162] B. Huang, "Research on target detection algorithm for FDA-MIMO radar," Ph.D. dissertation, University of Electronic Science and Technology of China, Chengdu, China, 2023,(Chinese).
- [163] Z. Qiu, Z. Liao, J. Xu, and K. Duan, "Range-ambiguous clutter suppression for space-based early warning radar using vertical FDA and horizontal EPC," *IEEE Geoscience and Remote Sensing Letters*, vol. 20, pp. 1–5, 2023.
- [164] Q. Kan, J. Xu, Y. Zhang, W. Wang, and Y. Xu, "Non-cooperative bistatic denial with EPC-MIMO radar transmitter," *IEEE Transactions on Aerospace and Electronic Systems*, 2025.
- [165] K. Yu, S. Zhu, L. Lan, J. Zhu, and X. Li, "Mainbeam deceptive jammer suppression with joint element-pulse phase coding," *IEEE Transactions on Vehicular Technology*, vol. 73, no. 2, pp. 2332–2344, 2023.
- [166] Y. Wang, L. Lan, S. Zhu, X. Li, and G. Liao, "Fast-moving target detection with frequency diverse element-pulse coding radar," *IEEE Transactions on Aerospace and Electronic Systems*, 2025.
- [167] P. Li, B. Huang, and W.-Q. Wang, "Knowledge-aided bayesian detection of distributed target for FDA-MIMO radar in gaussian clutter," *IEEE Transactions on Radar Systems*, vol. 2, pp. 344–354, 2024.
- [168] B. Huang, D. Orlando, W.-Q. Wang, W. Liu, and L. Lan, "Adaptive multiple targets detection for FDA-MIMO radar with gaussian clutter," *Signal Processing*, vol. 205, p. 108893, 2023.
- [169] B. Huang, J. Jian, A. Basit, R. Gui, and W.-Q. Wang, "Adaptive distributed target detection for FDA-MIMO radar in gaussian clutter without training data," *IEEE Transactions on Aerospace and Electronic Systems*, vol. 58, no. 4, pp. 2961–2972, 2022.
- [170] B. Huang, W.-Q. Wang, D. Orlando, A. Basit, and J. Liu, "Bayesian detection of distributed targets for FDA-MIMO radar in gaussian interference," *IEEE Signal Processing Letters*, vol. 29, pp. 2168–2172, 2022.
- [171] X. Chen, B. Chen, J. Guan, Y. Huang, and Y. He, "Space-range-doppler focus-based low-observable moving target detection using frequency diverse array mimo radar," *IEEE Access*, vol. 6, pp. 43 892–43 904, 2018.
- [172] Q. Kan, J. Xu, W. Wang, L. Lan, G. Liao, and H. C. So, "Joint DOA, DOD and range parameter estimation for bistatic FDA-MIMO radar via triangular geometry and maximum likelihood criterion," *IEEE Transactions on Aerospace and Electronic Systems*, 2025.
- [173] T. Zhong, H. Tao, H. Cao, and H. Liao, "Multiparameter estimation for monostatic FDA-MIMO radar with polarimetric antenna," *IEEE Transactions on Antennas and Propagation*, vol. 72, no. 3, pp. 2524–2539, 2024.
- [174] C. Xin, Q. Yang, L. Zhang, H. Wang, and K. Xu, "Joint range-angle estimation method for sparse terahertz frequency diverse arrays based on the music algorithm," in *2025 17th International Conference on Signal Processing Systems (ICSPS)*. IEEE, 2025, pp. 229–233.
- [175] J. Zhu, S. Zhu, J. Xu, L. Lan, and X. He, "Cooperative range and angle estimation with pa and fda radars," *IEEE Transactions on Aerospace and Electronic Systems*, vol. 58, no. 2, pp. 907–921, 2021.
- [176] S. L. Wang, Z.-H. Xu, X. Liu, W. Dong, and G. Wang, "Subarray-based frequency diverse array for target range-angle localization with monopulse processing," *IEEE Sensors Journal*, vol. 18, no. 14, pp. 5937–5947, 2018.
- [177] M. Fu, Z. Zheng, and W.-Q. Wang, "2-D DOA estimation for nested conformal arrays via sparse reconstruction," *IEEE Commun. Lett.*, vol. 25, no. 3, pp. 980–984, Mar. 2020.
- [178] T. G. Kolda and B. W. Bader, "Tensor decompositions and applications," *SIAM Rev.*, vol. 51, no. 3, pp. 455–500, Jul. 2009.
- [179] X. Guo, S. Miron, D. Brie, S. Zhu, and X. Liao, "A candecom/parafac perspective on uniqueness of doa estimation using a vector sensor array," *IEEE Trans. on Signal Process.*, vol. 59, no. 7, pp. 3475–3481, Jul. 2011.
- [180] C. Cui, J. Xu, R. Gui, W.-Q. Wang, and W. Wu, "Search-free DOD, DOA and range estimation for bistatic FDA-MIMO radar," *IEEE Access*, vol. 6, pp. 15 431–15 445, 2018.
- [181] B. Li, W. Bai, and G. Zheng, "Successive esprit algorithm for joint doa-range-polarization estimation with polarization sensitive fda-mimo radar," *IEEE Access*, vol. 6, pp. 36 376–36 382, 2018.
- [182] H. Ma, H. Tao, Y. Yue, T. Zhong, Y. Fang, and L. Wang, "Multiparameter estimation for bistatic EMVS-FDA-MIMO radar with arbitrarily configured arrays," *Digital Signal Processing*, p. 105928, 2026.
- [183] K. Wang, Z. Jin, Z. Yu, F. Zhong, L. Tang, and X. Tang, "Frequency diverse array with discrete fourier transform for single target estimation," *IEEE Transactions on Aerospace and Electronic Systems*, 2025.
- [184] S. Kay, *Fundamentals of Statistical Signal Processing, Volume II*. Prentice Hall, 1993.
- [185] E. Kelly, "An adaptive detection algorithm," *IEEE Transactions on Aerospace and Electronic Systems*, vol. AES-22, no. 2, pp. 115–127, 1986.
- [186] F. C. Robey, D. R. Fuhrmann, E. J. Kelly, and R. Nitzberg, "A CFAR adaptive matched filter detector," *IEEE Transactions*

- on Aerospace and Electronic Systems, vol. 28, no. 1, pp. 208–216, 1992.
- [187] A. D. Maio, “A new derivation of the adaptive matched filter,” *IEEE Signal Processing Letters*, vol. 11, no. 10, pp. 792–793, 2004.
- [188] A. De Maio, “Rao test for adaptive detection in gaussian interference with unknown covariance matrix,” *IEEE Transactions on Signal Processing*, vol. 55, no. 7, pp. 3577–3584, 2007.
- [189] L. Lan, M. Rosamilia, A. Aubry, A. D. Maio, G. Liao, and J. Xu, “Adaptive target detection with polarimetric FDA-MIMO radar,” *IEEE Transactions on Aerospace and Electronic Systems*, pp. 1–16, 2022.
- [190] C. Y. Chong, F. Pascal, J.-P. Ovarlez, and M. Lesturgie, “MIMO radar detection in non-gaussian and heterogeneous clutter,” *IEEE Journal of selected topics in signal processing*, vol. 4, no. 1, pp. 115–126, 2010.
- [191] W. Liu, Y. Wang, J. Liu, W. Xie, H. Chen, and W. Gu, “Adaptive detection without training data in colocated MIMO radar,” *IEEE Transactions on Aerospace and Electronic Systems*, vol. 51, no. 3, pp. 2469–2479, 2015.
- [192] W. Liu, J. Liu, C. Zhang, H. Li, and X. Wang, “Performance prediction of subspace-based adaptive detectors with signal mismatch,” *Signal Processing*, vol. 123, pp. 122–126, 2016.
- [193] W. Liu, J. Liu, Q. Du, and Y.-L. Wang, “Distributed target detection in partially homogeneous environment when signal mismatch occurs,” *IEEE Transactions on Signal Processing*, vol. 66, no. 14, pp. 3918–3928, 2018.
- [194] J. Liu, J. Han, Z. Zhang, and J. Li, “Bayesian detection for MIMO radar in Gaussian clutter,” *IEEE Transactions on Signal Processing*, vol. 66, no. 24, pp. 6549–6559, 2018.
- [195] N. Li, H. Yang, G. Cui, L. Kong, and Q. H. Liu, “Two-step bayesian detection for MIMO radar in compound-gaussian clutter with gamma texture,” in *2017 IEEE Radar Conference (RadarConf)*, Seattle, WA, USA, 2017, pp. 0146–0151.
- [196] E. Conte and A. De Maio, “Distributed target detection in compound-gaussian noise with Rao and Wald tests,” *IEEE Transactions on Aerospace and Electronic Systems*, vol. 39, no. 2, pp. 568–582, 2003.
- [197] L. Xu, J. Li, and P. Stoica, “Target detection and parameter estimation for MIMO radar systems,” *IEEE Transactions on Aerospace and Electronic Systems*, vol. 44, no. 3, pp. 927–939, 2008.
- [198] J. Liu, H. Li, and B. Himed, “Persymmetric adaptive target detection with distributed MIMO radar,” *IEEE Transactions on Aerospace and Electronic Systems*, vol. 51, no. 1, pp. 372–382, 2015.
- [199] Y. Sun, S. Shao, W.-Q. Wang, M. S. Greco, F. Gini, and S. Zhang, “Nonlinear frequency offset optimization strategy for solving secondary range ambiguity in planar FDA-STAP radar,” *IEEE Transactions on Aerospace and Electronic Systems*, 2025.
- [200] Z. Liu, S. Zhu, J. Xu, X. He, K. Duan, and L. Lan, “Range-ambiguous clutter suppression for STAP-based radar with vertical coherent frequency diverse array,” *IEEE Transactions on Geoscience and Remote Sensing*, vol. 61, pp. 1–17, 2023.
- [201] —, “Range-ambiguous clutter suppression for STAP-based radar with vertical coherent frequency diverse array,” *IEEE Transactions on Geoscience and Remote Sensing*, vol. 61, pp. 1–17, 2023.
- [202] Z. Qiu, K. Duan, X. Yang, and Y. Wang, “Range-ambiguous clutter suppression for space-based early warning radar via EPC-FDA-MIMO with nonorthogonal waveforms,” *IEEE Transactions on Aerospace and Electronic Systems*, vol. 60, no. 5, pp. 7106–7124, 2024.
- [203] Y. Wang and S. Zhu, “Range ambiguous clutter suppression for FDA-MIMO forward looking airborne radar based on main lobe correction,” *IEEE Transactions on Vehicular Technology*, vol. 70, no. 3, pp. 2032–2046, 2021.
- [204] R. Gui, W.-Q. Wang, A. Farina, and H. C. So, “FDA radar with Doppler-spreading consideration: Mainlobe clutter suppression for blind-Doppler target detection,” *Signal Processing*, vol. 179, p. 107773, 2021.
- [205] Z. Liu, S. Zhu, J. Xu, X. He, and Q. Liu, “Moving target detection in range-ambiguous clutter scenario with PA-FDA dual-mode radar,” *Digital Signal Processing*, vol. 135, p. 103942, 2023.
- [206] Z. Liu, S. Zhu, J. Xu, L. Lan, X. He, and X. Li, “Cooperated Moving Target Detection Approach for PA-FDA Dual-Mode Radar in Range-Ambiguous Clutter,” *Remote Sensing*, vol. 15, no. 3, p. 692, Jan. 2023.
- [207] B. Huang, P. Li, J. Jian, W.-Q. Wang, and A. Basit, “FDA-MIMO radar target detection with limited test samples,” *IEEE Transactions on Aerospace and Electronic Systems*, vol. 60, no. 4, pp. 4390–4406, 2024.
- [208] C. He, B. Huang, J. Wang, L. Liu, and R. Zhang, “Parametric GLRT-based adaptive target detection for FDA-MIMO radar in gaussian clutter,” *IEEE Transactions on Aerospace and Electronic Systems*, 2026.
- [209] B. Huang, D. Orlando, W.-Q. Wang, J. Jian, Y. Jia, W. Jia, and W. Liu, “GLRT-based adaptive target detection for FDA-MIMO radar in mainlobe deceptive jamming,” *IEEE Sensors Journal*, 2025.
- [210] L. Gui, B. Huang, and W.-Q. Wang, “Robust detector designing for FDA-MIMO radar with training data in gaussian noise,” *IEEE Transactions on Aerospace and Electronic Systems*, 2025.
- [211] B. Huang, W.-Q. Wang, P. Li, J. Jian, Y. Jia, W. Jia, and T. Liao, “Adaptive target detection for an FDA-MIMO radar in a mainlobe deceptive jamming and a partially homogeneous noise,” *Digital Signal Processing*, vol. 152, p. 104583, 2024.
- [212] J. Zhu, S. Zhu, J. Xu, L. Lan, and G. Liao, “Simultaneous detection and discrimination of mainlobe deceptive jammers in FDA-MIMO radar,” *IEEE Transactions on Aerospace and Electronic Systems*, pp. 1–15, 2023.
- [213] W. Jia, J. Jian, P. Li, M. Fu, B. Huang, and W.-Q. Wang, “Long-time coherent integration and range-angle beamforming for detecting high-speed maneuvering targets using FDA radar,” *IEEE Transactions on Aerospace and Electronic Systems*, 2025.
- [214] M. Jia, B. Huang, A. Basit, and W.-Q. Wang, “FDA-based maneuvering target detection with doppler-spread consideration,” *Digital Signal Processing*, vol. 159, p. 104990, 2025.
- [215] W. Wan, S. Zhang, and W.-Q. Wang, “Resolving doppler ambiguity of high-speed moving targets via FDA-MIMO radar,” *IEEE Geoscience and Remote Sensing Letters*, vol. 19, pp. 1–5, 2021.
- [216] R. Gui, W.-Q. Wang, A. Farina, and H. C. So, “FDA radar with doppler-spreading consideration: Mainlobe clutter suppression for blind-doppler target detection,” *Signal Processing*, vol. 179, p. 107773, 2021.
- [217] M. Liu, S. Zhang, and W. Wang, “Detecting moving target with doppler spread and range migration for FDA-MIMO radar,” in *IGARSS 2022-2022 IEEE International Geoscience and Remote Sensing Symposium*. IEEE, 2022, pp. 2809–2812.
- [218] J. Zhu, S. Zhu, L. Lan, and J. Xu, “Adaptive multi-target detection with FDA-MIMO radar,” in *2022 IEEE 12th Sensor Array and Multichannel Signal Processing Workshop (SAM)*, Trondheim, Norway, 2022, pp. 370–374.
- [219] R. Gui, W.-Q. Wang, and H. Shao, “General receiver design for FDA radar,” in *2018 IEEE Radar Conference (RadarConf18)*, Oklahoma, 2018, pp. 1–6.
- [220] Y. Lang, Z. Yang, L. Yang, and X. Chen, “Lamb wave frequency diverse array,” *IEEE Transactions on Ultrasonics, Ferroelectrics, and Frequency Control*, vol. 69, no. 8, pp. 2526–2539, 2022.
- [221] Z. Liu, B. Ma, J. Liu, K. Yang, and Y. Wang, “Joint DOA-Range estimation for coherent signals exploiting moving time-modulated frequency diverse coprime array,” *IEEE Signal Processing Letters*, 2025.
- [222] P. Li, B. Huang, W. Jia, and W.-Q. Wang, “Adaptive detection of distributed target for FDA-MIMO radar in compound-gaussian clutter,” *IEEE Transactions on Aerospace and Electronic Systems*, 2025.
- [223] L. Lan, J. Xu, G. Liao, S. Zhu, and H. C. So, “Mainlobe deceptive jammer suppression in SF-RDA radar: Joint transmit-receive processing,” *IEEE Transactions on Vehicular Technology*, vol. 71, no. 12, pp. 12602–12616, 2022.
- [224] M. Tan, J. Gong, and C. Wang, “Range dimensional monopulse approach with FDA-MIMO radar for mainlobe deceptive jamming suppression,” *IEEE Antennas and Wireless Propagation Letters*, vol. 23, no. 2, pp. 643–647, 2023.

- [225] Y. Hou and W.-Q. Wang, "Mainlobe deceptive jamming discrimination using distributed MIMO-FDA radar," *IEEE Signal Processing Letters*, 2025.
- [226] R. Wang, Y. Jia, W. Wang, and W. Wang, "UC-CNN: An u-shaped complex CNN for mainlobe deceptive jamming suppression with FDA-MIMO radar," in *2025 IEEE Radar Conference (RadarConf25)*. IEEE, 2025, pp. 682–686.
- [227] T. Yuan, F. He, Z. Dong, Y. Su, Z. Fan, and L. Yu, "Suppress mainlobe deceptive jamming target under unambiguous range compensation based on FDA-MIMO radar," *IEEE Transactions on Aerospace and Electronic Systems*, vol. 60, no. 5, pp. 6853–6868, 2024.
- [228] Y. Liu, C. Wang, J. Gong, and G. Chen, "Discrimination of mainlobe deceptive target with meter-wave FDA-MIMO radar," *IEEE Communications Letters*, vol. 26, no. 5, pp. 1131–1135, 2022.
- [229] T. Zhong, H. Tao, H. Cao, and H. Liao, "Mainlobe deceptive jamming suppression with polarimetric characteristic FDA-MIMO radar," in *IET Conference Proceedings CP874*, vol. 2023, no. 47. IET, 2023, pp. 2380–2383.
- [230] L. Lan, Y. Zhang, J. Xu, G. Liao, and H. C. So, "Suppressing mainlobe deceptive jammers via two-low-rank matrix decomposition in FDA-MIMO radar," *IEEE Transactions on Aerospace and Electronic Systems*, vol. 61, no. 2, pp. 2885–2898, 2024.
- [231] Q. Liu, C. Wang, D. Tian, W. Pu, X. Zhou, and Z. Liang, "A mainlobe jamming suppression method for an fda-mimo radar system with an ultralarge sparse aperture," *IEEE Transactions on Aerospace and Electronic Systems*, 2025.
- [232] P. Baizert, T. B. Hale, M. A. Temple, and M. C. Wicks, "Forward-looking radar GMTI benefits using a linear frequency diverse array," *Electronics Letters*, vol. 42, no. 22, pp. 1311–1312, 2006.
- [233] J. Xu, G. Liao, L. Huang, and H. C. So, "Robust adaptive beamforming for fast-moving target detection with FDA-STAP radar," *IEEE Transactions on Signal Processing*, vol. 65, no. 4, pp. 973–984, 2017.
- [234] C. Wen, M. Tao, J. Peng, J. Wu, and T. Wang, "Clutter suppression for airborne FDA-MIMO radar using multi-waveform adaptive processing and auxiliary channel STAP," *Signal Processing*, vol. 154, pp. 280–293, 2019.
- [235] F. Wan, J. Xu, Y. Xu, W. Wang, G. Liao, and Y. Zhang, "Clutter suppression for spaceborne FDA-MIMO radar with QPC," *IEEE Transactions on Aerospace and Electronic Systems*, 2025.
- [236] G. Haoliang, Z. Shunsheng, and W. Wenqin, "Passive localization countermeasure based on frequency diverse array," *Journal of Radar*, vol. 10, no. 6, 2021.
- [237] L. Wang, W.-Q. Wang, H. Guan, and S. Zhang, "LPI property of FDA transmitted signal," *IEEE Transactions on Aerospace and Electronic Systems*, vol. 57, no. 6, pp. 3905–3915, 2021.
- [238] W.-Q. Wang, "Moving-target tracking by cognitive rf stealth radar using frequency diverse array antenna," *IEEE Transactions on Geoscience and Remote Sensing*, vol. 54, no. 7, pp. 3764–3773, 2016.
- [239] Z. Chen, Z. Zhang, Y. Zhou, Q. Zhao, and W. Wang, "Elevated frequency diversity array: A novel approach to high resolution and wide swath imaging for synthetic aperture radar," *IEEE Geoscience and Remote Sensing Letters*, vol. 19, pp. 1–5, 2020.
- [240] Y. Zhou, W. Wang, Z. Chen, Q. Zhao, H. Zhang, Y. Deng, and R. Wang, "High-resolution and wide-swath SAR imaging mode using frequency diverse planar array," *IEEE Geoscience and Remote Sensing Letters*, vol. 18, no. 2, pp. 321–325, 2020.
- [241] K. Wang, G. Liao, J. Xu, Y. Xu, and Y. Zhang, "General bandwidth synthesis approach for multiresolution SAR imaging with frequency diverse array," *IEEE Transactions on Geoscience and Remote Sensing*, vol. 62, pp. 1–15, 2024.
- [242] B. Huang, W.-Q. Wang, S. Zhang, and Y. Liao, "FDA-based space-time-frequency deceptive jamming against SAR imaging," *IEEE Transactions on Aerospace and Electronic Systems*, vol. 58, no. 3, pp. 2127–2140, 2022.
- [243] C. Wang, J. Xu, G. Liao, X. Xu, and Y. Zhang, "A range ambiguity resolution approach for high-resolution and wide-swath SAR imaging using frequency diverse array," *IEEE Journal of Selected Topics in Signal Processing*, vol. 11, no. 2, pp. 336–346, 2016.
- [244] Y. Zhou, W. Wang, Z. Chen, Q. Zhao, Y. Deng, and R. Wang, "A novel high-resolution and wide-swath SAR imaging mode using frequency diverse planar array," in *EUSAR 2021; 13th European Conference on Synthetic Aperture Radar*. VDE, 2021, pp. 1–5.
- [245] Y. Wen, Z. Zhang, Z. Chen, H. Zhao, Y. Zhang, and H. Fan, "A frequency diverse array SAR processing framework based on the segmented phase code waveform for HRWS imaging," *IEEE Geoscience and Remote Sensing Letters*, vol. 20, pp. 1–5, 2023.
- [246] C. Lin, P. Huang, W. Wang, Y. Li, and J. Xu, "Unambiguous signal reconstruction approach for sar imaging using frequency diverse array," *IEEE Geoscience and Remote Sensing Letters*, vol. 14, no. 9, pp. 1628–1632, 2017.
- [247] J. Zhu, K. Yu, S. Zhu, B. Wang, R. Wang, and L. Wang, "Application of frequency diverse array to resolve range ambiguity for SAR imaging," in *2019 6th Asia-Pacific Conference on Synthetic Aperture Radar (APSAR)*. IEEE, 2019, pp. 1–5.
- [248] W.-Q. Wang, "Forward-looking SAR imaging with frequency diverse array antenna," in *2016 IEEE International Geoscience and Remote Sensing Symposium (IGARSS)*, Beijing, China, 2016, pp. 4191–4194.
- [249] J. Shen, K. Liao, S. Ouyang, H. Wang, and Q. Yu, "Front-downward-looking 3D SAR imaging using frequency diversity array," in *2021 IEEE International Geoscience and Remote Sensing Symposium IGARSS*. IEEE, 2021, pp. 3967–3970.
- [250] M. Zhang, G. Liao, X. He, and S. Zhu, "Unambiguous forward-looking SAR imaging on HSV-R using frequency diverse array," *Sensors*, vol. 20, no. 4, p. 1169, 2020.
- [251] H. Wang, S. Zhang, W. Wang, B. Huang, Z. Zheng, and Z. Lu, "Multi-scene deception jamming on SAR imaging with FDA antenna," *IEEE Access*, vol. 8, pp. 7058–7069, 2020.
- [252] B. Huang, W. Wang, S. Zhang, H. Wang, R. Gui, and Z. Lu, "A novel approach for spaceborne sar scattered-wave deception jamming using frequency diverse array," *IEEE Geoscience and Remote Sensing Letters*, pp. 1–5, 2019.
- [253] Y. Zhu, H. Wang, S. Zhang, Z. Zheng, and W. Wang, "Deceptive jamming on space-borne sar using frequency diverse array," in *IGARSS 2018 - 2018 IEEE International Geoscience and Remote Sensing Symposium*, July 2018, pp. 605–608.
- [254] B. Huang, S. Y. Nusenu, S. Zhang, W.-Q. Wang, Y. Liao, and Z. Wang, "A deceptive jamming against high and low orbit bistatic sar using frequency diversity array," in *2019 6th Asia-Pacific Conference on Synthetic Aperture Radar (APSAR)*. IEEE, 2019, pp. 1–5.
- [255] H. Zhang, G. Jin, H. Zhang, Y. Wang, Y. Cheng, Z. Guo, S. Ye, and D. Zhu, "A fast repeater mainlobe deceptive jamming suppression method for FDA-MIMO SAR under complex motion condition," *IEEE Transactions on Aerospace and Electronic Systems*, 2025.
- [256] J. Yu, W. Nie, M. Zhou, Z. Tian, and B. Huang, "Scattered wave deception jamming against squint sar using frequency diverse array," in *2020 IEEE Asia-Pacific Microwave Conference (APMC)*. IEEE, 2020, pp. 979–981.
- [257] M. Lou, J. Yang, Z. Li, H. Ren, H. An, and J. Wu, "Joint optimal and adaptive 2-d spatial filtering technique for FDA-MIMO SAR deception jamming separation and suppression," *IEEE Transactions on Geoscience and Remote Sensing*, vol. 60, pp. 1–14, 2022.
- [258] P. Ji, S. Xing, D. Dai, B. Pang, and D. Feng, "A template-modulation jamming against sar based on frequency-diverse array," *IEEE Geoscience and Remote Sensing Letters*, vol. 20, pp. 1–5, 2023.
- [259] Z. Wang, S. Yang, M. Shi, and K. Qin, "FDA-SSD: fast depth-assisted single-shot multibox detector for 3d tracking based on monocular vision," *Applied Sciences*, vol. 12, no. 3, p. 1164, 2022.
- [260] A. Basit, W.-Q. Wang, and S. Y. Nusenu, "Adaptive transmit array sidelobe control using FDA-MIMO for tracking in joint radar-communications," *Digital Signal Processing*, vol. 97, p. 102619, 2020.
- [261] A. Basit, W.-Q. Wang, S. Y. Nusenu, and Z. Zheng, "Cognitive FDA-MIMO with channel uncertainty information for target tracking," *IEEE Transactions on Cognitive Communications and Networking*, vol. 5, no. 4, pp. 963–975, 2019.
- [262] W.-Q. Wang, "Moving-target tracking by cognitive RF stealth radar using frequency diverse array antenna," *IEEE Transac-*

- tions on Geoscience and Remote Sensing, vol. 54, no. 7, pp. 3764–3773, 2016.
- [263] Y. Sun, Z. Zheng, W.-Q. Wang, and T.-x. Liao, “DOA estimation and tracking for FDA-MIMO radar signal,” *Digital Signal Processing*, vol. 106, p. 102858, 2020.
- [264] Y. Wang, W. Li, G. Huang, and J. Li, “Time-invariant range-angle-dependent beam pattern synthesis for fda radar targets tracking,” *IEEE Antennas and Wireless Propagation Letters*, vol. 16, pp. 2375–2379, 2017.
- [265] R. Gui, W.-Q. Wang, Y. Pan, and J. Xu, “Cognitive target tracking via angle-range-doppler estimation with transmit subaperturing FDA radar,” *IEEE Journal of Selected Topics in Signal Processing*, vol. 12, no. 1, pp. 76–89, 2018.
- [266] Z. Wang, W.-Q. Wang, and J. Xiong, “Cognitive target tracking using FDA radar for increased SINR performance,” in *2016 IEEE Radar Conference (RadarConf)*. IEEE, 2016, pp. 1–4.
- [267] B. Yang, S. Zhu, X. He, L. Lan, and X. Li, “Cognitive FDA-MIMO radar network for target discrimination and tracking with main-lobe deceptive trajectory interference,” *IEEE Transactions on Aerospace and Electronic Systems*, vol. 59, no. 4, pp. 4207–4222, 2023.
- [268] R. Gui, Z. Zheng, and W.-Q. Wang, “Cognitive FDA radar transmit power allocation for target tracking in spectrally dense scenario,” *Signal Processing*, vol. 183, p. 108006, 2021.
- [269] Y. Yan, H. Tao, J. Guo, and B. Yang, “Cognitive FDA-MIMO radar network’s transmit element selection algorithm for target tracking in a complex interference scenario,” *Remote Sensing*, vol. 17, no. 1, p. 59, 2024.
- [270] W.-Q. Wang, “DM using FDA antenna for secure transmission,” *IET Microwaves, Antennas & Propagation*, vol. 11, no. 3, pp. 336–345, 2017.
- [271] J. Xiong, S. Y. Nusenu, and W.-Q. Wang, “Directional modulation using frequency diverse array for secure communications,” *Wireless Personal Communications*, vol. 95, pp. 2679–2689, 2017.
- [272] A. Basit, W. Wang, S. Y. Nusenu, and S. Wali, “FDA based QSM for mmwave wireless communications: Frequency diverse transmitter and reduced complexity receiver,” *IEEE Transactions on Wireless Communications*, pp. 1–1, 2021.
- [273] T. Zhang, Y. Zou, G. Wang, A. Chaaban, G. Liu, and J. Cheng, “RIS-Aided index modulation for OFDM systems: Analysis and code design for flat-fading channels,” *IEEE Transactions on Communications*, vol. 72, no. 10, pp. 6192–6208, 2024.
- [274] Y. Xu, D. Ma, Y. Fang, L. Lv, and Y. Zhou, “Polar-coded modulation schemes for multiple-mode OFDM with index modulation system,” *IEEE Wireless Communications Letters*, vol. 13, no. 12, pp. 3668–3672, 2024.
- [275] E. Aydin, F. Cogen, and E. Basar, “Code-index modulation aided quadrature spatial modulation for high-rate MIMO systems,” *IEEE Transactions on Vehicular Technology*, vol. 68, no. 10, pp. 10257–10261, 2019.
- [276] B. Huang, S. Shang, and M.-S. Alouini, “Movable-antenna index modulation (MA-IM): System framework and performance analysis,” 2026. [Online]. Available: <https://arxiv.org/abs/2603.26153>
- [277] G. Huang, S. Ouyang, Y. Ding, and V. Fusco, “Index modulation for frequency diverse array,” *IEEE Antennas and Wireless Propagation Letters*, vol. 19, no. 1, pp. 49–53, 2020.
- [278] J. Jian, W.-Q. Wang, B. Huang, L. Zhang, M. A. Imran, and Q. Huang, “MIMO-FDA communications with frequency offsets index modulation,” *IEEE Transactions on Wireless Communications*, 2023.
- [279] J. Jian, Q. Huang, B. Huang, and W.-Q. Wang, “FDA-MIMO-based integrated sensing and communication system with frequency offsets permutation index modulation,” *IEEE Transactions on Communications*, 2024.
- [280] S. Y. Nusenu, S. Huaizong, Y. Pan, and A. Basit, “Space-frequency increment index modulation approach for fifth generation and beyond wireless communication systems,” *IEEE Transactions on Vehicular Technology*, vol. 69, no. 6, pp. 6286–6298, 2020.
- [281] A. Basit, W.-Q. Wang, S. Y. Nusenu, and S. Wali, “FDA based QSM for mmwave wireless communications: Frequency diverse transmitter and reduced complexity receiver,” *IEEE Transactions on Wireless Communications*, vol. 20, no. 7, pp. 4571–4584, 2021.
- [282] B. Qiu, L. Wang, J. Xie, Z. Zhang, Y. Wang, and M. Tao, “Multi-beam index modulation with cooperative legitimate users schemes based on frequency diverse array,” *IEEE Transactions on Vehicular Technology*, vol. 69, no. 10, pp. 11028–11041, 2020.
- [283] H. Huang and W.-Q. Wang, “FDA-OFDM for integrated navigation, sensing, and communication systems,” *IEEE Aerospace and Electronic Systems Magazine*, vol. 33, no. 5-6, pp. 34–42, 2018.
- [284] M. Wachowiak, A. Bourdoux, and S. Pollin, “Frequency diverse array ofdm system for joint communication and sensing,” in *2025 IEEE 5th International Symposium on Joint Communications & Sensing (JC&S)*. IEEE, 2025, pp. 1–6.
- [285] S. Y. Nusenu and W.-Q. Wang, “Range-dependent spatial modulation using frequency diverse array for OFDM wireless communications,” *IEEE Transactions on Vehicular Technology*, vol. 67, no. 11, pp. 10886–10895, 2018.
- [286] S. Y. Nusenu, S. Huaizong, and P. Ye, “Power allocation and equivalent transmit fda beamspace for 5g mmwave noma networks: Meta-heuristic optimization approach,” *IEEE Transactions on Vehicular Technology*, vol. 71, no. 9, pp. 9635–9646, 2022.
- [287] S. Y. Nusenu, S. Huaizong, Y. Pan, and A. Basit, “Space-frequency increment index modulation approach for fifth generation and beyond wireless communication systems,” *IEEE Transactions on Vehicular Technology*, vol. 69, no. 6, pp. 6286–6298, 2020.
- [288] B. Huang, J. Xu, and M.-S. Alouini, “Generalized code-frequency-space index modulation: A next-generation green communication solution,” *IEEE Transactions on Wireless Communications*, 2025.
- [289] P. Gandotra and R. K. Jha, “A survey on green communication and security challenges in 5g wireless communication networks,” *Journal of Network and Computer Applications*, vol. 96, pp. 39–61, 2017.
- [290] F. Cogen, E. Aydin, N. Kabaoglu, E. Basar, and H. Ilhan, “Generalized code index modulation and spatial modulation for high rate and energy-efficient mimo systems on rayleigh block-fading channel,” *IEEE Systems Journal*, vol. 15, no. 1, pp. 538–545, 2020.
- [291] S. Ji, H. Chen, Q. Hu et al., “A dual-function radar-communication system using frequency diverse array,” in *Proc. IEEE Radar Conf. (RadarConf)*, 2018, pp. 224–229.
- [292] S. Y. Nusenu, W.-Q. Wang, and A. Basit, “Time-modulated fd-mimo array for integrated radar and communication systems,” *IEEE Antennas Wireless Propag. Lett.*, vol. 17, no. 6, pp. 1015–1019, 2018.
- [293] X. Zhou, L. Tang, Y. Bai et al., “Performance analysis and waveform optimization of integrated FD-MIMO radar-communication systems,” *IEEE Trans. Wireless Commun.*, vol. 20, no. 11, pp. 7490–7502, 2021.
- [294] M. Li and W.-Q. Wang, “Joint radar-communication system design based on FDA-MIMO via frequency index modulation,” *IEEE Access*, vol. 11, pp. 67722–67736, 2023.
- [295] J. Jian, Q. Huang, B. Huang et al., “FDA-MIMO-Based integrated sensing and communication system with frequency offsets permutation index modulation,” *IEEE Trans. Commun.*, vol. 72, no. 11, pp. 6707–6721, 2024.
- [296] J. Jian, B. Huang, W. Jia et al., “FDA-MIMO-Based integrated multi-target sensing and communication system with complex coefficients information embedding,” *arXiv preprint arXiv:2409.02447*, 2024.
- [297] Q. Xu, L. Lan, G. Liao, K. Wang, and T. Zheng, “Transceiver design for an FDA-MIMO Radar and MIMO communication spectral coexistence system,” *Journal of Radars*, 2025.
- [298] J. Jian, W. Jia, W.-Q. Wang et al., “Dual-function system for area surveillance and multi-user communications with FDA-MIMO,” *IEEE Trans. Veh. Technol.*, 2025, early access.
- [299] H. Yang, S. Gong, H. Liu et al., “Frequency diverse array-enabled RIS-aided integrated sensing and communication,” *IEEE Trans. Wireless Commun.*, 2025, early access.
- [300] A. Hassanien and S. A. Vorobyov, “Phased-MIMO radar: A tradeoff between Phased-Array and MIMO radars,” *IEEE Transactions on Signal Processing*, vol. 58, no. 6, pp. 3137–3151, 2010.